ELECTRICAL CHARACTERIZATION OF ARCING FAULT BEHAVIOR ON 120/208V SECONDARY NETWORKS

A Dissertation

by

JEFFREY ALAN WISCHKAEMPER

Submitted to the Office of Graduate Studies of
Texas A&M University
in partial fulfillment of the requirements for the degree of

DOCTOR OF PHILOSOPHY

December 2011

Major Subject: Electrical Engineering

Electrical Characterization of Arcing Fault Behavior

On 120/208V Secondary Networks

ELECTRICAL CHARACTERIZATION OF ARCING FAULT BEHAVIOR ON 120/208V SECONDARY NETWORKS

A Dissertation

by

JEFFREY ALAN WISCHKAEMPER

Submitted to the Office of Graduate Studies of
Texas A&M University
in partial fulfillment of the requirements for the degree of

DOCTOR OF PHILOSOPHY

Approved by:

Chair of Committee,	B. Don Russell
Committee Members,	Karen L. Butler-Purry
	Deepa Kundur
	Warren Heffington
Head of Department,	Costas Georghiades

December 2011

Major Subject: Electrical Engineering

ABSTRACT

Electrical Characterization of Arcing Fault Behavior on 120/208V Secondary Networks.

(December 2011)

Jeffrey Alan Wischkaemper, B.S., Texas A&M University

Chair of Advisory Committee: Dr. B. Don Russell

Arcing faults have been a persistent problem on power systems for over one hundred years, damaging equipment and creating safety hazards for both utility personnel and the public. On low-voltage secondary networks, arcing faults are known to cause specific hazards collectively called “manhole events”, which include smoke and fire in underground structures, and in extreme cases explosions. This research provides the first comprehensive attempt to electrically characterize naturally occurring arcing fault behavior on 120/208V secondary networks.

Research was performed in conjunction with the Consolidated Edison Company of New York, whereby a single low-voltage network was instrumented with thirty high-speed, high-fidelity data recording devices. For a nominal one year period, these devices collected detailed, high-speed waveform recordings of arcing faults and other system transients, as well as statistical power system data, offering new insights into the behavior of arcing faults on low-voltage networks.

Data obtained in this project have shown the intensity, persistence, and frequency of arcing faults on low-voltage networks to be much higher than commonly

believed. Results indicate that arcing faults may persist on a more-or-less continuous basis for hours without self-extinguishing, may recur over a period of hours, days, or weeks without generating enough physical evidence to be reported by the public or operate conventional protective devices, and may draw enough current to be observed at the primary substation serving the network. Additionally, simultaneous fault current measurements recorded at multiple locations across the network suggest the possibility of using multi-point secondary monitoring to detect and locate arcing faults before they cause a manhole event.

DEDICATION

dixitque Deus fiat lux et facta est lux et vidit Deus lucem quod esset bona et lux in tenebris lucet et tenebrae eam non conprehenderunt.

ACKNOWLEDGEMENTS

This research would not have been possible without the hard work and dedication of multiple people, and this dissertation would not be complete without acknowledging their efforts:

I express tremendous gratitude to my committee chair, Dr. B. Don Russell, for his outstanding mentorship, and for granting me the opportunity to work alongside him.

Thanks also go to my committee members, Dr. Butler-Purry, Dr. Kundur, and Dr. Heffington, for their service, and for indulging me and my flirtation with multiple deadlines.

Special thanks go to Carl Benner, whose knowledge of arcing faults and power system waveforms is unrivaled. Carl's tremendous insight contributed in no small way to the ideas contained in this dissertation.

The data collection platform used in this project would not exist without the work of Karthick Manivannan, my fellow researcher in the Power System Automation Laboratory. His capable management of a team of graduate students ensured the smooth operation of my data monitors. In particular, Jagadish Chandar's diligent effort in maintaining the DFA platform software had significant impact on the success of this project.

Jessica Meadors and Sharon Loe deserve unending thanks for their tireless work behind the scenes in our laboratory.

I am also tremendously grateful to Tammy Carda, our graduate student advisor, who never rolled her eyes when I asked silly questions.

A host of employees of the Consolidated Edison Company of New York contributed to this project. In particular, Serena Lee, Leslie Philp, Neil Weisenfeld, Yingli Wen, Frank Doherty, Stan Lewis and Pete Hoffman contributed their significant expertise and knowledge about the operation of low-voltage networks. Special thanks also go to Gerard Johnson, who installed the data collection devices under the streets of New York City.

Additional personal thanks go to Dr. Warren Heffington, and his wife Donna, for their support and encouragement across my collegiate career. I appreciate Dr. Heffington's work on my committee, but I appreciate more his kind and gentle spirit, and his quiet example of life well lived.

Dr. Brian Perkins became a trusted friend during my graduate school experience. His encouragement and example of professionalism did not go unnoticed.

Kelly and Sara Davidson were mentors throughout my college years. They opened their home to me, and became a second set of parents. Their wisdom and guidance helped shape who I am.

Dr. James Fisher was, and remains, the best of friends. There are no words to describe the respect and admiration I have for his intellect, his humility, and his character. James is not only a wonderful friend, but an incredible human being.

To my sister and longtime roommate, Lisa, I extend a special thanks: you'll always be #1 in my book.

My parents, Jay and Dianna, challenged me to accomplish great things. Their love, support, and financial assistance made this document possible. Their spirit of generosity to those around them is a testament to the kind of people they are, and the kind of person I hope to become.

And finally, I could not have completed this work without the support and love of my wife, Katie. Her encouragement and company make life that much more sweet.

TABLE OF CONTENTS

Page

Page

LIST OF FIGURES

Page

Page

Page

Page

Page

Page

LIST OF TABLES

Page

1. INTRODUCTION TO LOW-VOLTAGE ARCING PROBLEM

1.1 Historical Background

Arcing faults have been a persistent problem since the construction of the first electrical power systems. Unlike bolted faults which usually trip protective devices, intermittent arcing faults may produce bursts of significant electrical activity interrupted by long quiescent periods (e.g. hours, days, weeks) before progressing to a sustained low-impedance, high-current electrical condition sufficient to operate a conventional protective device, or generating physical evidence to be noticed by the public. When incipient arcing conditions go undetected, they pose a variety of problems for system operators, as well as a safety hazard to utility crews and the public.

A significant body of work exists exploring detection of arcing on medium and high-voltage systems [1-75]. Recent years have seen an increasing interest in arcing on low-voltage (<1,000V) systems, but this work is almost exclusively focused on 480V [76-85] systems, where arcing faults can both readily sustain themselves, and produce fires, explosions, and arcs with a tremendous release of energy. Very little work has been done on faulted 120/208V class systems, partially because conventional wisdom has always held that arcing faults cannot sustain themselves at such a low-voltage level [83, 86-90].

This dissertation follows the style of *IEEE Transactions on Industry Applications.*

The lack of significant research on 120/208V class systems does not mean the problem is entirely unknown. Early published papers on arcing in low-voltage networks date to 1924 [91], followed by two papers in 1931 [86, 87]. The next mentions of arcing on low-voltage networks in published literature comes almost two decades later in the classic Westinghouse text [88], and the Edison Electric Company's reference on underground systems [89]. All of these early documents express the same basic conclusion: arcing at 120/208V does not sustain itself, and cables on such systems, when properly designed, should burn themselves clear in relatively short order. In general, these books still form the foundation of conventional wisdom related to arcing faults on 120/208V networks: arcing faults typically clear themselves "with relatively low current," "without damage to the cable except at the fault," and "in less than a tenth of a second"[88, 89].

Following the Edison Electric book, little mention is made of low-voltage network arcing until 1983, when a paper discussing the protection of Vepco's 480V spot networks was published by Roop [92]. Koch and Carpentier published a work detailing manhole explosions caused by arcing faults on BC Hydro's 480V networks in 1992 [93], and a 1993 paper focused on the detection of high impedance faults on low-voltage networks in laboratory tests [90]. Again, sustained arcing on 120/208V class systems was not discussed, or when discussed, was declared to not be possible.

In spite of the theoretical objections and conventional wisdom to the contrary, the experience of personnel operating 120/208V class systems indicated that significant arcing activity did exist on these systems, evidenced by substantial operational evidence.

While researchers had not been successful at sustaining an arc at 120/208V in the laboratory, arcing faults certainly seemed to sustain themselves in conduits underground. Furthermore, the degradation of underground cables on 120/208V systems due to arcing produced smoke, fires, and explosions in underground structures, which collectively became known as “manhole events” [77, 90, 92-95].

Even though arcing faults caused noticeable operational problems on 120/208V systems, understanding of the behavior of naturally occurring arcing phenomena at this voltage level was not significantly different in 1994 than when the first underground alternating current networks were installed almost 100 years before. Several factors contributed to this general lack of understanding.

First, underground low-voltage arcing is an intermittent phenomenon, the occurrence of which is almost impossible to predict. As a result, recording current and voltage measurements produced by naturally occurring arcing events is a non-trivial task. Any experiment would need to monitor multiple points on the secondary network for a period of weeks or months to have a high probability of detecting a naturally occurring arcing fault. Additionally, arcing faults often have magnitudes equal to or less than normal system transients, meaning any device set sensitively enough to record incipient arcing signatures will also record large numbers of non-arcing events, creating a significant data storage and data management problem. Also, because arcing faults can endure over a period of minutes to hours, properly characterizing them requires a data collection device capable of recording long waveform files, on the order of minutes, a feature not typically available on even exotic relays or power quality devices.

Second, as documented in literature, attempts to induce arcing at 120/208V in laboratory settings proved elusive. It was clear arcing occurred in underground structures and persisted at least long enough to produce serious physical damage, but replicating this phenomenon in the laboratory was very difficult. The physical conditions which enabled arcing in underground conduits was unknown, and by the time a major arcing event was reported, all evidence of those conditions had been obliterated by the event itself. Research conducted in [90] explains the difficulty of initiating arcing faults below 200V in a laboratory. It was not until a comprehensive study on gasses produced by the degradation of cable insulation that researchers were able to consistently produce stable arcs at 120V [96]. This study is discussed in detail in Section 2.1.1.

Finally, even if one could model and understand the behavior of the naturally occurring phenomena, it was unclear how this knowledge would lead to improved system operation based on available technology. Even as recently as the last decade, following the report of [96], arcing faults were considered to be “an industry problem that presently has no available solution” [97]. Recent advances in distributed communication and intelligent relays have made systems for the detection and location of arcing faults on a secondary network technologically feasible, which in turn has generated new interest in research on this topic. Indeed, one of the recommendations of [96] was that such a system might be possible. In the years following this report, limited research has been published exploring this possibility [76, 81, 98]. These research efforts will be detailed in a subsequent section.

1.2 Low-voltage Networks

1.2.1 History

The first low-voltage alternating current network is believed to have been installed in Memphis, TN in 1907, though this date is uncertain. It is clear, however, that by the early 1920's, multiple networks existed in major cities across the United States. Due to perceived advantages including superior reliability and economic benefits serving dense urban loads, low-voltage networks became the de facto standard for any application where there was a high load density, or where high reliability was a requirement[88, 89]. By 1974, over 300 companies in the United States operated low-voltage networks [99].

Low-voltage networks remain a power delivery system of choice for urban centers today, with most major cities operating at least one network. Ironically, despite their widespread use, many utility personnel are unaware of their existence. When the subject is discussed, experienced personnel from utilities without operational networks are often surprised to learn that such systems exist.

Functionally, low-voltage networks have experienced only incremental improvements since they were first installed. Their general topology and operation has remained relatively unchanged over the past 90 years, with the most major architectural advances being the introduction of the automatic network protector in 1924 [91], which served as the sine qua non of low-voltage networks, and the development of cable limiters to protect against fault currents in 1938 [100-103]. A variety of incremental changes have improved components like cable insulation, network transformers, and

network protector relays, but most networks operate today in more or less the same fashion as when they were first installed. Particularly telling is that the main reference texts in this field remain books published in the 1950's, with low-voltage networks receiving only a passing mention in newer texts, if they are mentioned at all [88, 89, 104].

1.2.2 Typical Configuration

Low-voltage networks consist of a highly interconnected secondary cable system fed by multiple primary feeders. The network is structured in such a way that the secondary can be thought of as a more-or-less continuous "grid," with each network transformer serving as a current injection point, and each load as a current sink. Network transformers are arranged in such a way that an outage on one primary feeder, even though it may take out several secondary transformers, does not result in an interruption in customer load. Likewise, the loss of a single secondary main cable does not result in the interruption of load to customers.

A typical network protection scheme is as follows: in the event of a fault on a primary feeder, each network transformer is equipped with a network protector, which serves in essence as a circuit breaker that trips on reverse power flow [88, 89, 91]. If a fault is detected on a primary feeder, the substation breaker and all network protectors attached to transformers served by that feeder will open, de-energizing the circuit from both sides. In actual practice, the substation breaker will operate first, followed by network protectors tripping out based on their respective protection curves. After the substation breaker has opened, but before any network protectors have operated, the

network itself continues to feed the primary feeder fault from the secondary side. Initially, the primary fault will be fed from the network preferentially through secondary transformers electrically closest to the fault point, resulting in those transformers' network protectors operating first. Once these network protectors have opened, the fault current shifts to flow through other transformers connected to the faulted primary feeder whose network protectors have not yet operated. This process continues until all network protectors on transformers connected to the affected feeder have operated. After operation of all protective devices, no intentional reclosing is attempted. The feeder remains out of service until the fault is located and repairs are complete. During the course of this research, several examples of this phenomenon were observed and recorded, enabling new insights into primary feeder fault behavior.

Due to their low nominal voltage and high load density, low-voltage secondary networks are designed to carry relatively high currents. For example, a 120/208V 1,000kVA transformer has a nominal per-phase current rating of over 2,600A at its secondary terminals at full rated load. These current levels require multiple, large diameter cables, and give rise to the possibility of unusually high fault currents. Typical numbers cited for available secondary fault currents are on the order of 35,000-50,000A. Because this fault current is served from multiple transformers, no single transformer sees the "total" fault current, making system protection a more challenging task. This problem is compounded during the occurrence of an arcing fault, which typically does not draw as much current as a full "bolted" fault. In foundational texts describing network operations, arcing faults are allowed to burn clear by design [88, 89]. A major

emphasis of good network design in these texts is making sure enough current is available to burn a cable clear in the event of an arcing fault at any point on the network. In essence, arcing faults that self-clear by burning free are a part of intended system operation, though the effects they cause are undesirable, often destructive and sometimes dangerous.

Secondary transformer impedances in low-voltage networks are generally higher than those on medium voltage radial systems, with most units having 5% impedance [88, 89]. This higher value prevents currents from “circulating” on primary feeders in normal system operation. In the absence of this artificially high impedance, current could flow from the network through the secondary transformer onto the primary feeder, and then back onto the secondary network through a different transformer attached to that primary feeder, under certain network load conditions.

While some utilities employ SCADA-type systems on their secondary networks, in truth little is known about the actual behavior and distribution of current flows on secondary networks, both for loads and faults. Conventional wisdom dictates that “every load (or every fault) is served by every transformer,” but few scientific measurements exist to provide a basis for modeling how load and fault current are distributed as a wide range of controlling parameters vary.

1.3 Low-voltage Arc Fault Problem

1.3.1 Evolution

Arcing faults on 120/208V systems are known to cause a variety of operational and public safety hazards. Faults occur when cable insulation is sufficiently damaged to allow the formation of a conductive path between the phase conductor and a grounded or semi-grounded object. In general, this initial contact is not a “bolted” fault condition, but rather occurs through a high-impedance medium such as mud, water, slurry, etc. The resultant electrical current produces an arc, which in turn produces high temperatures and expulsion of gasses and metals, further degrading cable insulation, and increasing the probability of the fault continuing and/or recurring. Additionally, the localized heating, which has been measured to be several hundred degrees Celsius, liberates flammable, explosive, and toxic gases. Finally, the arc contains significant energy which by itself can produce powerful shockwaves [95, 105]. The calculation and mitigation of arc flash hazards is a problem affecting a wide range of industries, and is well documented in literature [105-121].

1.3.2 Manhole Events

Operational safety hazards produced by network arcing faults are commonly referred to as “manhole events.” This term serves as an omnibus phrase to describe a wide variety of phenomena which may evolve along different electrical and mechanical paths, but ultimately produce undesirable hazards to equipment, utility personnel, and the public.

The most serious categories of manhole events are fires and explosions. While manhole fires and explosions are not common, they have become increasingly damaging to utility public relations in an age where many passersby have the ability to video an explosion or fire occurring in a manhole or transformer vault and upload it to the internet before the utility is aware of the problem. A quick search of internet video sites reveals no shortage of footage related to manhole events. While the public is unaware of and unconcerned with the mechanism causing these events, they are generally quite concerned with the end result. In addition to exposure on social networking and internet video sites, major events also tend to draw the attention of larger news outlets. Figure 1 shows a photo published on the New York Times website on February 11, 2010 following an event which damaged a building in downtown Manhattan. A similar photo, published on the social media site Gawker, is shown in Figure 2.

Figure 1: Explosion in a transformer vault, February 11, 2010.

Photo by Stephanie Derogue for the New York Times

Figure 2: Photo of February 11, 2010 manhole explosion.

Photo by Austin Riggs, published on Gawker

The degradation of cable insulation produces a wide range of flammable and explosive gasses, as described in [96]. These gasses are produced at the point of the fault. When the fault occurs in conduit, explosive gasses are believed to constitute a low fire and explosion risk, at least initially, primarily due to the lack of oxygen in the immediate area surrounding the fault. Over time, the gasses are believed to migrate out of the conduit into adjacent structures, mixing with oxygen. When the proper ratio of oxygen and explosive gasses combine, additional arcing may trigger a fire or explosion.

Even in the absence of explosive gasses, the shockwave from the arc itself can, in some instances, be enough to displace manhole covers[95].

Insulation degradation can also produce significant amounts of smoldering and smoke, which can sometimes be visible emerging from structures. These events are generally referred to as “smoking manholes,” and are significantly more common than manhole fires and explosions. Without swift attention, however, a smoking manhole may escalate into a more serious event. Additionally, the composition of gasses produced by degrading insulation may contain compounds like hydrogen chloride and sulfur dioxide which are toxic, especially when inhaled.

A subcategory of manhole event not generally seen or discussed in literature is the presence of elevated carbon monoxide in structures or buildings. Carbon monoxide is produced when carbon-containing material combust without sufficient oxygen to completely oxidize the organic material. Carbon monoxide is a known product of arcing fault-induced insulation degradation, and poses perhaps the greatest safety risk to the public [96]. Carbon monoxide is odorless, colorless, and tasteless, but also extremely flammable and highly toxic. As a result, any report of an elevated carbon monoxide level in a building or structure is generally investigated by the utility and considered a manhole event for the purposes of internal reporting.

2. DISCUSSION OF RECENT WORK ON 120/208V ARCING

2.1 Prior Work by the Consolidated Edison Company of New York

2.1.1 1996 EPRI/UL Gas Evaluation Study

2.1.1.1 Summary of Results

The Consolidated Edison Company of New York (ConEdison) is the largest domestic operator of low-voltage secondary network power systems. Recognizing the significance of manhole events, ConEdison contracted with EPRI in 1995 to conduct research on the low-voltage arcing phenomenon, targeting systems operating at less than 480V [96]. The specific emphasis of that project was to characterize gasses generated from decomposition of cable insulation in the presence of high currents and electric arcs. Measurements were taken of arcing induced on a 600V-rated cable. A recorded waveform from the project's final report is presented in Figure 3.

Interestingly, waveforms observed in Figure 3 closely resemble arcing waveshapes previously observed on medium voltage systems, though in this laboratory setting they appear much more stable than naturally observed events, with significantly less cycle-to-cycle variability. The lack of variability may have been due to the relatively stable mechanical configuration of the experimental setup, which does not necessarily represent the dynamic mechanical conditions occurring during actual faults. This project also marked the first time stable arcing was achieved in a laboratory setting at 120/208V. Previous attempts to initiate and sustain arcs at or below 200V had little success. Together, these results were a significant advancement, representing one of the first

major contributions to foundational knowledge about arcing behavior below 480V in 70 years.

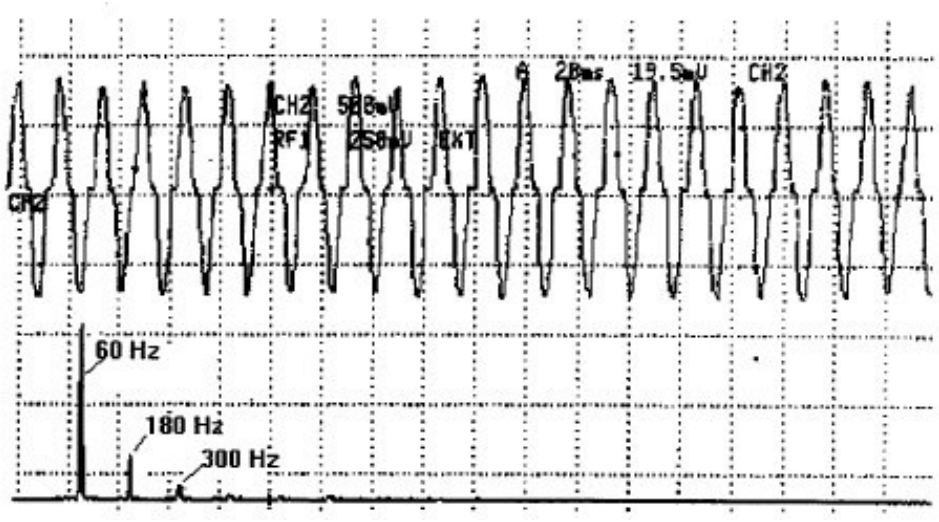

Figure 3: Recorded arcing current waveform from gas evolution testing

Experimentally, testing for gas evolution occurred in two phases. In the first phase, researchers attempted to measure decomposition effects due to ohmic (I^2R) heating, and in the second phase they attempted to measure effects due to electric arcing. The arcing research was conducted by physically damaging cable insulation and conditioning the cable in order to produce a carbonized path. In some tests, a salt water solution was dripped into the conduit to simulate what is believed to happen as salt solution seeps into underground structures when roads are salted during snow and ice events.

Research indicated that thermal decomposition of cable insulation occurred when the cable's temperature exceeded 200 C. The composition of the gasses varied based on temperature, but it was observed that the primary combustible gasses were methane, ethylene, and carbon monoxide, though acetylene could be generated as the cable approached 400 C. Decomposition caused by electrical arcing produced similar results, with methane, ethylene, acetylene and carbon monoxide all observed. Certain cables also produced hydrogen chloride, sulfur dioxide, and hydrogen gas. Research indicated that gas generation rates were higher when the concentration of oxygen was reduced.

A notable finding from this research was the suggestion that conditions could exist which would allow sporadic arcing to continue on a system in a high-impedance state for an indefinite period. This was very important finding, which raised several key questions. Does sporadic arcing occur weeks or months before a final event, only to die out until additional water, mud, sludge, etc. creates a semi-conductive path? Does the level of activity grow over time, finally reaching levels that produce enough gasses to cause explosions? At the time, these and other questions did not have concrete answers, but this conclusion from the gas evolution study, and prior fault anticipation work at Texas A&M both suggested there might be a substantial period of intermittent arcing episodes prior to final failures [16]. If the answer to the questions was determined to be "yes," it could provide the means to detect and locate arcing faults well in advance of manhole events, thereby enabling crews to prevent the final catastrophic failure altogether. Furthermore, the EPRI report itself suggested it might be possible to detect

the electrical signals produced by the arcing faults generated in the lab as a means of mitigating the arcing fault problem.

While the answers to the questions raised in this report were unknown and technology did not exist to adequately investigate them at the time, in many ways these questions form the first formulation of the hypotheses explored in this research.

2.1.2 3rd Avenue Yard Staged Arc Fault Tests

2.1.2.1 Summary of Results

One recommendation of EPRI's Gas Evaluation study was to investigate the potential for detecting arcing by monitoring electrical signals. In 1997 ConEdison began an internal project researching this possibility with staged experiments at their 3rd Avenue Yard facility in Brooklyn. Partial results of this research were published in [80]. For the 3rd Avenue Yard tests, cable faults were created in a section of cable added above ground, in conduit, between two manholes on one of ConEdison's networks. Electrical behavior was recorded in two locations with a high-speed data acquisition system (20,000 samples per second) monitoring directly at the end of the faulted cable section and in one vault location. Electrical behavior also was recorded with modified ETI relays in five locations.

Figure 4 was taken from a report on the 3rd Avenue Yard tests and shows waveforms captured during one of the 3rd Avenue Yard trials. Spectral analysis of the data showed significant activity below 1,000Hz. Specifically, the activity was described as "pink" noise, increasing the general noise floor below 1,000Hz. The shape of the waveforms generated in the 3rd Avenue Yard tests look very similar to waveforms

captured during the gas evolution study. In the case shown in Figure 4, we can note that the fault occurred on Phase B, with current exceeding 3,300 amps in the positive half-cycle. Both Phase A and C have much lower magnitudes, suggesting that they are inductively or capacitively induced sympathetic effects caused by the fault on Phase B.

Figure 5 and Figure 6 show arcing current waveforms obtained from multiple locations during another staged event during the 3rd Avenue Yard tests. Figure 5 contains fault measurements recorded directly at the point serving the fault, and thus represents the actual fault current served to the fault. Figure 6 shows waveforms recorded from a remote point in the network during the same fault. This is believed to be the first time a staged fault was recorded at multiple points in the network, suggesting the possibility of remote detection of arcing currents produced by naturally occurring faults.

The report on the 3rd Avenue Yard Tests described data collected from the ETI relays as inconclusive, but it was noted that some disturbances were detected by the relays. Due to the nature of the Power Spectral Density below 1,000Hz, it was believed that such arcing faults would be detectable by relays, and a prototype program was recommended.

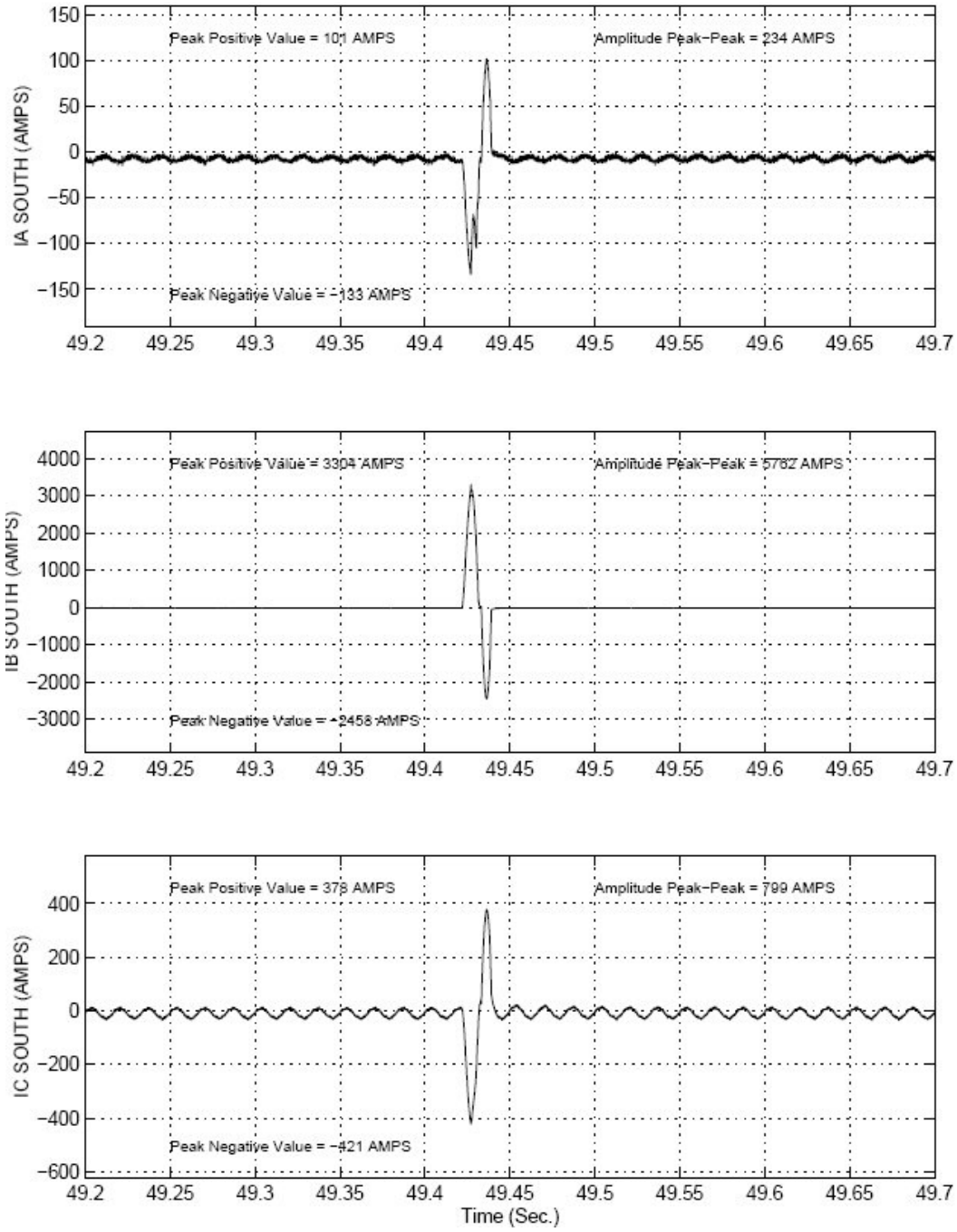

Figure 4: Current waveforms recorded during 3rd Avenue Yard tests

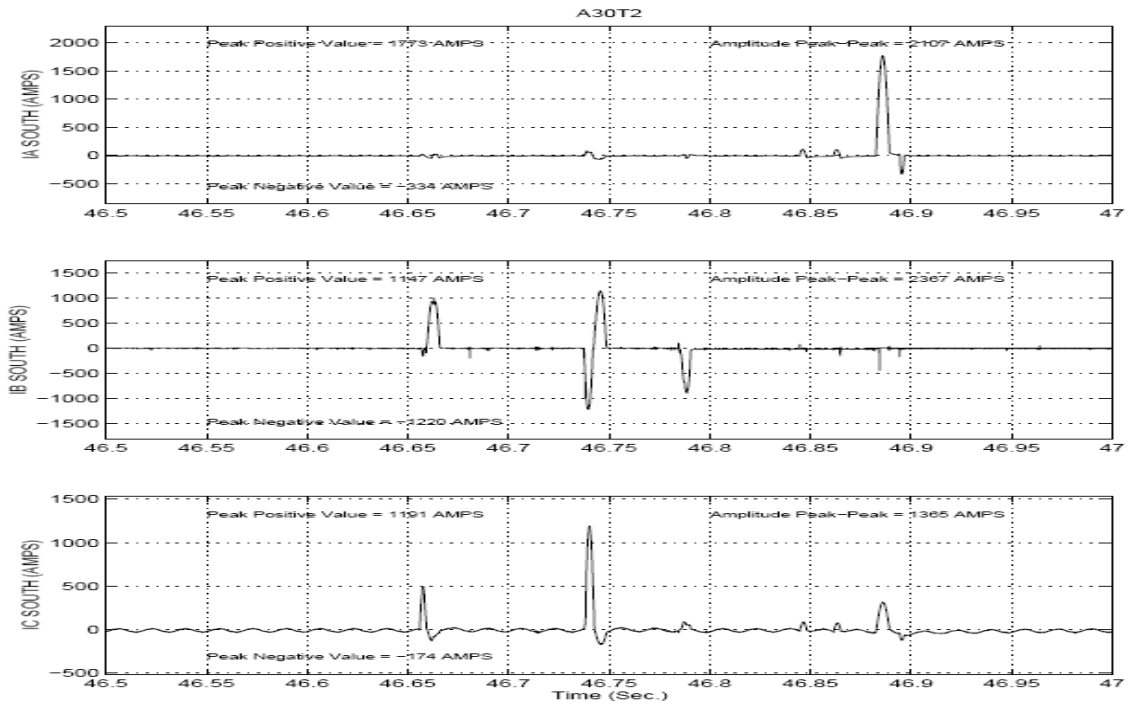

Figure 5: Arcing waveforms from 3rd Avenue Yard tests, Location “A”

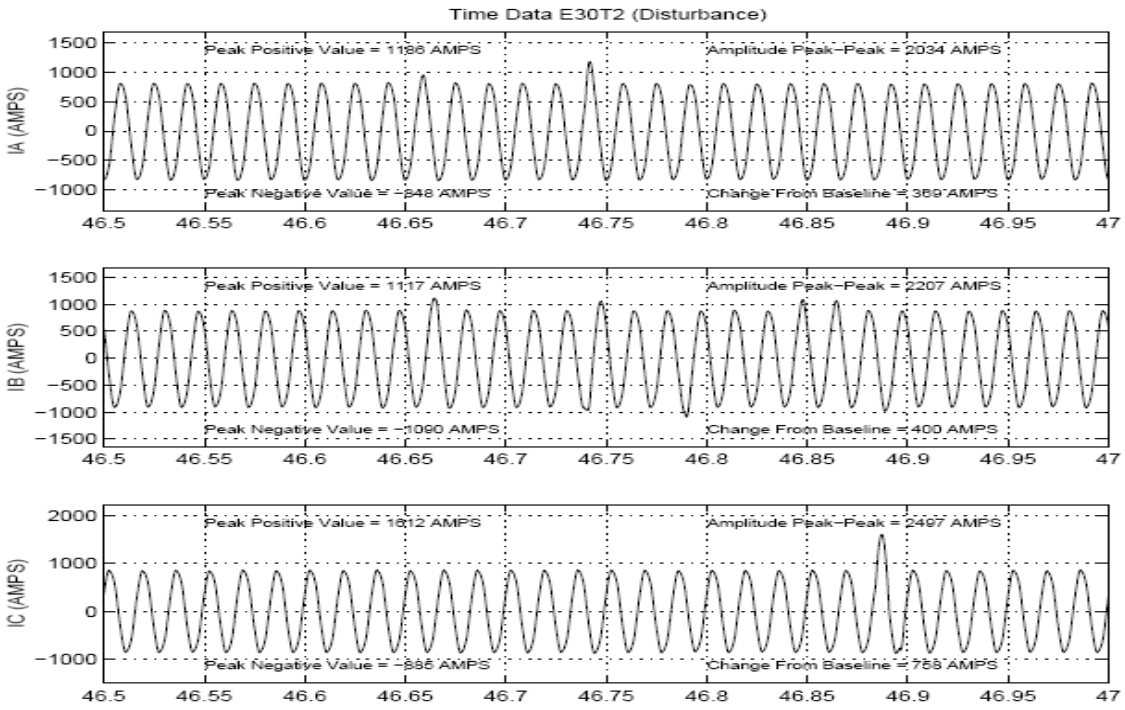

Figure 6: Arcing waveforms from 3rd Avenue Yard tests, Location “E”

2.1.3 Fashion Network Data Collection Project

2.1.3.1 Summary of Results

Following the recommendation of the 3rd Avenue Yard test final report, ConEdison began an internal project to explore the possibility of using a broad deployment of relays to detect the electrical signatures produced by arcing faults. In 2005 ConEdison installed 50 Siemens model 7SJ64 relays in selected transformer vaults on the Fashion network. The Fashion network is a relatively small secondary network, and 50 monitored points represented a substantial percentage of the network’s 114 network transformers. Figure 7 shows an enclosure containing one of the 7SJ64 relays,

as installed by ConEdison. For approximately two years, ConEdison used the oscillographic data capture capability of these relays to record waveforms from the network. These devices were capable of storing a maximum of nine records in a circular buffer with each waveform capture having a length of slightly over 1 second, at a sample rate of 960Hz. The three-phase currents were measured directly and the relays calculated a neutral current as the point-by-point sum of the three-phases. Event records were stored in the COMTRADE format, which is an industry standard file format for relay data. The records were managed by a proprietary Siemens software package.

In order to retrieve the data, an engineer with a laptop physically travelled to each of the locations when an indication had been received that the buffer in a device was full and downloaded the data. This process was prone to some delay, however, and the circular buffer used in the device introduced the possibility that valuable data could be overwritten. At the end of the project, ConEdison had retrieved approximately 550 data records, though due to various data management issues, only 64 were determined to be unique. These records were subsequently analyzed by Texas A&M for indications of arcing.

Figure 7: Installed enclosure containing Siemens 7SJ64 relay

2.1.3.2 Case Studies

Figure 8 contains normal, unaltered waveforms for an event that is designated as Sample Event A for purposes of this dissertation. Because this measurement is taken from a network transformer serving load, the measurements contain a pseudo steady-state load component plus the transient current produced by the event of interest. To distinguish event current from the total current, a simple numerical technique was applied to remove the ambient load component. The resulting waveforms approximate the current of the event of interest alone and are shown in Figure 9 for Sample Event A.

Sample Event A is one of a handful of records retrieved in the project which researchers determined contained arcing signatures. The Fashion network project was significant as it produced the first known record of any naturally occurring arcing activity. Unfortunately, due to a variety of limitations, as discussed in Section 2.1.3.3, little could be said about this data in terms of fundamentally characterizing the arcing signatures themselves. Waveforms captured in the project resembled both waveforms collected in the 3rd Avenue Yard tests, the EPRI gas evolution study, and arcing faults observed on medium voltage systems, but serious questions remained about the actual behavior of arcing faults on the network. In particular, how arcing faults developed over time was still virtually unknown.

The Siemens relays only captured about one second of data per event. As a result, it remained unknown whether there might be significant numbers of bursts over a substantial period of time leading up to a report of a manhole event, although past experience with other incipient failures suggested this was likely the case.

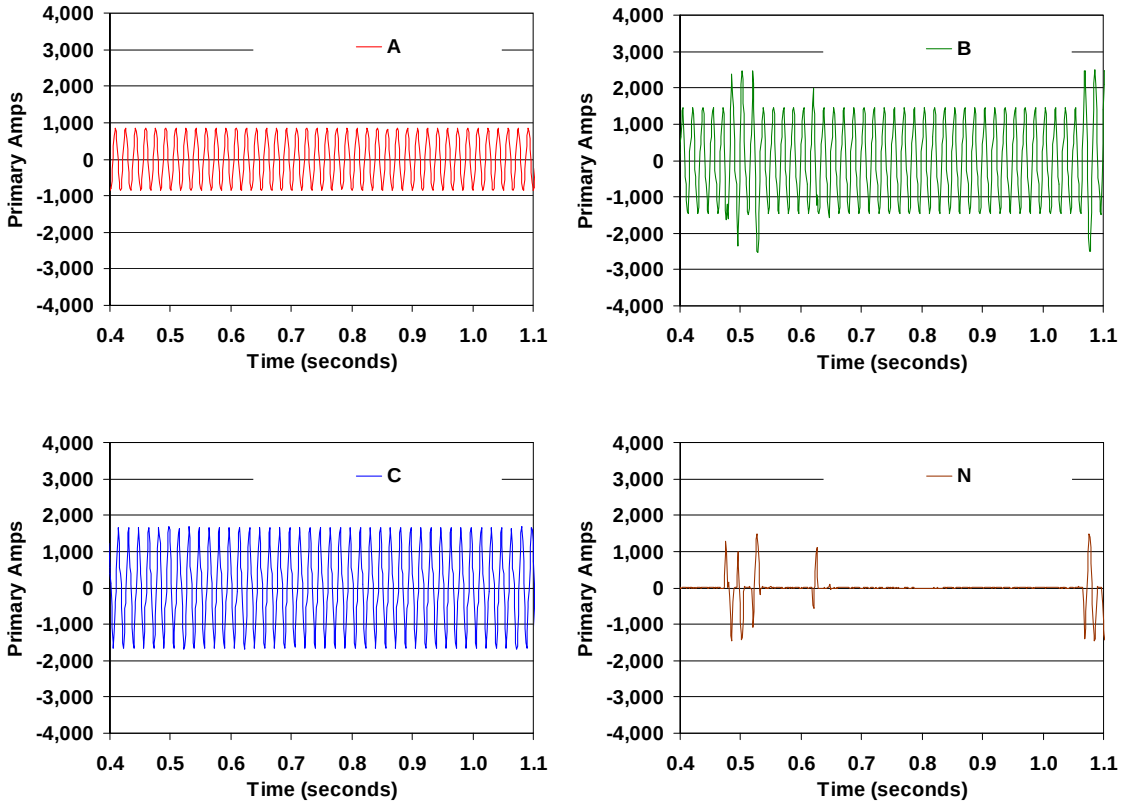

Figure 8: Unaltered waveforms measured during Event A

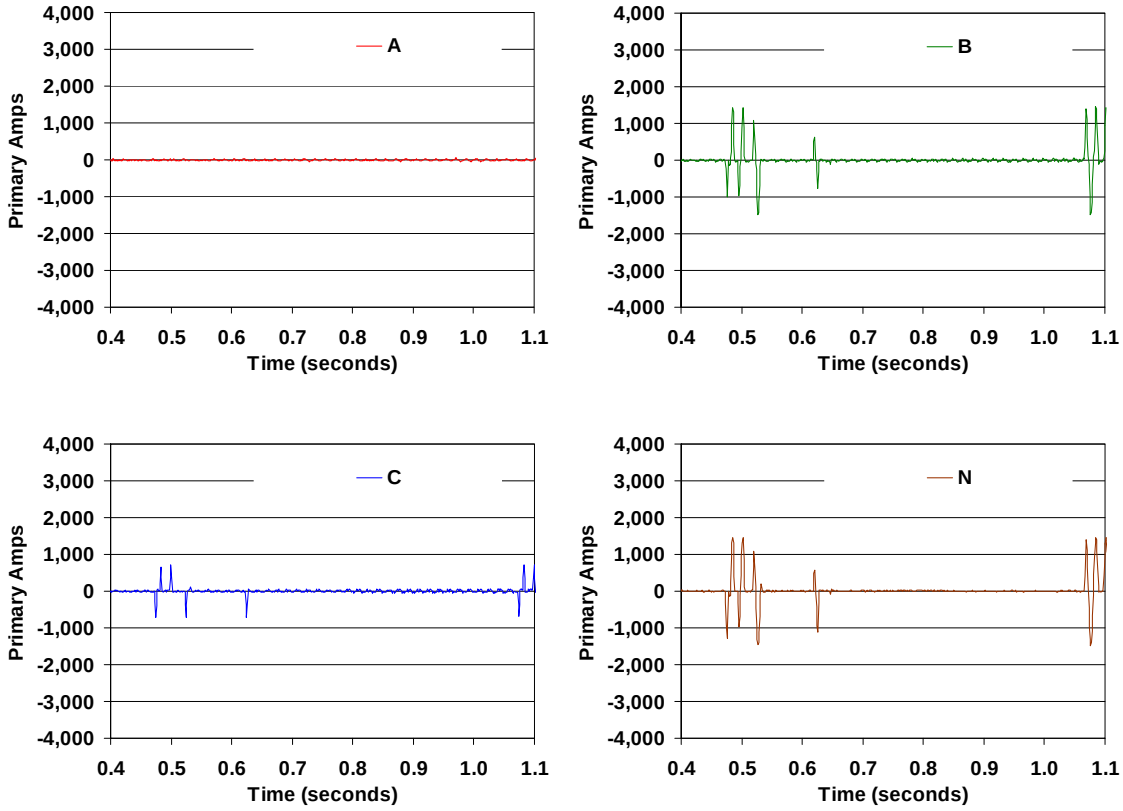

Figure 9: Waveforms from Event A, ambient load removed

ConEdison contracted with researchers at Texas A&M to analyze data retrieved from the Fashion network project. Researchers qualitatively compared the shape and temporal behavior of these waveforms to their knowledge base of the behavior of arcing faults on overhead medium-voltage systems. These analyses revealed a number of similarities.

In a general sense, the shape and temporal behavior of low-voltage arcing fault current mimicked characteristics of arcing faults on medium-voltage systems. More

specifically, there were apparent similarities in the shapes of the arcing waveforms. Also, waveforms appeared rich in harmonic and non-harmonic components, and exhibited significant cycle-to-cycle variations within a burst. Recorded cases also suggested that individual bursts of arcing current lasted cycles, with quiescent periods lasting cycles, seconds, or longer. These characteristics were again consistent with behavior observed in many instances of arcing faults on medium-voltage systems.

While initial analysis suggested similarities between arcing on low-voltage networks and arcing on higher voltage systems, it also suggested significant differences. Most notably, arcing faults on medium-voltage systems almost always involve a single-phase and ground. Multi-phase faults on medium-voltage systems tend to be conventional, low-impedance faults that can be cleared by conventional protection. Data from the Fashion network suggested this might not be the case for low-voltage arcing faults, as all of the events measured contained phase-to-phase activity. In their summary report, researchers noted this surprising finding, including the mention of a roundtable discussion held with ConEdison engineers where all parties speculated about the mechanical configurations that could bring about such electrical characteristics. The report clearly stated, however, that none of the theories advanced rose above the level of conjecture, since none were supported by actual data.

In summary, researchers felt the data obtained in the Fashion network study offered encouraging similarities to data observed in previous tests and on medium voltage systems, but simultaneously highlighted all the outstanding questions about the

unknown fundamental characteristics of naturally occurring arcing faults on low-voltage networks.

2.1.3.3 Limitations of Data Collected

The Siemens relays used in the Fashion Network project were designed primarily to provide system protection, with data capture capabilities included as a secondary feature. While the collected data provided encouraging results, the analysis was limited significantly by the capabilities of the data collection device.

For instance, the relays sampled data at 960Hz, or a nominal 16 points per cycle. This data rate is more than sufficient for relaying, but is inadequate for describing the high range of frequency components typically found in arcing events. While the lower sample rate was enough to say quantitatively “something” happened, and that the resulting waveforms might be arcing, it was not enough to define the actual characteristics of the fault sufficiently.

More importantly, waveform recordings from the device were time limited to 65,535 samples, which resulted in in records of slightly over one second in length. Furthermore, the device was only capable of holding nine such records at any given time in a circular buffer.

Another significant limitation involved the labeling of the data captures from the Siemens relays. There were numerous demonstrable instances of data records that were labeled with the incorrect location (i.e., box number) or date and time. For example, there might be ten absolutely byte-by-byte identical waveforms that were labeled as having occurred at multiple locations over a span of months. Unfortunately there was no

key that would allow this mislabeling to be corrected. Out of approximately 550 data records retrieved by ConEdison, only 64 records were determined to be unique. Because of the widespread labeling errors, researchers had no confidence in any of the time or location information, and therefore could not match any of the records with any date, time or incident in utility operations records. In summary data from the Siemens relays provided multiple records where waveform data appeared quite valid, but with unreliable time and location information.

Finally, the Siemens data collection devices were programmed to initiate data captures based on sensing multiple, rapid changes in neutral current over a short period of time. Normal system events (e.g., line switching, large load starting, etc.) can cause sudden changes in current as well. Because the data collection devices held only a very limited number of event records, setting the threshold for data capture sensitively could result in normal system events filling the available buffers and leaving little or no room for those events truly of interest.

This problem was complicated by the reality of ConEdison personnel needing to visit each location on a regular basis to retrieve records. If the interval between visits allowed more than nine records to be captured, data would be lost. These factors combined to result in a tradeoff between sensitivity, data retention, and reasonable intervals between visits. Consequently, the devices were set to trigger only on relatively high levels of current. The result is that arcing events that might have occurred without reaching the threshold were ignored.

2.1.4 Summary

These experiments and field measurements collectively captured the existence of arcing at 120/208V. However, many questions remained unanswered and a true model of fault behavior did not exist.

3. RESEARCH HYPOTHESES, METHODS, AND GOALS

While extensive research has been performed to characterize and detect naturally occurring arcing faults on medium voltage systems [1-75], very little information exists on naturally occurring arcing faults on low-voltage systems, particularly those operated at 120/208V. While studies have been performed measuring staged arcing faults in laboratory conditions, there is very limited information about how these faults behave on operational power systems. In particular, almost nothing is known about how such faults develop and recur over time, how long they may persist without being reported or cleared by conventional means, how far from their point of origin they can be electrically observed, and whether they can be located.

One objective of this research was to collect an extensive database of naturally occurring arcing fault signatures on low-voltage, 120/208V networks, and subsequently analyze them to create a comprehensive record of how such faults behave on an operational secondary network.

3.1 Hypotheses

In particular, this research was designed to demonstrate conclusively the following hypotheses to be true:

1) Arcing faults can persist for minutes, hours, days, or weeks before producing enough physical or electrical evidence to be detected by a utility company or the public.

2) Arcing faults at 120V can persist near-continuously for hours without self-extinguishing or operating any protective device.
3) Arcing faults on low-voltage secondary networks can be detected by monitoring primary feeders serving network transformers geographically proximate to the faulted location.
4) Arcing faults can be readily detected by electrically monitoring secondary cables; both low and high current faults can be detected.
5) Arcing fault current is served predominantly by network transformers closest to the fault location.
6) Monitors not electrically near the fault location do not observe the fault.
7) Faults can be located using multiple, simultaneous measurements of fault current on secondary cables.

3.2 Goals

The ultimate goal of this research is to provide a foundational, scientific basis for the detection, location, and mitigation of network arcing faults. If the above hypotheses are true, future systems can be developed which may allow network operators to substantially reduce the occurrence of catastrophic failures and public safety hazards on their systems, thereby improving reliability and reducing the potential for harm to the public.

4. EXPERIMENTAL METHODOLOGY

4.1 Overview and Timeline

Based on findings from previous research projects at Texas A&M and ConEdison, both parties undertook a fundamental study to explore the behavior of arcing faults on 120/208V secondary networks. To this end, an experiment was devised where 30 underground points would be monitored for a nominal period of one year, to be extended based on observed results. ConEdison selected the Cooper Square network in Manhattan as the installation site for the project. The project also included instrumenting one of the 26 primary feeders serving the networks.

4.1.1 Project Questions for Investigation

At the beginning of the project, there were several unanswered questions about the behavior of arcing faults on secondary networks:

1) Would incipient arcing faults produce enough current to be observed by underground monitoring points?
2) Would the current distribution of such faults be so broad across the network that virtually every underground monitor would record every network arcing fault?
3) How long might an arcing fault remain in an incipient condition before resulting in a final, catastrophic failure?

- Do most secondary network arcing faults clear themselves permanently "in less than a tenth of a second," as proposed by conventional wisdom[89]?
- How many faults would be cleared by conventional system protection?
- Do some faults occur at detectable levels with enough advanced warning to enable crews to fix the condition and prevent a manhole event, assuming the fault location can be found?

4) Would secondary network arcing faults be visible on primary feeders serving the network?
5) If they could be observed, would the characteristics of arcing faults on low-voltage systems resemble those of arcing on medium-voltage systems?
6) Would it be possible to locate faults based on electrical measurements?

4.1.2 Project Timeline

To assess the survivability of the proposed data collection devices (DCDs) underground, ConEdison ordered four initial units to be installed prior to the remaining twenty-six. These four units were delivered to ConEdison and became operational in March 2009. Communication was lost to one of the units within a few weeks. Site visits revealed the cell modem at the site had suffered a catastrophic failure, possibly due to water incursion in its enclosure. A replacement modem was ordered, and installed in July. Within weeks of the replacement modem installation, communication was again lost with the unit. Ultimately, it was determined that the underground structure had been flooded, resulting

in the malfunction of both the second cell modem and the DCD. The other three original DCDs functioned without incident.

ConEdison ordered the remaining twenty-six DCDs following the successful installation of the original four units. The units were delivered in two shipments to ConEdison over the summer months. By the end of April 2010, most of the twenty-six units were installed and operational. Intermittent communication failures have generally meant that nominally twenty-five DCDs are operational and communicating at any given time. Monitoring of these units continues as of the writing of this dissertation.

> Winter is traditionally the active season for manhole events in New York, and winter weather activity was expected to result in significant arcing. The winter of 2010-2011 turned out to be exceptionally harsh in New York City, with near record levels of snowfall. On several occasions, the severe weather produced an extremely high volume of arcing-related waveform captures on DCDs.

4.2 Cooper Square Network

4.2.1 Network Overview

The Cooper Square Network serves approximately 65,000 electric customers in Manhattan and is bounded by Broadway on the west, the East river on the east, 14th and 15th Streets on the north, and Canal and Market streets on the south, as shown in Figure 10. The estimated network peak load was 247MW in 2007, and weekend loads were expected to peak at 197MW.

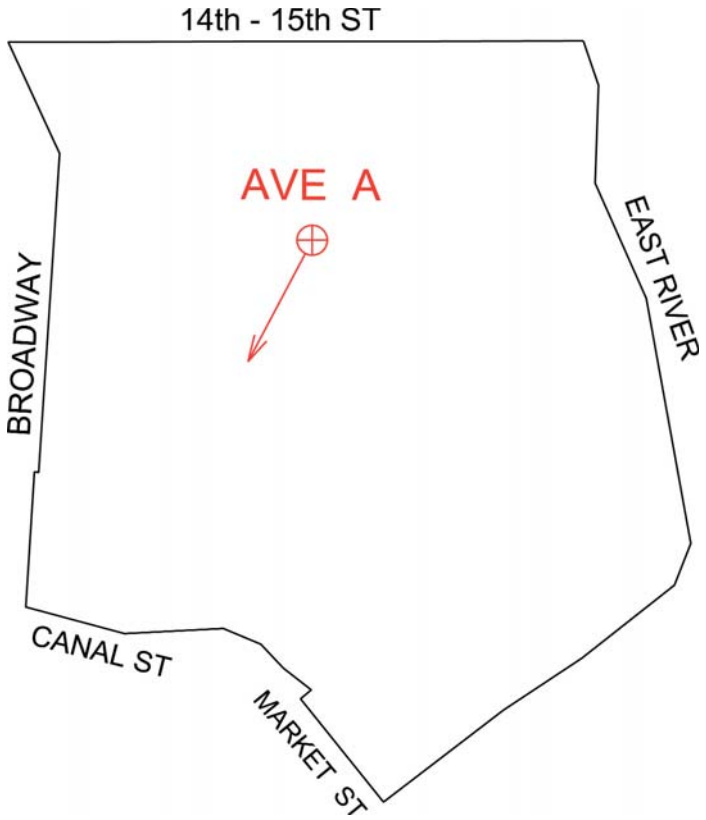

Figure 10: Map of Cooper Square Network

(source: ConEdison Distribution Engineering Manual, 2007)

The network is supplied by 26, 13.8kV primary feeders served from the Ave. A Area Substation. Ave. A is the only area substation serving the Cooper Square network, and Cooper Square is the only network served by Ave. A. Each primary feeder serves multiple network transformers, predominantly 1,000kVA, with some 500kVA and 2,000kVA transformers at selected installations. A table of the primary feeders and load projections, along with number of network transformers is supplied in Figure 11. Cooper Square contains a total of 428 network transformers with a total connected capacity of 373MVA.

COOPER SQUARE NETWORK						
		2007				
		SUMMER LOAD		SUMMER RATING		
FEEDER NUMBER	Note	NORMAL (Proj.Amps)	EMERGENCY (Proj.Amps)	NORMAL (Amps)	EMERGENCY (Amps)	NETWORK TRANSFORMERS SUPPLIED
7M20		574	756	680	980	18
7M21		372	528	680	1,039	12
7M22		575	874	680	980	21
7M23		600	867	680	972	21
7M24		466	576	520	776	20
7M25		606	859	680	970	21
7M26		573	851	680	981	20
7M27		343	463	469	668	12
7M28		261	375	520	835	8
7M29		277	416	530	849	13
7M31		570	687	677	774	20
7M32		434	633	520	794	16
7M33		484	730	680	1,012	17
7M34		567	892	680	983	22
7M35		346	536	520	833	12
7M36		415	614	500	690	17
7M37		578	895	680	979	22
7M38		574	864	673	964	19
7M39		466	654	557	840	18
7M51		294	399	429	579	9
7M52		515	804	680	1,002	18
7M53		468	615	584	827	18
7M54		296	391	451	571	12
7M55		324	503	597	995	15
7M56	(new)	320	523	449	649	15
7M57	(new)	357	527	494	699	12
					TOTAL	428

Figure 11: Table of feeders with normal load and network transformers supplied

(Source: Con Edison, 2007 Distribution Engineering Manual)

4.2.2 Selection of Monitoring Sites

Thirty underground sites were selected for monitoring. These sites were selected by analyzing historical data to determine the geographical distribution of manhole events on the Cooper Square network. The network is mapped into various “M&S Plates,” which form a grid across the network. Each plate is identified by a number and letter combination, for example 14J. The plates containing the Cooper Square network are

numbered 17 to 10, from north to south, and I to O from west to east. For example, the geographic center of the network would be located somewhere in plate 14L. ConEdison keeps records of all manhole events, including the street address at which they occurred. Seven years of data was analyzed, and each plate was assigned a number equal to the total number of manhole events which had occurred during the time period of available data. These values were then normalized and used to distribute the thirty underground monitoring sites based on plate location. The results of this process are shown in Table 1 and Table 2.

.

Table 1: Number of manhole events by plate, Cooper Square Network, 2000-2007

	J	**K**	**L**	**M**	**N**	**O**
17	5	10	15	7	6	-
16	12	6	3	9	10	-
15	8	11	3	1	5	0
14	20	10	14	7	7	0
13	8	10	8	3	4	0
12	6	7	12	7	1	2
11	7	21	6	3	4	1
10	30	15	14	11	2	1
9	13	0	17	6	2	0

This method of distribution did not yield whole numbers, as can be seen in Table 2. Additionally, it was understood that some locations might not be suitable for installation of devices because, for example, if they were prone to flooding. As a result, a total of forty locations were submitted to ConEdison for evaluation as installation sites for DCDs, as shown in Table 2. The final sites selected for device installation are shown on a map of Manhattan in Figure 12. A table of all vault numbers and street addresses is given in Table 3.

Table 2: Proposed distribution of data collection devices

	J	**K**	**L**	**M**	**N**	**O**
17	0	1	1.5	1	0	
16	1	0	0	1	1	
15	1	1	0	0	0	0
14	2	1	1.5	1	1	0
13	1	1	1	0	0	0
12	0	1	1	1	0	0
11	1	2	0	0	0	0
10	2.5	1.5	1.5	1	0	0
9	1	0	1.5	0.5	0	0

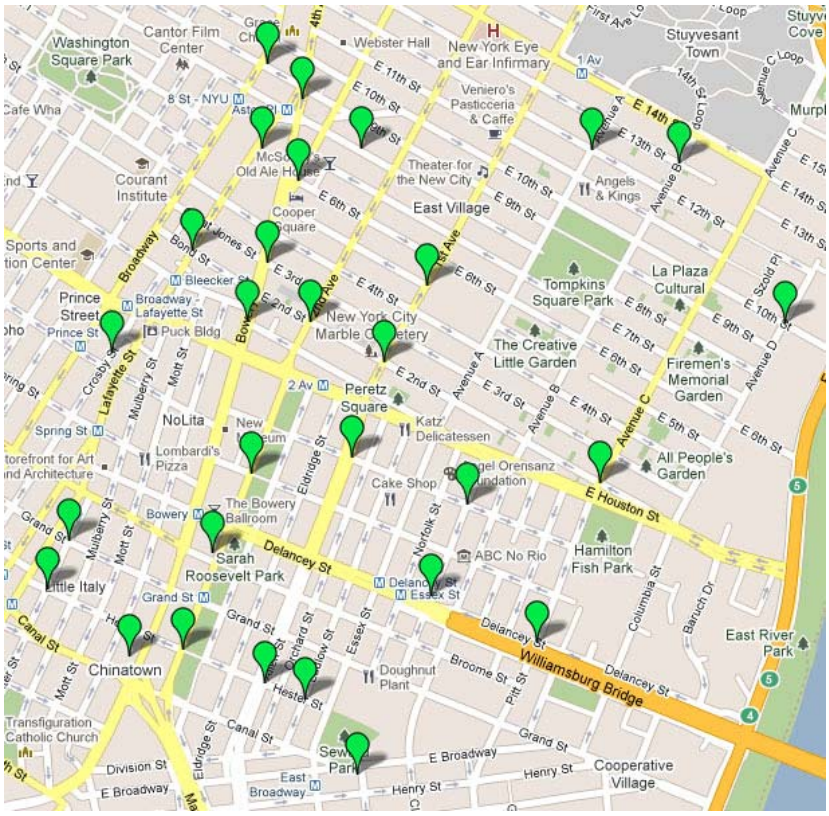

Figure 12: Data collection device installation sites

Table 3: Data collection device installation sites

Vault Number	Primary Feeder	Plate	Address
5445	07M25	10J	BAXTER ST E22N HESTER ST
3544	07M35	10K	BOWERY 74 NLY
7755	07M23	10K	HESTER ST S72W CHRYSTIE ST
6839	07M31	10L	ALLEN ST E33N HESTER ST
7385	07M32	10L	HESTER ST N136E LUDLOW ST
1109	07M22	10M	E BROADWAY 189
6561	07M53	11J	BAXTER ST E51S GRAND ST
3283	07M20	11K	BROOME ST 324
7369	07M21	11K	BOWERY ST E30N GRAND ST
2855	07M23	12K	RIVINGTON ST 45
0199	07M38	12L	SUFFOLK ST 87
5083	07M57	12M	DELANCEY ST N26E PITT ST
7475	07M51	13I	CROSBY ST 116
7926	07M35	13J	E 1 ST BOWERY
8185	07M31	13K	ALLEN ST C34S STANTON ST
3888	07M37	13L	SUFFOLK ST W28N STANTON ST
8292	07M53	14J	E 3 ST S90E BOWERY
9698	07M24	14J	BOND ST S33W LAFAYETTE ST
8442	07M23	14K	E 2 ST N25E 1 AV
9742	07M32	14K	2 ST S32W 2 AVE
9116	07M33	15J	COOPER SQ PARK_48N E 6 ST
9326	07M24	15J	LAFAYETTE ST 427
4238	07M24	15K	E 5 ST S32E 1 AV
4413	07M36	16J	4 AV 42 2ND NLY
8106	07M39	16J	E 9 ST 71 ELY
9216	07M52	16J	ST MARKS PL 19
6361	07M54	17L	E 12 ST S47W AV A
5847	07M28	17M	E 13 ST N E AV B

4.3 Measurement Equipment

4.3.1 Overview

The measurement devices selected for this data collection project were based on devices developed for the Distribution Fault Anticipation project at Texas A&M University under grants from EPRI and the U.S. Department of Energy. This platform was developed over a period of 15 years to provide high-speed, high-fidelity measurements of power system events with the aim of anticipating incipient fault conditions and providing actionable information to utilities. In addition to high quality measurement data, the chosen platform includes advanced data management and viewing software allowing for automated retrieval and convenient analysis of large numbers of captured waveforms.

4.3.2 Data Collection System

4.3.2.1 Field Units

The DCDs used in this project were designed and developed for the Distribution Fault Anticipation (DFA) project at Texas A&M University. The standard DFA hardware was designed to be contained in a 19” rack-mount chassis for installation in a substation. Because DCDs used in this project were to be mounted underground in a NEMA enclosure, heat dissipation was a significant concern. As a result, a second mechanical packaging using the same electronics was designed and designated the “open frame” chassis. This mechanical configuration allowed heat to escape more easily from the electronics, reducing temperatures near the boards themselves. The two alternative configurations of DFA hardware are shown in Figure 13 and Figure 14. Figure 13 shows

the standard 19-inch rack-mount DFA unit. One of these units was installed at the Ave. A area substation on a single primary feeder. Figure 14 shows the open-frame chassis, which was subsequently mounted in a NEMA enclosure for installation underground described further in Section 4.3.2.2.

Figure 13: 19-inch rack-mount DFA unit

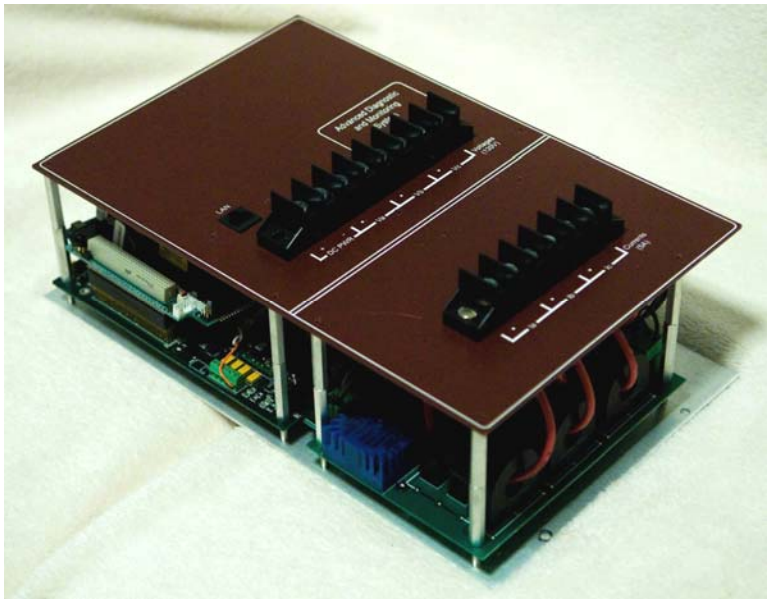

Figure 14: Open frame chassis used as DCD

The electronics onboard the DCD consist of an off the shelf single board computer (SBC) and two custom designed interface boards. The SBC connects to the "analog board," which holds a programmable logic controller (PLC) and custom signal processing circuitry. The analog board is responsible for all data conditioning and sampling, as well as low level functions like a watchdog timer. The analog board pairs with a "magnetics board" containing current transformers (CTs) and potential transformers (PTs) which accept inputs at the terminals of the device and convert them to signal levels. These signals are then passed to the analog board for processing.

The magnetics board accepts inputs from standard 120V/5A power system PTs and CTs, which are the de facto standard used for inputs to power system relays. The voltage inputs are directly connected to PTs on the magnetics board, which transform them to the appropriate range for sampling.

There are three sets of CTs on the magnetics board, each of which has a single-phase current passing through it. Two sets of CTs are used to sample the individual phase currents at different resolutions. One set measures a nominal 0-7A (“normal”) range, and the other a nominal 0-100A (“fault”) range, with both channels sampling at 16-bits using the same sample clock. Because power system faults can produce very large currents (on the order of 50A+ at the input terminals of the device), it is necessary to have the range of the fault channel to accurately measure these events. However, during normal system operation, the DCD will see only a nominal 5A at its input terminals, meaning that 95% of the fault channel’s converter range is unused. To more accurately characterize small incipient signals and provide the highest fidelity data possible, the normal range currents are used whenever they are not saturated. If the normal channel converters are saturated, the fault channel data is available. The third set of CTs produce a sampled neutral current for the normal channels. The outputs of each of these CTs are summed electrically and the result sampled at the same range as the normal current channels. The neutral of the fault channels, by contrast, is produced by a mathematical sum of the fault channel phase currents.

All current and voltage waveforms are sampled at 15,360Hz, or a nominal 256 points per cycle. Because the power system frequency constantly varies from its nominal 60Hz value, the converters employ a Phase Lock Loop (PLL) to track power system frequency as closely as possible. The DCDs are capable of recording 15 channels at this rate, as listed in Table 4.

Normal and fault channels have previously been described in discussion of CTs on the magnetics board. High frequency current channels are produced from the normal data channel after being processed by a 120dB digital high-pass filter with bandpass frequency of 2,000Hz.

In addition to high-speed waveforms, the DCDs also produce a number of calculated values which are stored on a per-cycle or 2-cycle basis. These values include:

- the RMS of each of the sampled signals
- the RMS of a cycle-by-cycle subtraction of normal current, fault current, high-frequency current, and voltage waveforms
- individual components of a 2-cycle FFT of normal current, up to 960Hz
- cycle-by-cycle values of real power (P), reactive power (Q), complex power (S), and power factor, calculated both from the high-speed waveforms (RMS power) and the 60Hz component of high-speed waveforms (Phasor power)
- phase angles for both voltage and current waveforms.

Table 4: Desciptions of high-speed waveform channels

Signal	Description
V_A	Voltage, Channel A
V_B	Voltage, Channel B
V_C	Voltage, Channel C
$I_{Norm}A$	Normal Current, Channel A
$I_{Norm}B$	Normal Current, Channel B
$I_{Norm}C$	Normal Current, Channel C
$I_{Norm}N$	Normal Current, Channel N
$I_{Fault}A$	Fault Current, Channel A
$I_{Fault}B$	Fault Current, Channel B
$I_{Fault}C$	Fault Current, Channel C
$I_{Fault}N$	Fault Current, Channel N
$I_{HF}A$	High Frequency Current, Channel A
$I_{HF}B$	High Frequency Current, Channel B
$I_{HF}C$	High Frequency Current, Channel C
$I_{HF}N$	High Frequency Current, Channel N

Each of these quantities are available on demand in recorded waveform files. It is also often important to have an idea of how system behavior changes over longer periods of time. To this end, the DCDs also record the minimum, maximum, average, and standard deviation of every quantity they measure over a configurable period of time, nominally set at 15 minutes. This data is invaluable when attempting to set thresholds for triggering waveform captures, discussed further in Section 4.4.2.1. These statistical values are referred to as “interval data.”

4.3.2.2 Underground Enclosures

To survive exposed conditions in underground vaults, the DCD electronics were installed in a NEMA 4 enclosure measuring 20”x16”x10.” Inside the enclosure, a power supply converted the 120V AC line voltage obtained directly from ConEdison’s secondary network to 14VDC, supplying power both to the DCD and a battery installed for backup power. All three voltage inputs were fused with 2A fuses, and CT terminals were attached directly to the DCD. Also included was a temperature cutoff switch, designed to turn the DCD off if temperature in the enclosure exceeded 168F to prevent damage to the device itself. A picture displaying the final configuration is located in Figure 15.

4.3.2.3 Master Station

Each DCD independently communicates with a “master station” located at Texas A&M. This communication is performed over a standard TCP/IP connection via cell modem. The communication system itself is described in more detail in Section 4.3.3. The master station is responsible for data retrieval and storage, as well as updating settings for the device in the field. During the communication interval, the master station retrieves all available waveform files, all interval data, and then updates whatever system settings have changed (e.g. triggering thresholds, CT/PT settings, etc), and finally performs software updates to the field device, if any are available.

Figure 15: NEMA enclosure with DCD installed

The master station serves as a common collection point, maintaining a full database of all events recorded and retrieved, as well as all interval data collected on all units. Data contained at the master station can be opened by a custom software package (DFAGui) which allows for advanced analysis of large numbers of waveforms, as well as viewing interval data.

One important feature of the DFAGui software is its load removal, or “phasor-differencing” function. This function will be explained in more detail in Section 5. Another important function of the DFAGui software is its ability to sort and organize waveform files. The DFAGui allows a user to assign a classification to each waveform record, which can then be used to filter waveform files of interest. For example, a user

can easily select all files which have been given a classification related to arcing over a specified time period, if so desired.

4.3.3 Communication System

ConEdison contracted with AT&T to provide communication to underground monitors for the Arc Fault Data Collection Project. Each device communicated via a cell modem installed external to the DCD in a separate NEMA enclosure. The cell modems each obtained a static IP address from AT&T's network, and allowed the DCD to communicate over the internet to the master station at Texas A&M.

While communication was intended to be "always on," it was not uncommon for devices to lose communication, sometimes for days or weeks at a time. DCDs continued to operate and record data in the event of a communication loss, and were equipped with sufficient storage that, except in rare cases, no data was lost.

While no speed tests were explicitly performed to determine the data rate at which the communication system was able to transfer, in general performance was considered "good enough" given the research nature of the project. In most instances, waveform files were retrieved within 15 minutes of their occurrence, though in cases of extreme backlog and slow communications, some units took months to fully retrieve all recorded waveforms.

4.3.4 Instrumentation Transformers

Direct measurement of high currents and voltages are not generally possible with high precision measurement devices. To convert system-level currents and voltages to signal-level magnitudes, current transformers and potential transformers are used.

Typical installations of DFA devices have used meter-quality substation CTs and PTs to provide 120V/5A inputs at the device terminal. Because DCDs for this project were installed underground, different sensors were required.

Since the nominal voltage of the network is already 120/208V, no PTs were required to provide device level inputs. Each phase was connected to the voltage input terminals of the DCD through a 2 amp fuse. Phase A had an additional connection through a temperature switch, and was also connected to an AC/DC power supply input. There was an initial question of whether the switching power supply would adversely affect signal quality on Phase A voltage. A test installation at the Annex substation in Bryan, Texas, used as a burn-in site by Texas A&M, showed significant dips in Phase A voltage, particularly when the backup battery was charging. This test installation was powered by the relay PT output, which was determined to be a significant contributing factor to the voltage distortions. Reconnecting the Phase A input to a 120V wall outlet at the Annex substation alleviated the problem. Installed devices on ConEdison's 120/208V network experienced no issues with distortion due to the switching power supply.

The CTs selected for the project were required to have high ratios due to the large available fault currents on the network. Estimates for fault current in many structures exceeded 50,000A. Additionally, multiple cables are generally run per phase, and the selected CTs would be required to measure current on all cables. ConEdison's previous data collection projects on the secondary network had used a CT produced by Flex Core, a division of Morlan & Associates Inc. These CTs were offered in a variety

of ratios and sizes. While the specification sheets only claimed to pass frequencies between 50-400Hz, results from data collected on Siemens relays during the Fashion network project suggested that performance should be sufficient to characterize arcing faults adequately. The particular models selected for use in this project were 3000:5 CTs with an 11” inner diameter. At the selected CT ratio, the DCD’s “normal” current channel saturates at 4200 amperes (RMS), and the “fault” channel saturates at 60,000 amperes (RMS).

4.4 Recorded Data

4.4.1 Interval Data

The values of the minimum, maximum, average, and standard deviation for each of the measured and calculated parameters obtained by the DCD are recorded in a database at a configurable interval of time, typically set to 15 minutes. This includes both high-speed waveform data and calculated parameters such as harmonic spectra. Figure 16 shows values for the average RMS current over each 15 minute interval recorded during calendar year 2010. This data is useful for determining when load shifts occurred on the network, as there are generally step changes in the average current at affected locations. One such shift can be observed on the right fifth of Figure 16.

Other interval plots that are of particular use for longer periods of time are the maximum current and minimum voltage recorded at 15 minute intervals, shown in Figure 17 and Figure 18 respectively. The minimum voltage plot can be useful for locating events which substantially affect the power system voltage, such as large arcing

events, or overcurrent faults on a primary feeder, or the transmission system, while the maximum current plot can be used to see high current events located on the network.

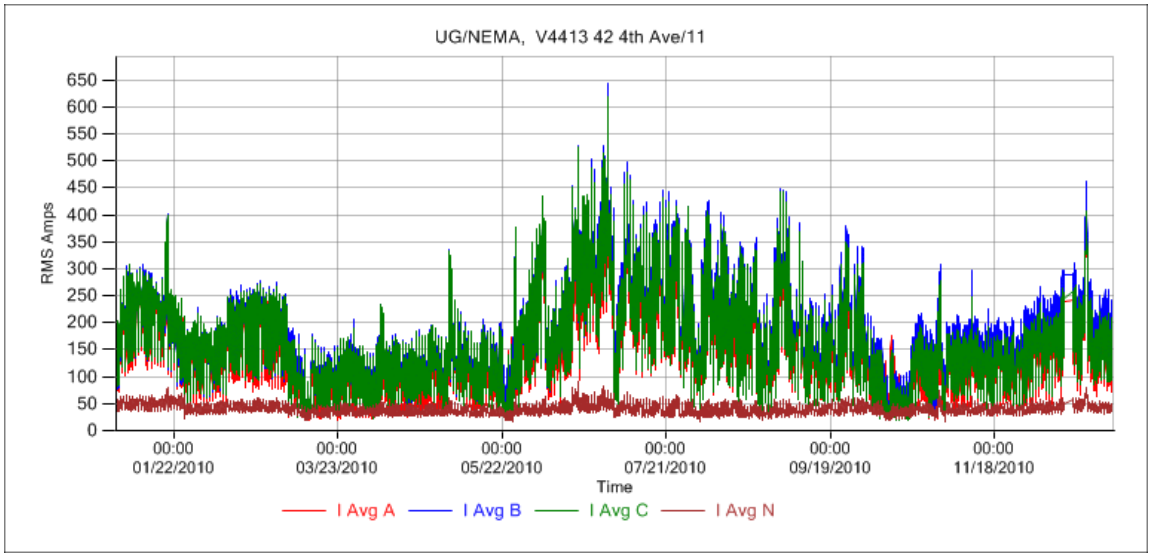

Figure 16: Average RMS current (15 minute interval) for one year period, V4413

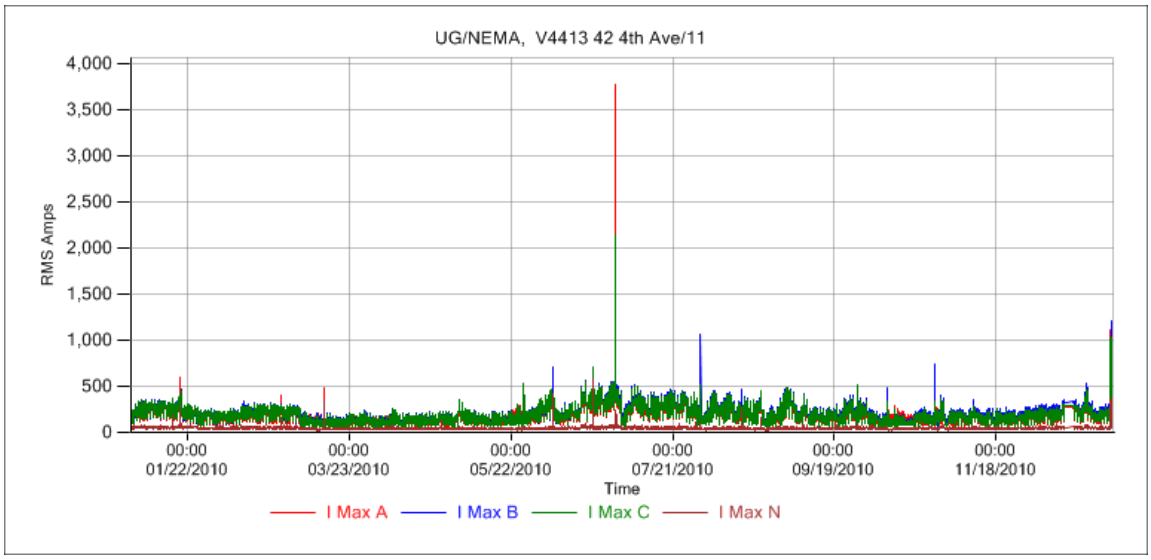

Figure 17: Maximum RMS current (15 minute interval) for one year period, V4413

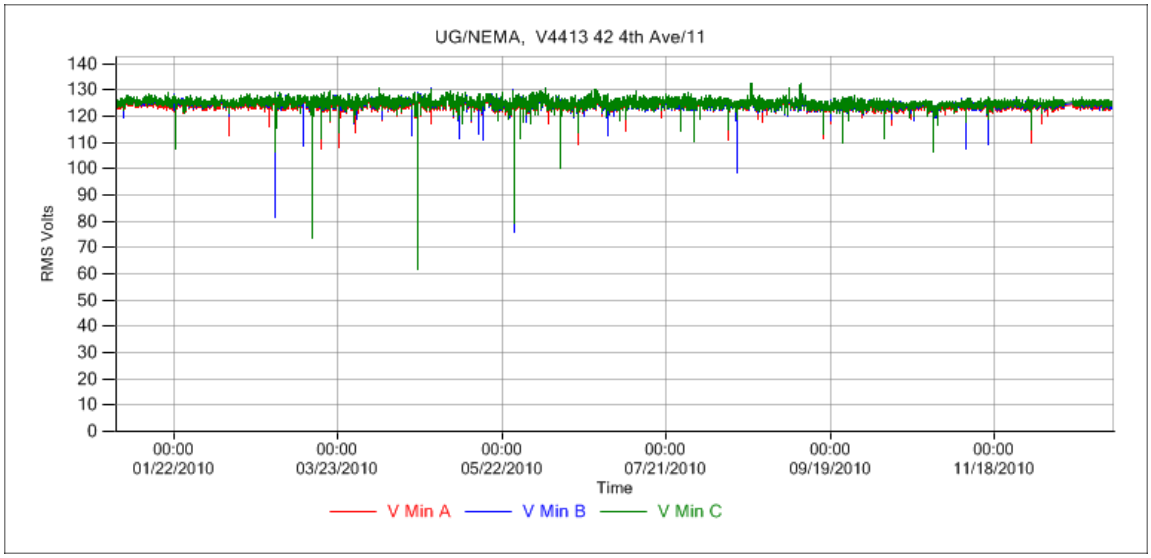

Figure 18: Minimum RMS voltage (15 minute interval) for one year period, V4413

4.4.2 Waveform Files

4.4.2.1 Triggering

The main sources of recorded data in this project are waveform files. Each DCD continually monitors both current and voltage waveforms looking for power system transients. Most transients which occur on a power system are “normal” system events, and not of any special interest. These may include motors starting, capacitors switching, overcurrent faults, and inrush transients. Previous research has shown that incipient arcing faults often produce transients with currents less than or equal to the transients produced by many of these “normal” system events [14]. Because incipient arcing transients are extremely important to this project, devices were set to trigger sensitively, recording relatively small transients. As a result, devices also captured large numbers of normal power system transients, including all of the events mentioned above.

Each underground device served loads primarily in its own geographic area, and as a result each device observed certain local transient conditions not common to other devices. For instance, a motor located in a building proximate to a certain vault would be served primarily by that vault, and might not be seen by a location even a block away. These locally specific transient events required each device’s triggering thresholds to be specifically tuned to capture the maximum number of events of interest, while avoiding large numbers of unnecessary normal events.

Ideal triggering parameters are sensitive to arcing faults, but insensitive to normal system events. Ineffective triggering parameters have no such selectivity. To determine appropriate parameters for use as triggering thresholds, a basic understanding

of the types of signatures typically produced by arcing faults and normal system transients is essential.

In the majority of previous work focusing on arcing faults, arcing was assumed to be phase-to-ground, as any phase-to-phase contact almost immediately resulted in a low-impedance bolted fault. Phase-to-ground events are generally easier to detect than phase-to-phase events, because they produce variations in the neutral current. Normal system transients, by contrast, tend to be three-phase events, and result in little to no change in neutral current. As an example, a three-phase motor might produce several hundred amperes of transient current on each phase, but might produce less than 10 amperes of current on the neutral conductor. By contrast, a small phase-to-ground arcing fault would produce many times this amount of current on the neutral, simply due to its nature as a single-phase event. While any single-phase event would behave in a similar fashion, non-arcing-related single-phase events large enough to be observed at transformer vaults are rare on the secondary network.

As the project progressed, it became clear that many secondary network arcing faults were not phase-to-ground, but rather exhibited phase-to-phase or complex three-phase interactions. These faults might not be detected by focusing exclusively on the neutral channel. Another characteristic of arcing faults is their broad spectrum frequency content. Many normal system transients also produce harmonic content, but in the case of most normal transients, this content tends to be dominated by odd as opposed to even harmonics. Arcing faults, by contrast, produce large harmonic currents in both odd and

even harmonics. Consequently, both the 120Hz and 240Hz bands were targeted as being appropriate parameters for triggering.

Three-phase arcing events were found to be sensitive to both of the parameters mentioned above. Additionally, large three-phase arcing events tended to produce currents sufficiently large enough to affect system voltage. The architecture of a secondary network results in an extremely stiff voltage, meaning that very large changes in current are required to significantly affect the voltage observed remotely from the fault point. In practice on the network, an event of several thousand amperes was required to change the local voltage magnitude by more than 2%. In some cases, major three-phase events were observed to produce voltage sags to 90% of nominal, though this was a rare occurrence.

As discussed above, each location exhibited a unique signature of transients based on the loads in its geographical area. Each location therefore needed thresholds tuned to the particular loads in its area. Four parameters were primarily used for triggering thresholds: 120Hz magnitude, 240Hz magnitude, the RMS of a point-by-point cycle difference, and a percentage change in RMS voltage. The harmonic components are calculated from an FFT performed over a 2-cycle window, and represent the magnitude of energy at that harmonic value. The RMS of the difference of two cycles is calculated as a “simple” difference, where each cycle is subtracted from the preceding cycle on a point-by-point basis, and the RMS calculated from the resulting signal. Each of these parameters is reasonably decoupled from absolute system load conditions. In the case of harmonic currents, even harmonics are not generally sustained on a normal

power system for any length of time. As an example, a location with over 1,000 amperes of RMS load current would generally contain less than 5 amperes at the second harmonic (120Hz), as shown in Figure 19 and Figure 20. These figures contain interval data from a selected unit for a one week period.

Figure 19 shows the average RMS currents measured at V9326 over a one week period. These graphs are derived from the interval data stored by each DCD as discussed in Section 4.4.1. Each day begins with a relatively low load in the night, rising sharply in the morning, and peaking in the early afternoon before returning to nighttime levels. The two days with significantly lower peaks represent a weekend period, while the five days with highest peaks represent weekdays. Figure 20 shows the average 120Hz components of current measured at 15 minute intervals during this same time period. While the same diurnal cycle can be seen, the absolute current level is much lower, with an absolute peak of 3.5 amperes, compared to a total-load peak of over 1,300 amperes. Finally, Figure 21 shows the maximum value of 120Hz current recorded at each 15 minute interval over the same one week period of time. In this graph, clear peaks indicate transient activity. Another important feature of this graph can be observed in a transition of “steady state” maximum values during the day on May 12. This transition was caused by a load shift within the network, which is typical in the event of a primary feeder being removed from service, or restoration of a primary feeder which had previously been out of service.

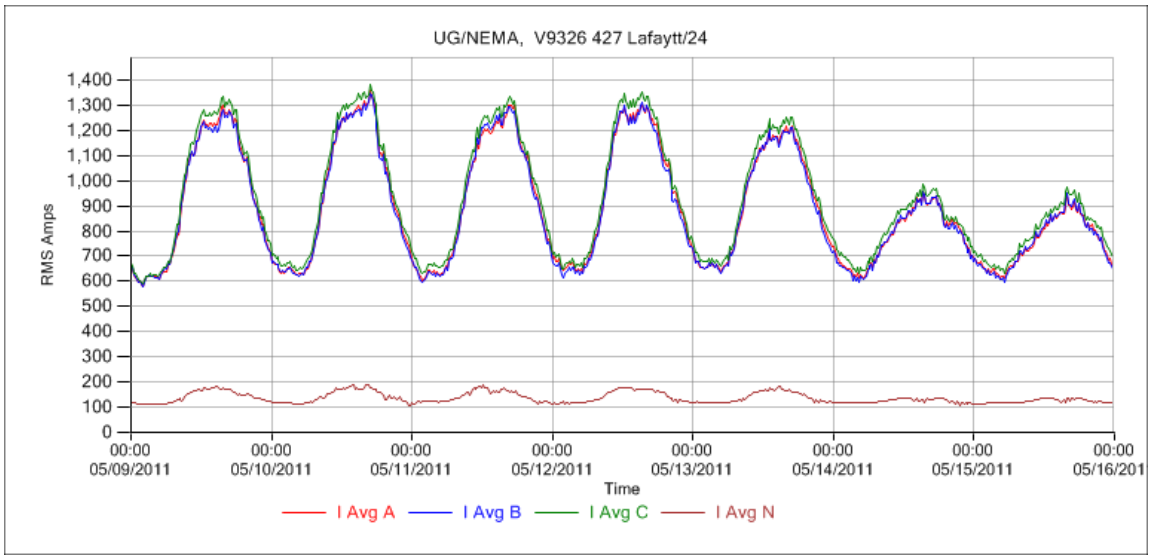

Figure 19: Average RMS currents (15 minute interval) over one week period, V9326

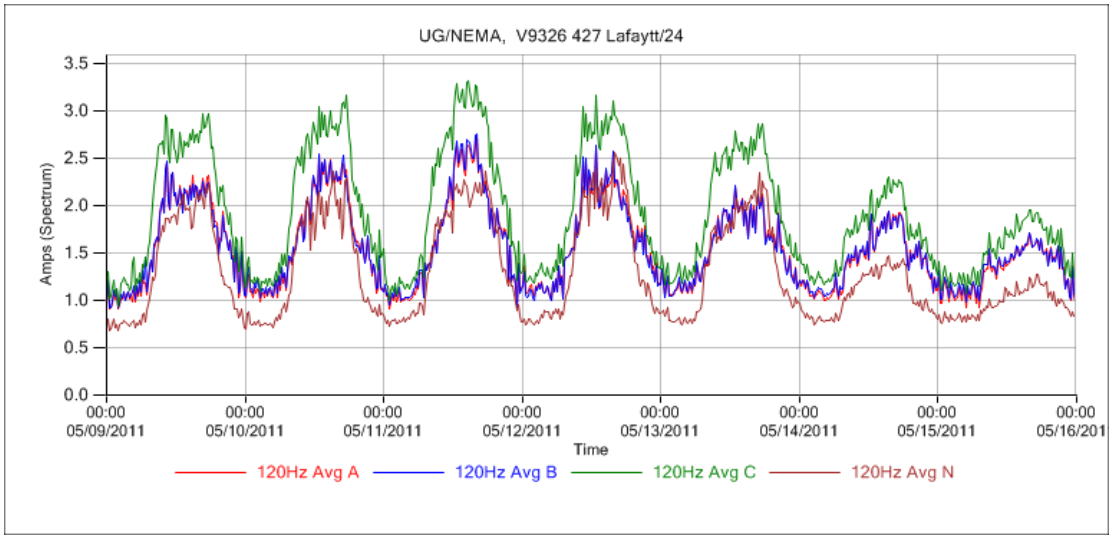

Figure 20: Average 120Hz component of current (15 minute interval) over one week period, V9326

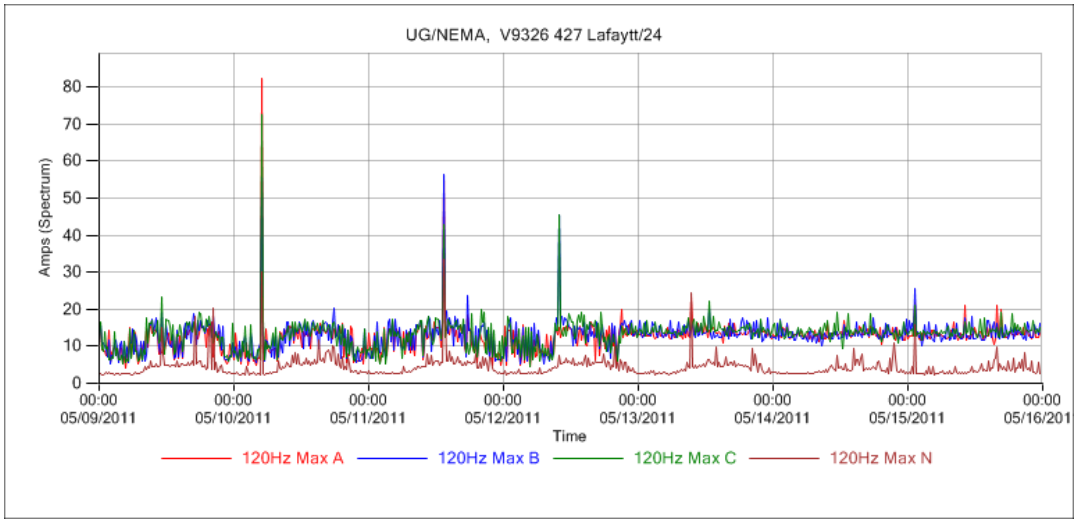

Figure 21: Maximum 120Hz component of current (15 minute interval) over one week period, V9326

The third parameter used for triggering is the RMS of a cycle-to-cycle "simple" difference, where each cycle is subtracted from the previous cycle on a point-by-point basis. This parameter is a measure of cycle-to-cycle variability typically produced by transient events. Figure 22 shows the average value of this parameter as measured during each 15 minute interval over the same one week period used in the examples of harmonic current. Figure 23 shows the maximum value of this parameter as measured over the same time intervals and time period. As shown in Figure 22, there is a more or less constant level of average transient activity loosely correlated to system load. When viewing the maximum transient observed in a given interval, as in Figure 23, clear "spikes" corresponding to major transient events are visible. In particular, the neutral current clearly shows activity indicative of single-phase transient events.

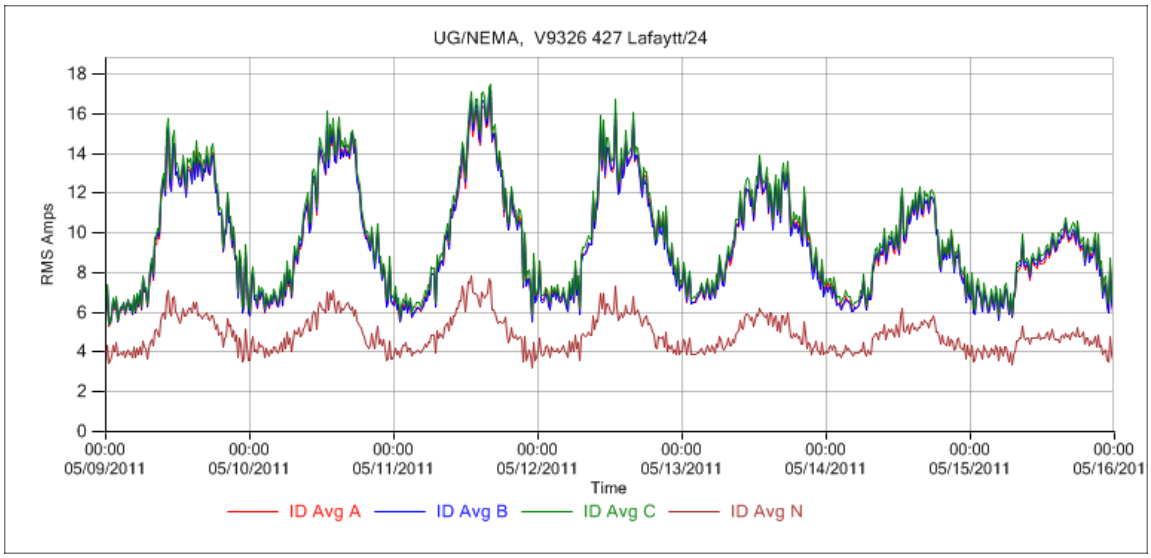

Figure 22: Average RMS "differenced" current (15 minute interval) over one week period, V9326

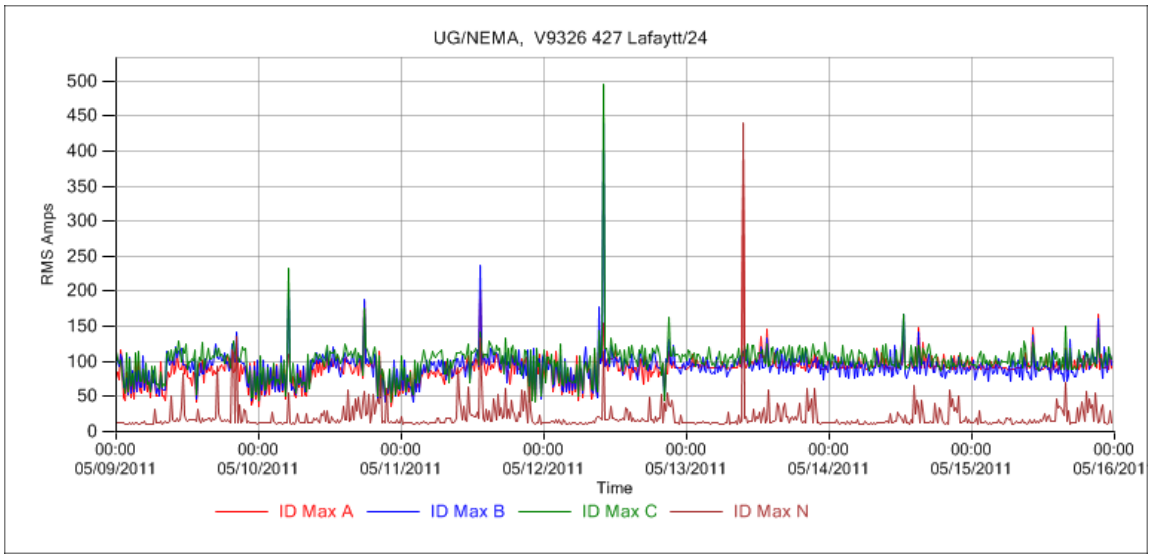

Figure 23: Maximum RMS "differenced" current (15 minute interval) over one week period, V9326

The physical locations of these DCDs are shown in Figure 24. As previously mentioned, each device has its own unique fingerprint associated with loads served in its local geographic area. By way of comparison, Figure 25-Figure 29 are provided from the closest DCD to V9326, which is V9116. Even though these devices are less than an electrical block from each other, the transient currents seen by each device differ significantly.

Figure 24: Locations of V9326 and V9116

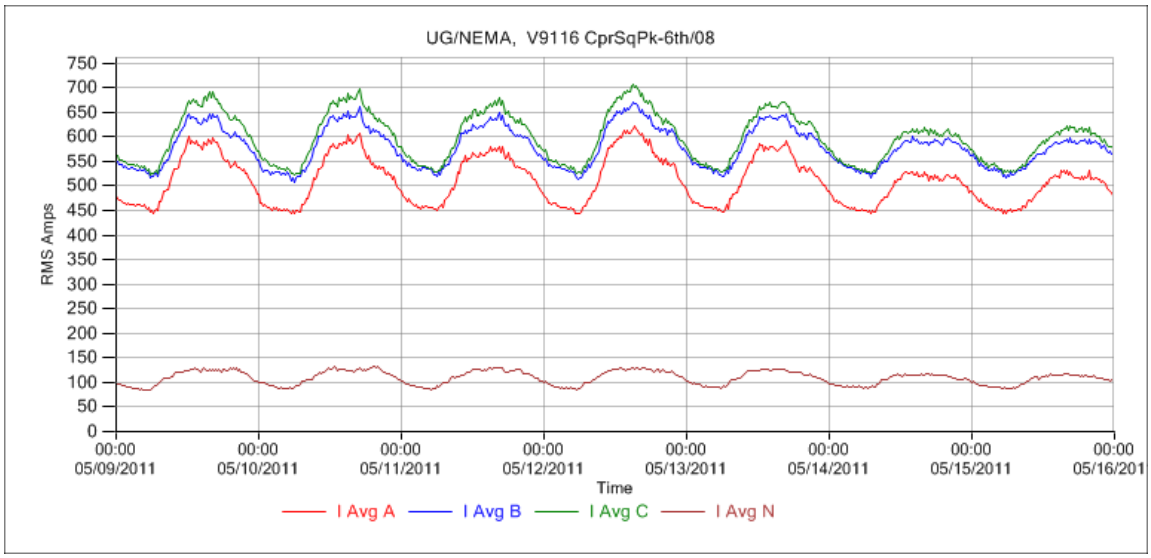

Figure 25: Average RMS currents (15 minute interval) over one week period, V9116

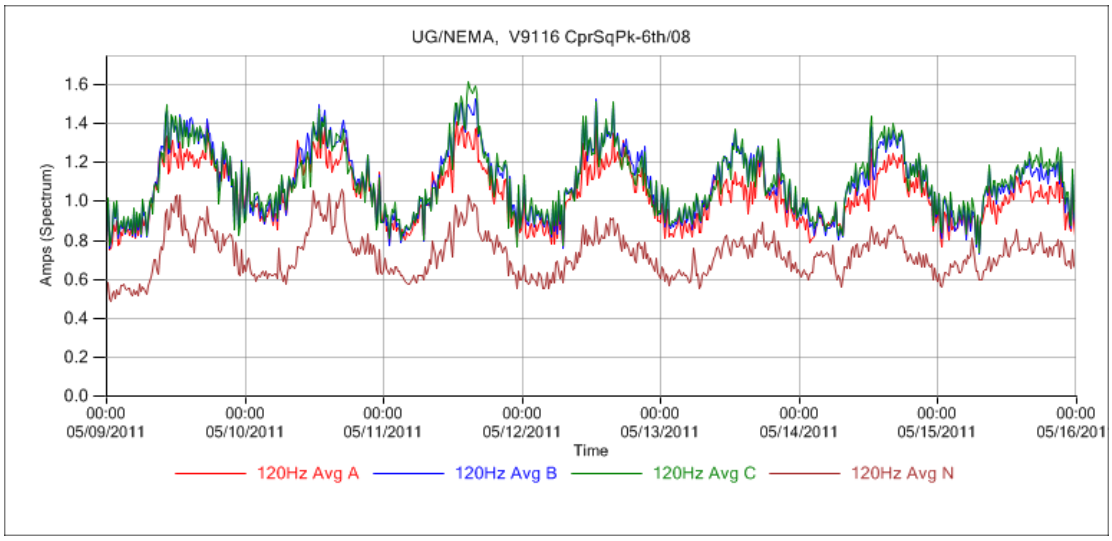

Figure 26: Average 120Hz component of current (15 minute interval) over one week period, V9116

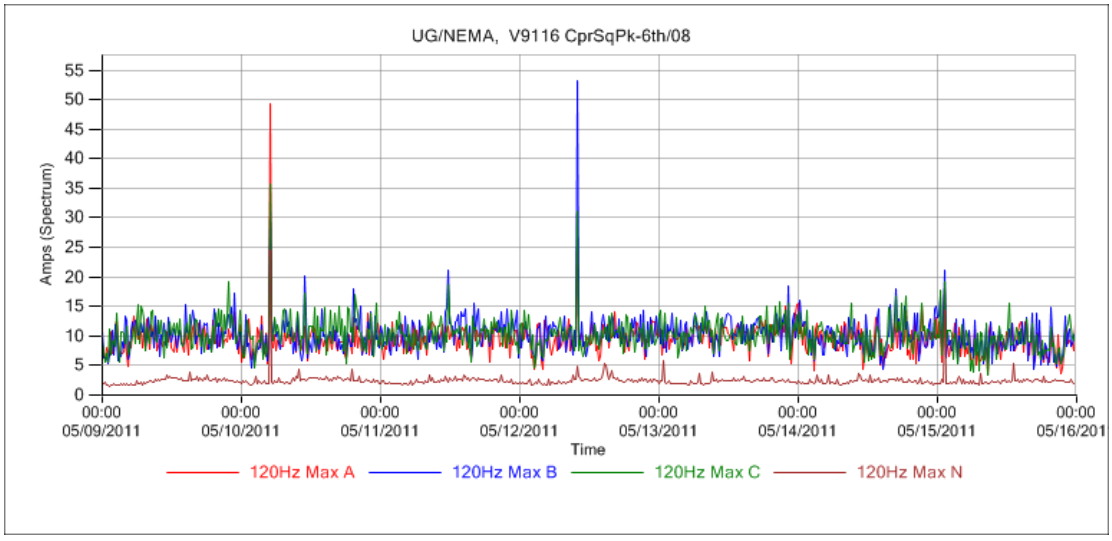

Figure 27: Maximum 120Hz component of current (15 minute interval) over one week period, V9116

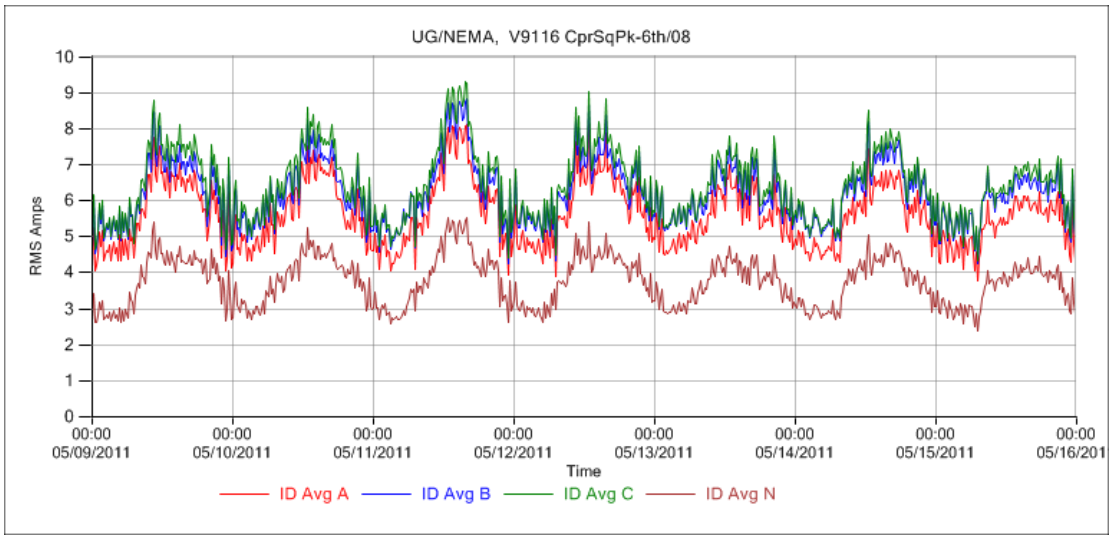

Figure 28: Average RMS "differenced" current (15 minute interval) over one week period, V9116

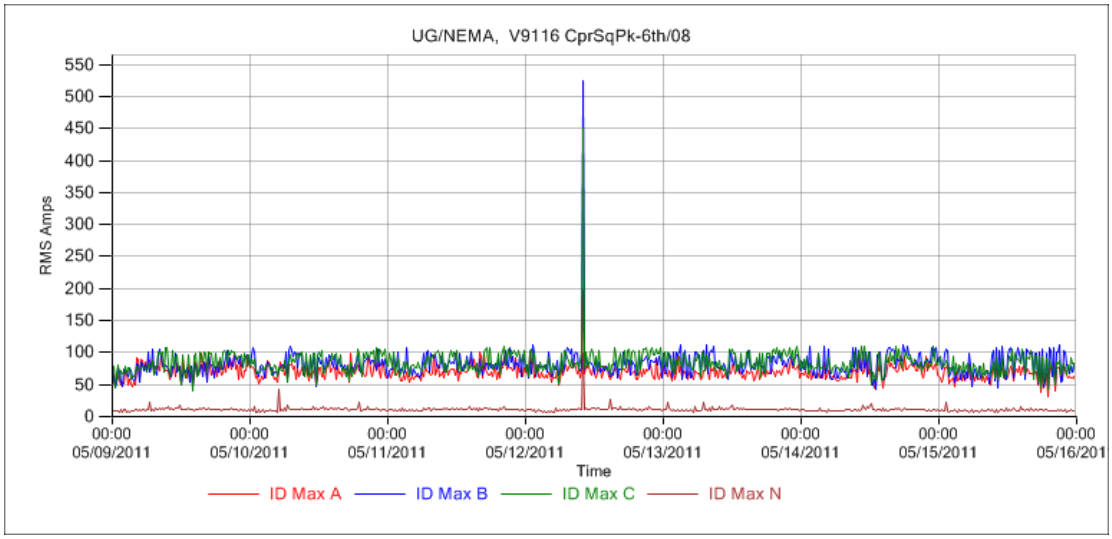

Figure 29: Maximum RMS "differenced" current (15 minute interval) over one week period, V9116

One inherent drawback to the secondary network architecture is that certain monitored locations are significantly less sensitive than other locations, depending on loads in the immediate geographic area. Figure 30-Figure 34 contain the same series of graphs at a location with a very large local load, which has a startup transient shown in Figure 35. If Figure 30 is contrasted with Figure 19, the absolute load levels are approximately the same, with daytime peaks of roughly 1,300A. Figure 34 and Figure 23 show a significantly different picture, however. While V9326 has a baseline maximum differenced current of approximately 100 amperes for each phase current, V8442 has a similar baseline of between 350 and 500 amperes, depending on the phase. This effectively means that in any given 15 minute interval, V8442 can expect to see at least one load with a startup transient of between 350 and 500 amperes. Thus, the RMS difference parameter cannot be set close to this value without resulting in an excessive number of captures. The end result is that events which would be easily detectible at V9326 are undetectable at V8442 because of the higher transient baseline.

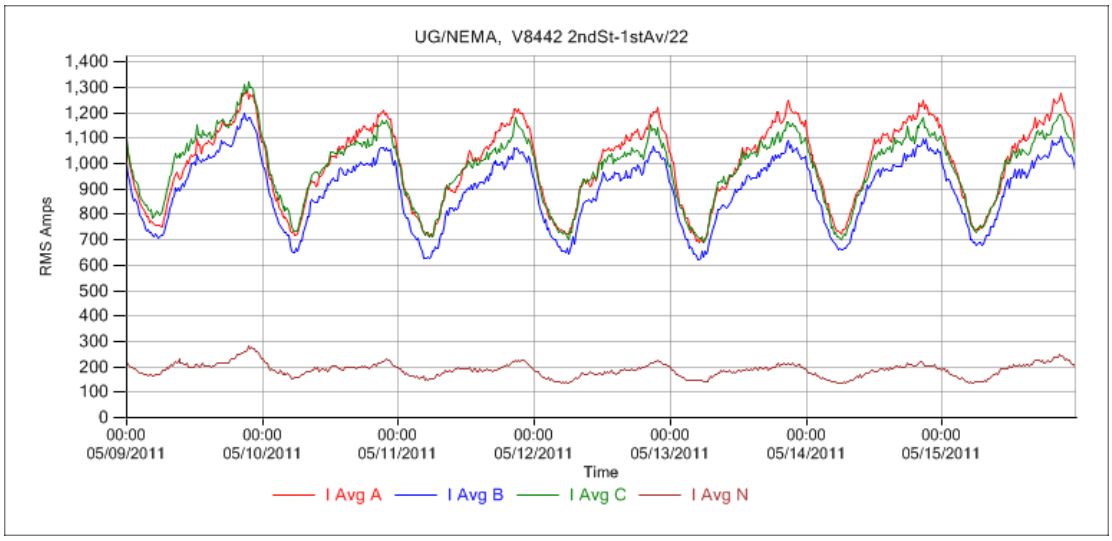

Figure 30: Average RMS currents (15 minute interval) over one week period, V8442

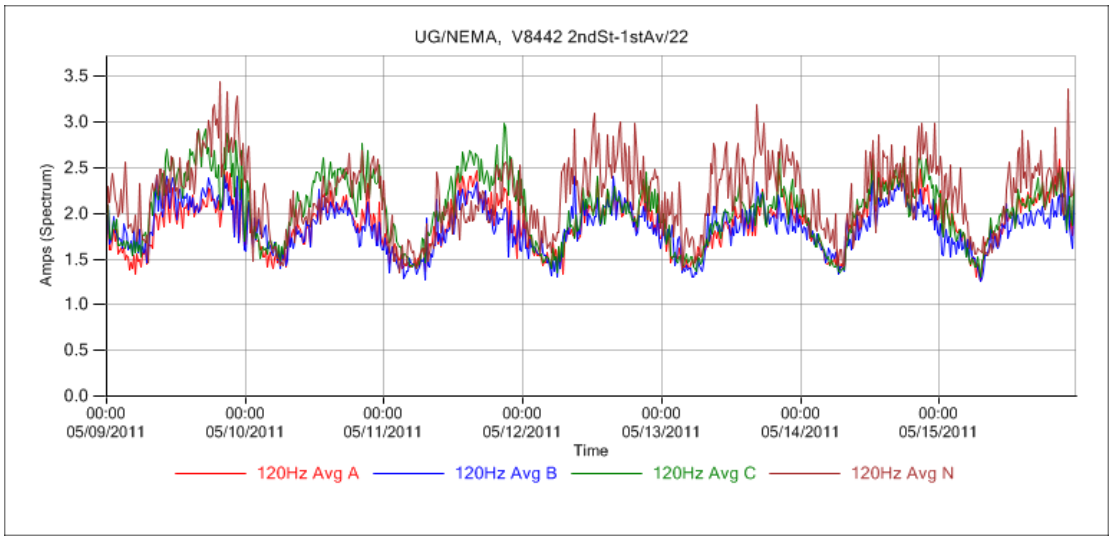

Figure 31: Average 120Hz component of current (15 minute interval) over one week period, V8442

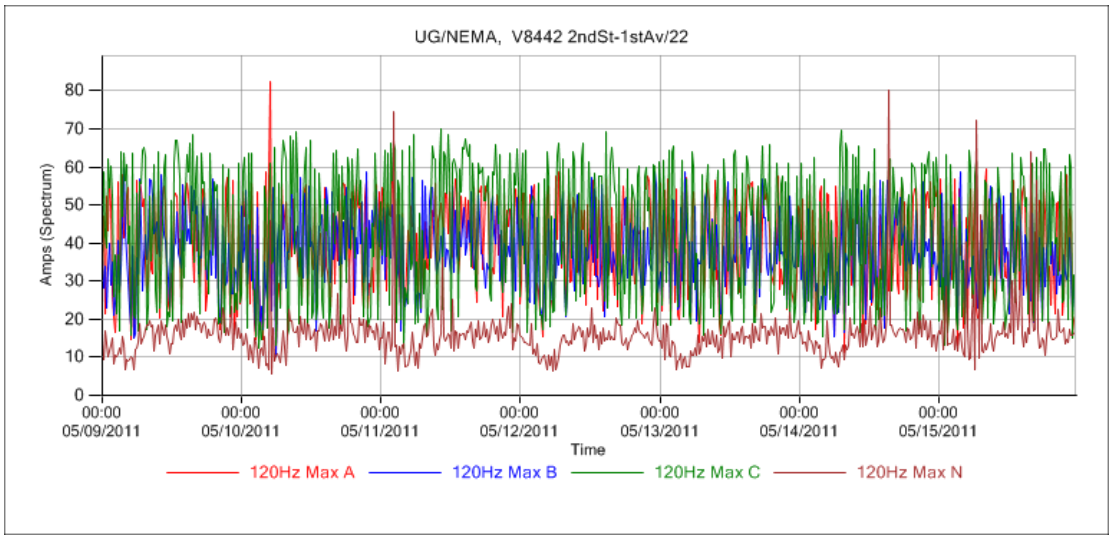

Figure 32: Maximum 120Hz component of current (15 minute interval) over one week period, V8442

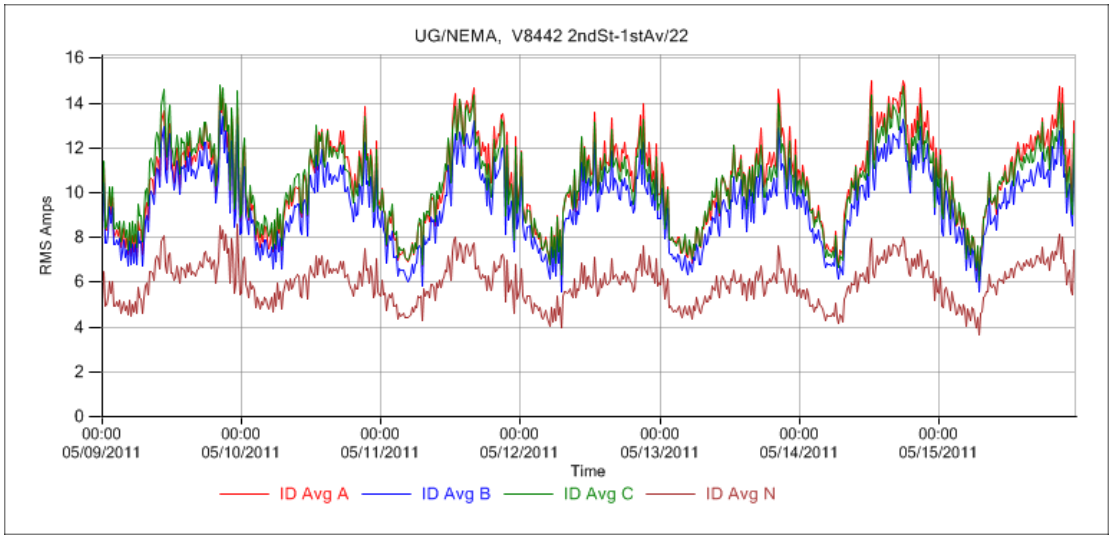

Figure 33: Average RMS "differenced" current (15 minute interval) over one week period, V8442

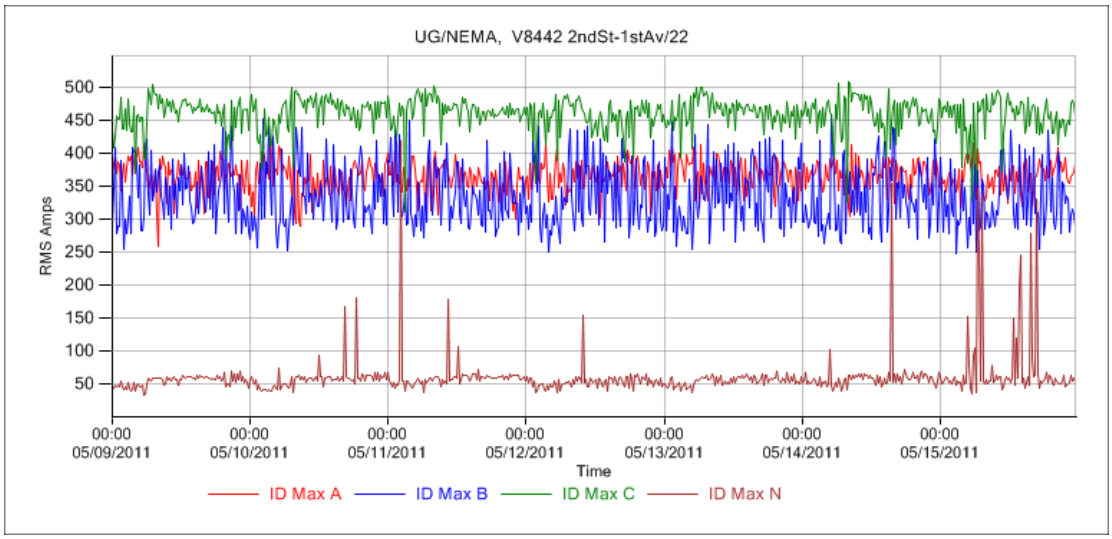

Figure 34: Maximum RMS "differenced" current (15 minute interval) over one week period, V8442

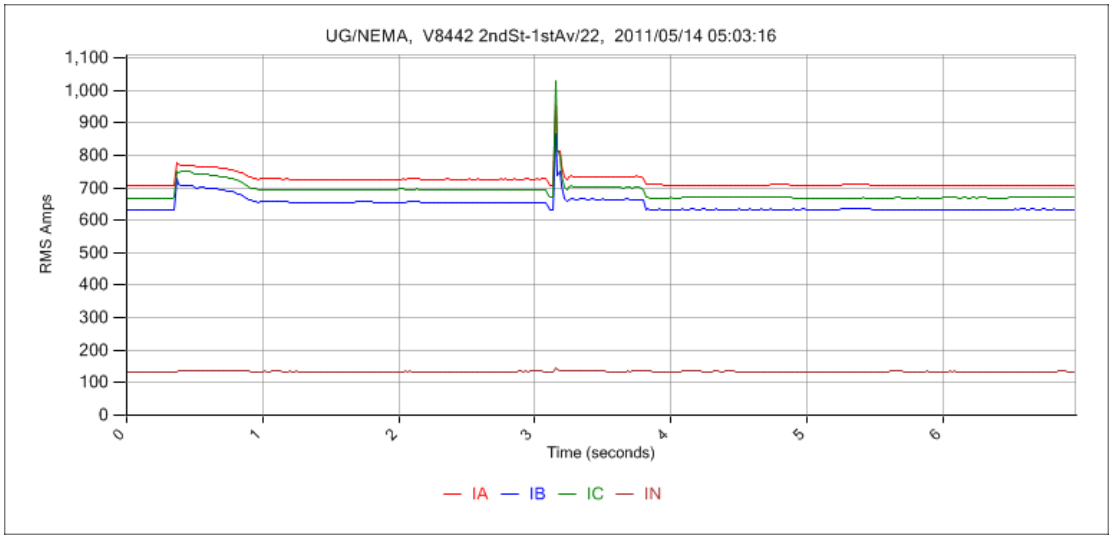

Figure 35: RMS currents from a large motor start, V8442

4.4.2.2 Contents of recorded waveform files

Information written into the permanent recorded waveform files is configurable. At first, DCDs in this experiment were configured to record all available channels. This included the fifteen high-speed channels in Table 4, as well as all harmonic and other calculated parameters.

Previous projects using DFA hardware were served by communication systems which offered high data bandwidth and unmetered data limits, making waveform file size a secondary concern. The cell modems used in this project were both considerably slower than systems used in other projects, and were programmed to shut off for the remainder of the calendar month once a 5GB data limit was reached. Complicating this situation was the discovery that network arcing faults could generate tremendous amounts of data in short periods of time, something not previously observed in other projects. The largest data cards, used in 26 of the 30 DCDs, were capable of holding one hour and eighteen minutes of data with all channels stored.

Decreasing the number of bytes in each file for a given period of recorded data would reduce the number of bytes transferred back to the master station, thereby effectively increasing transfer rates. Reduction in the data rate would also effectively increase the length of captured waveform data that could be stored locally on the DCD. To accomplish this, multiple channels were eliminated from stored waveform files, generally under the justification that they could later be recreated digitally if necessary.

Since high-speed channels consumed the most data within a file, elimination of these channels, where possible, was given top priority. Because the maximum current

that could be reasonably measured by the “normal” range currents was approximately 4,200A RMS, it was judged that the “fault” range channels were necessary to properly characterize large events. The neutral for the fault range, however, is calculated from the three individual phases, rather than being sampled separately. As a result, it could be eliminated and recreated from the three-phase channels.

A similar evaluation was performed with the high-frequency channels. After capturing initial test data, it became clear that arcing was easily detectable without using the high frequency channels. Additionally, the channels themselves were derived from the application of a digital high-pass filter to the normal range currents, and could be recreated after the fact. However, it was judged that unless there were some way to easily determine whether useful information might exist in the high frequency channels, it was unlikely they would ever be recreated, even if the procedure were possible. To preserve some of the high frequency information, the neutral high-frequency channel was retained, while the phase high-frequency channels were eliminated.

While calculated quantities did not consume as many bytes per channel as the high-speed waveform data, eliminating unnecessary channels was still beneficial. By default, each individual harmonic component up to 960Hz was stored in the capture file every two cycles. Because most of the harmonic energy is contained in the first few harmonics, analysis was performed on initial data to determine whether any additional value was gained by retaining higher order harmonics. It was determined that, in general, the magnitudes of harmonics above 330Hz did not offer enough value to keep them in the capture file, given that all harmonics could be recreated on demand if necessary.

Additionally, previous research on the DFA project has suggested that calculated RMS power values (P, Q, S, PF) are of questionable validity during transient conditions, particularly compared to values calculated from quantities derived from the 60Hz components of currents and voltages. As a result, all RMS power quantities were removed.

The resultant waveform files were approximately 73% of the size of waveform files containing all signals. This increased the amount of waveform data which could be recorded on disk to approximately one hour and forty-seven minutes.

4.4.3 Summary

The triggering and data management procedures described have been very effective in creating a competent database of recorded network arcing faults for investigation. This database will be of significant value to future researchers.

5. EXPERIMENTAL RESULTS

Over a period of two years, DCDs installed on ConEdison's Cooper Square network monitored and recorded transient events. From the installation of the first units in March 2009 through the end of March 2011, DCDs recorded over 145,000 unique waveform transients, comprising over 205 hours of recorded waveform data. Approximately 43,500 of the waveform files contained distinct arcing signatures. Additionally, approximately 3,500 of the transients were tied to 42 separate manhole events reported to ConEdison by conventional means.

Information obtained from captured waveform files was groundbreaking, and provided a unique opportunity to characterize and document the behavior of naturally occurring arcing faults. It would be difficult to summarize and discuss all the lessons learned from the study of data recorded during this project. Addressing my specific research goals for this dissertation and the most important findings, the following can be said:

- Waveform data from this project contain what are believed to be the first high-fidelity, full duration recordings of naturally occurring arcing faults on a 120/208V secondary network simultaneously seen at multiple locations. Appendix A presents a case study of an event recorded simultaneously at two underground monitoring points which led to a manhole event.

- Recorded waveform transients demonstrate that arcing events can exist for long periods of time, many times on the order of hours, without self-extinguishing. The project recorded multiple instances where arcing faults persisted on an almost continual basis for hours before crews located the fault and cut cables, or the fault eventually burned clear. The most dramatic instance of this behavior is detailed in Appendix B, where a network arcing fault continued intermittently for approximately 72 hours without causing a conventional report of a manhole event. During the 72 hour period, over 2,000 unique waveform records with distinct arcing transients were observed and recorded, with many of the waveform records containing multiple arcing transients.
- Project data are also believed to contain the first ever observations of naturally occurring arcing faults located on a secondary network that were simultaneously recorded on both the network itself, and on a primary feeder serving transformers proximate to the faulted location. Appendix C presents a case study involving measurements of the same network arcing fault simultaneously sampled at three underground monitors and a primary feeder serving other transformers in the geographic area of the faulted location. This particular event began over a seven hour period where arcing was persistently, but intermittently observed at two underground locations and the primary feeder. Following the initial seven hour period, no arcing was observed for the next fifteen-

hours. Twenty-two hours after the initial arcing observation, the two original underground monitors, a third underground monitor, and the substation-based DCD recorded arcing on a near-continuous basis over the next four-hours. This electrical activity resulted in two manhole fires.

- Recordings from multiple events have demonstrated that arcing faults can recur persistently for extended periods of time before progressing to final failure or generating enough physical evidence to be observed by the public. Appendix D presents a case study of an event which was observed over a period of eighteen days before being located and repaired by a utility crew.
- Finally, several recordings exist where the same arcing fault was observed by multiple underground monitors, providing new insight into fault current distributions on secondary networks. In particular, Appendix E details a pioneering event where measurements from five underground monitoring points were used to accurately determine the location of an arcing fault which lay dormant for four months.

These case studies represent only a small fraction of data observed, recorded, and analyzed over the course of this project. For each of the case studies presented here, additional examples exist which serve to confirm the general findings outlined above.

6. DATA ANALYSIS

6.1 Load Extraction Via Signal Processing

Measurement of transient events on operational systems occurs in the presence of nominal load current. Often, the magnitude of the load current during the transient condition far exceeds the magnitude of the transient event itself. Even if the transient magnitude is large compared to the load, adequately characterizing the event is complicated by the presence of load current. As a result, a critical component of analysis related to transient conditions in general and arcing faults in particular is the development of a method to estimate pre-event load current so it can be removed from the measured signal, with the resulting signal being as good an estimate as possible of the event current alone.

In general, transient currents and load currents have different phase angles and harmonic contents, and as a result a simple cycle-by-cycle subtraction is not a good estimate of fault current. In previous research conducted at Texas A&M's Power System Automation Laboratory, advanced digital signal processing techniques have been developed to account for these variations and produce a low-noise estimate of event current during transient conditions. This process is internally known as "phasor differencing," and was used extensively in this project.

Figure 36-Figure 39 illustrate the importance of such load removal algorithms. Figure 36 shows a six-second period of high-speed waveforms recorded during the course of this research. From this view, it is not immediately obvious that any transient

condition has occurred. Figure 37 shows the same six seconds of data after processing through the phasor differencing routines. From the same zoom level, it is clear that a half-cycle arc burst with magnitude of approximately 300 amperes has occurred at approximately 3.5 seconds in this waveform capture.

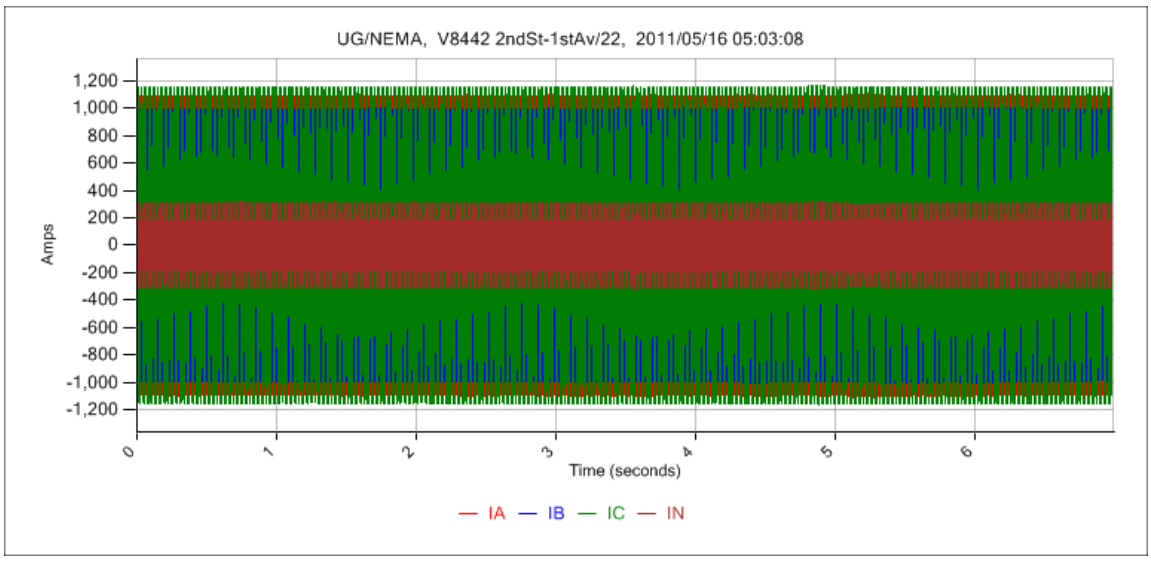

Figure 36: Six-second waveform capture containing single half-cycle arc burst, unprocessed current waveforms

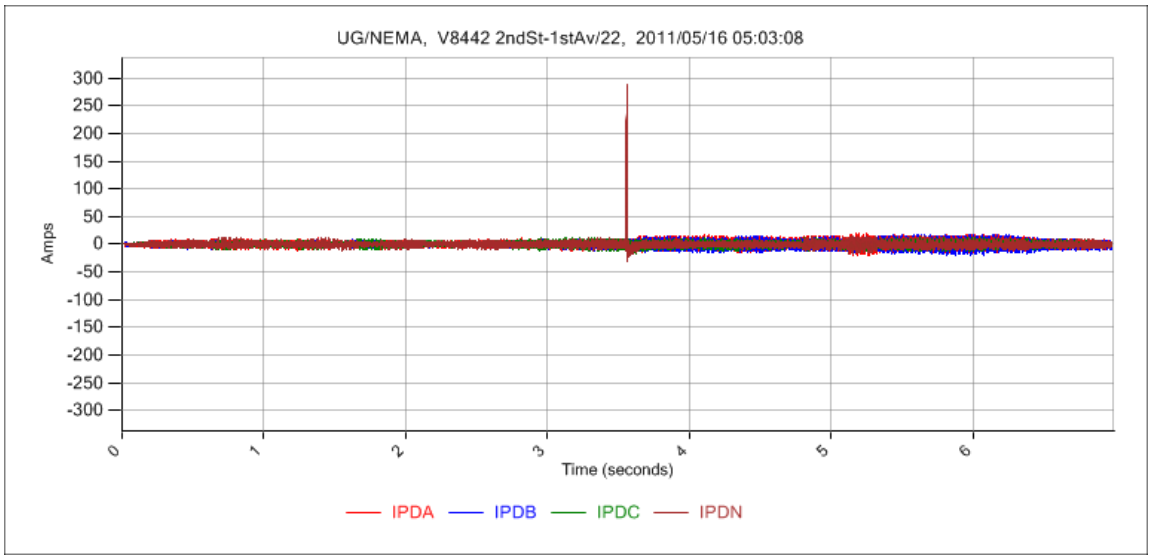

Figure 37: Six-second waveform capture containing single half-cycle arc burst, phasor differenced currents

Figure 38 shows a portion of the same data zoomed to show the faulted section of the waveform recording in greater detail. The fault is visible upon close inspection as a slightly distorted peak on Phase C between 3.560 and 3.565 seconds. While this current peak is clearly different from those around it, a detailed analysis of differences in characteristics between the peaks is not readily accessible. By contrast, Figure 39 shows the same period of data after processing through the phasor differencing algorithms. In this graph, the nature of the transient condition can be clearly identified and studied.

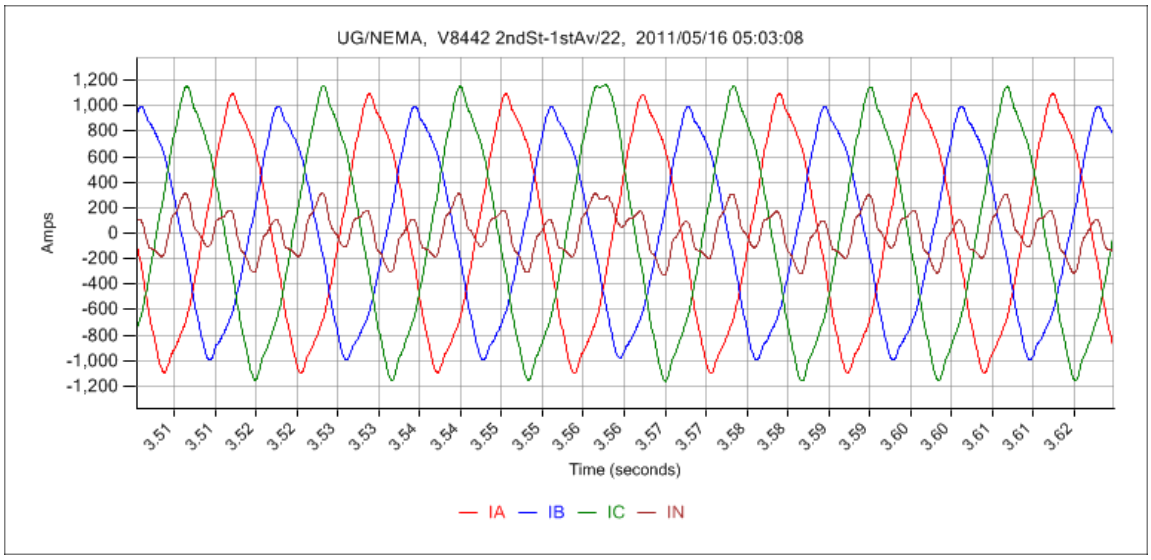

Figure 38: Half-cycle arc burst, unprocessed current waveforms

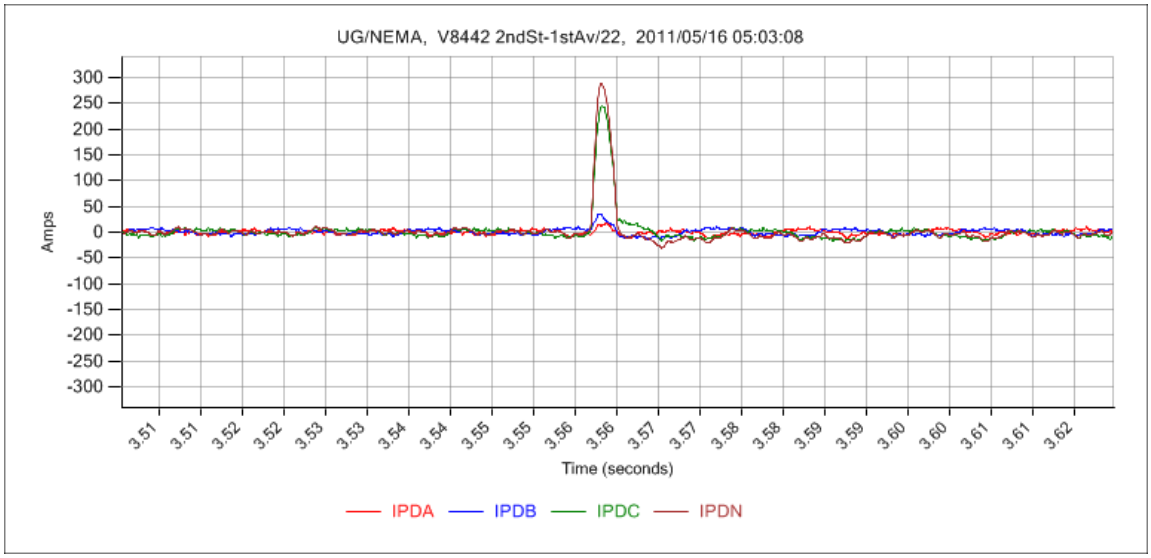

Figure 39: Half-cycle arc burst, phasor differenced current waveforms

While the case presented above shows a relatively short, low magnitude transient, even cases with larger magnitudes and longer durations are difficult to adequately characterize without load current removed, as shown in Figure 40 and Figure 41. While Figure 40 contains clear transient activity, it is unclear exactly what is happening on a subcycle basis without the removal of the pre-event load. Figure 41, by contrast, shows the interaction between all phases much more clearly.

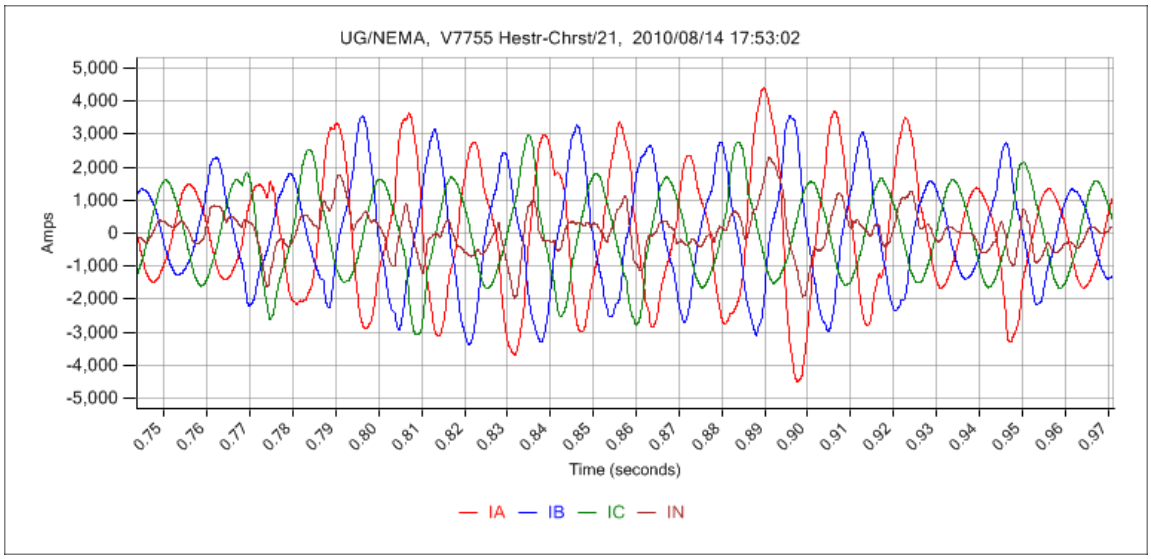

Figure 40: Multi-cycle three-phase arc fault, unprocessed current waveforms

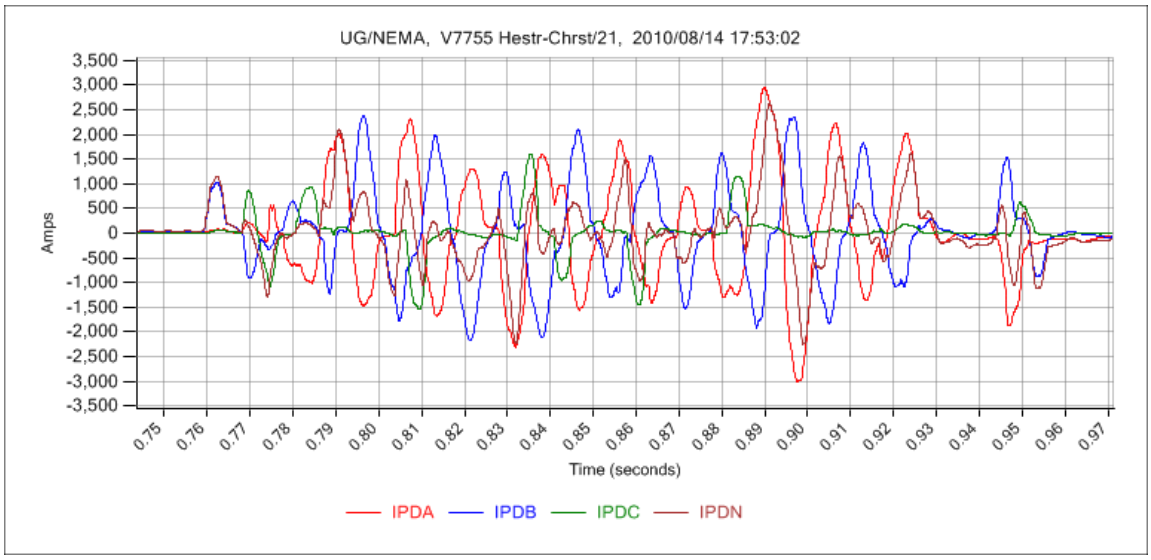

Figure 41: Multi-cycle three-phase arcing fault, phasor differenced current waveforms

6.2 Typical Arcing Fault Waveforms

6.2.1 Single-phase Arcing Events

Single-phase arcing events represent the majority of arcing transients on 120/208V secondary networks. It is not inaccurate to say that sporadic, half cycle, single-phase arc bursts similar to those in Figure 38 and Figure 39 occur multiple times daily on the secondary network regardless of weather conditions.

Bursts which persist for longer periods of time, however, exhibit general characteristics predicted by mathematical arcing fault models and resembling arcing fault waveforms observed on medium voltage class systems[10, 11, 83]. Figure 42 and Figure 43 show typical behavior during an extended arc burst period for a single-phase

arc. Figure 44 shows similar behavior on a medium voltage 12kV class system, recorded as part of Texas A&M's ongoing DFA project on distribution feeders.

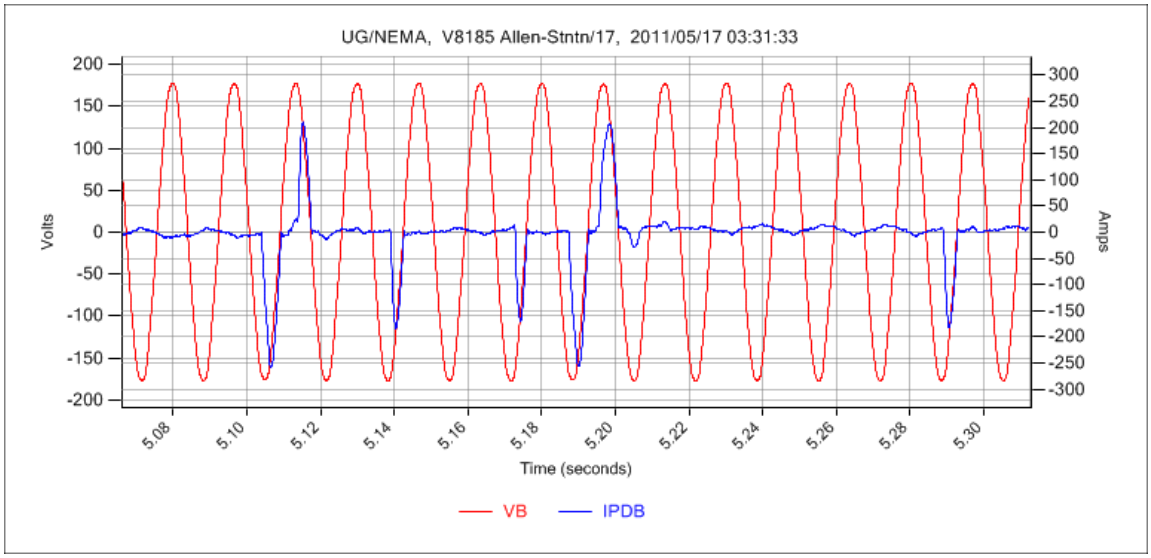

Figure 42: Multi-cycle single-phase arc burst, voltage and differenced current waveforms

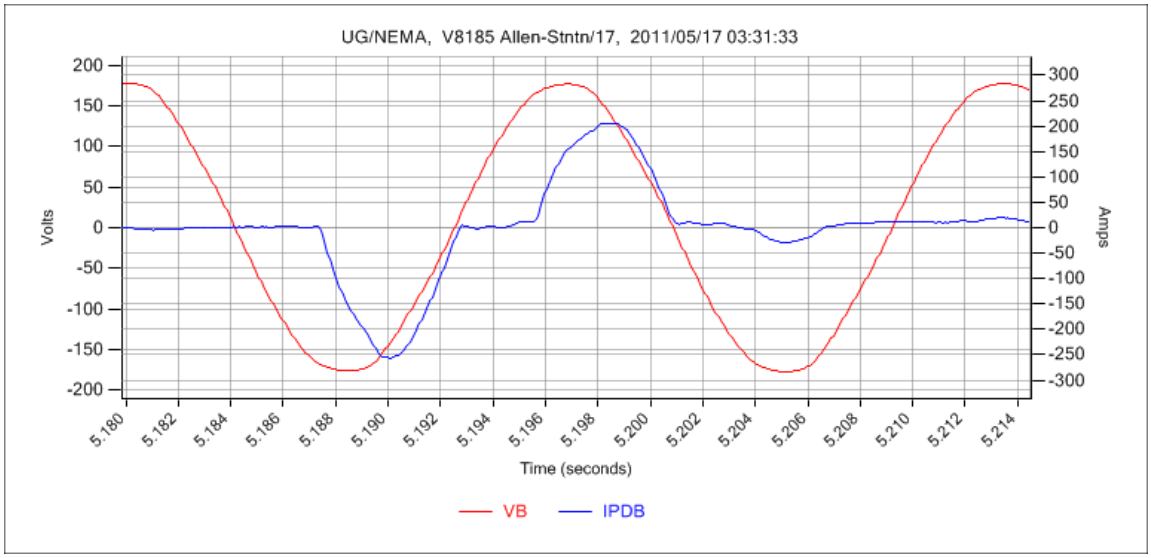

Figure 43: Full-cycle single-phase arc burst, voltage and differenced current waveforms

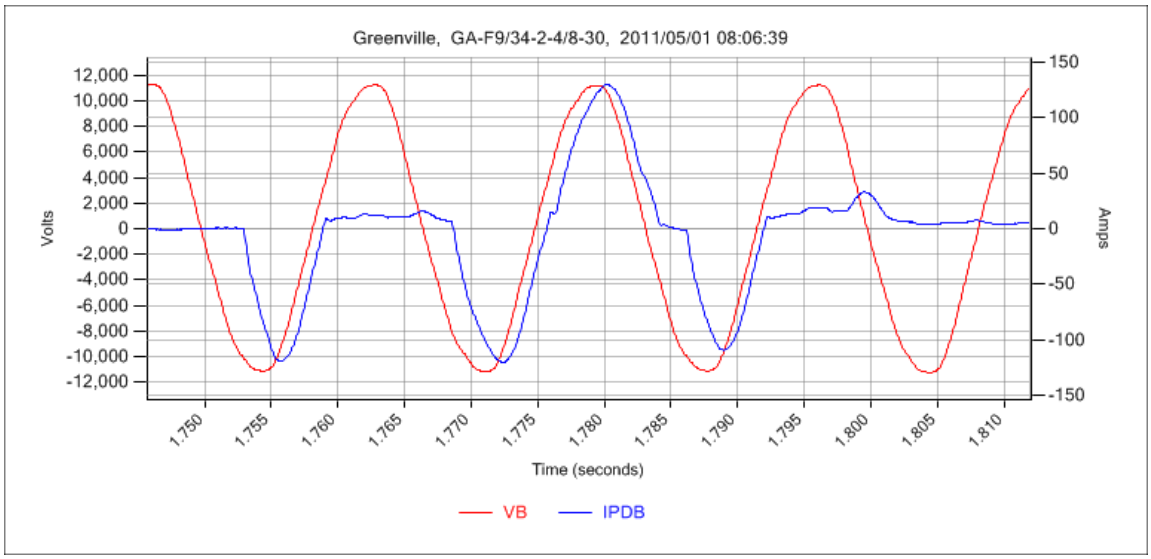

Figure 44: 1.5 cycle medium-voltage single-phase arc burst, voltage and differenced current waveforms

6.2.2 Phase-to-phase Arcing Events

As previously discussed, phase-to-phase arcing events are considered unusual on higher voltage class systems. As a result, very few recordings exist of phase-to-phase arcing. Figure 45 shows a typical phase-to-phase arcing burst observed during the course of this research. Figure 46 and Figure 47 show each individual faulted phase along with its phase voltage. As can be seen in both individual phase plots, the arcing fault currents in a phase-to-phase arcing fault maintain some characteristics of single-phase arcing, but the previously straightforward relationship between voltage and current no longer holds. In contrast, the arcing current in this example is driven by the difference in phase voltages, rather than the individual voltages themselves. Current waveforms do still exhibit significant nonlinearities, and clearly contain significant harmonic and non-harmonic components. Events of this type are, in general, the simplest recorded phase-to-phase cases.

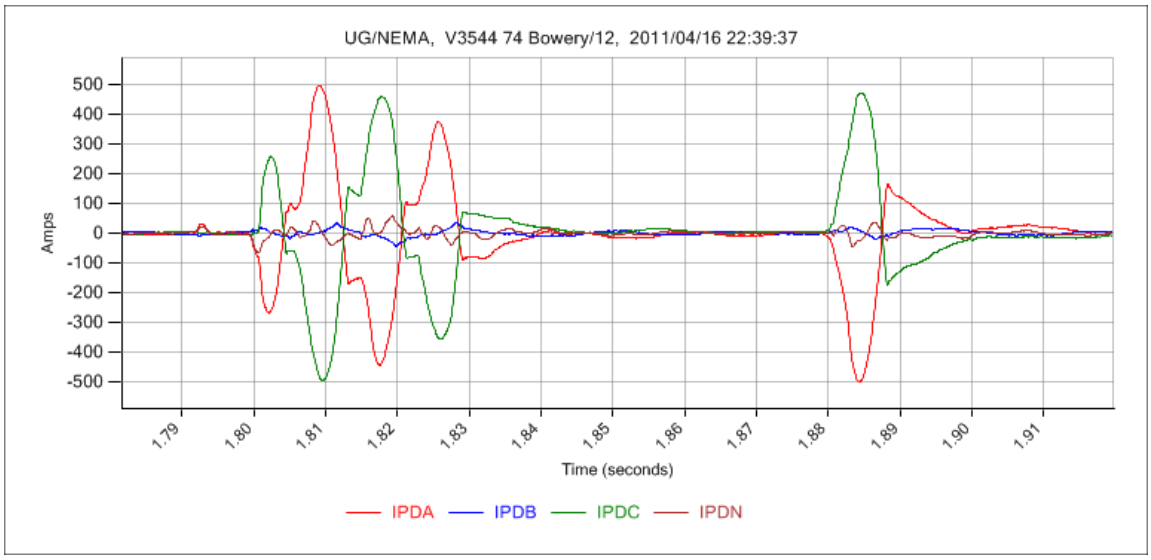

Figure 45: Phase-to-phase arcing fault, phasor difference currents

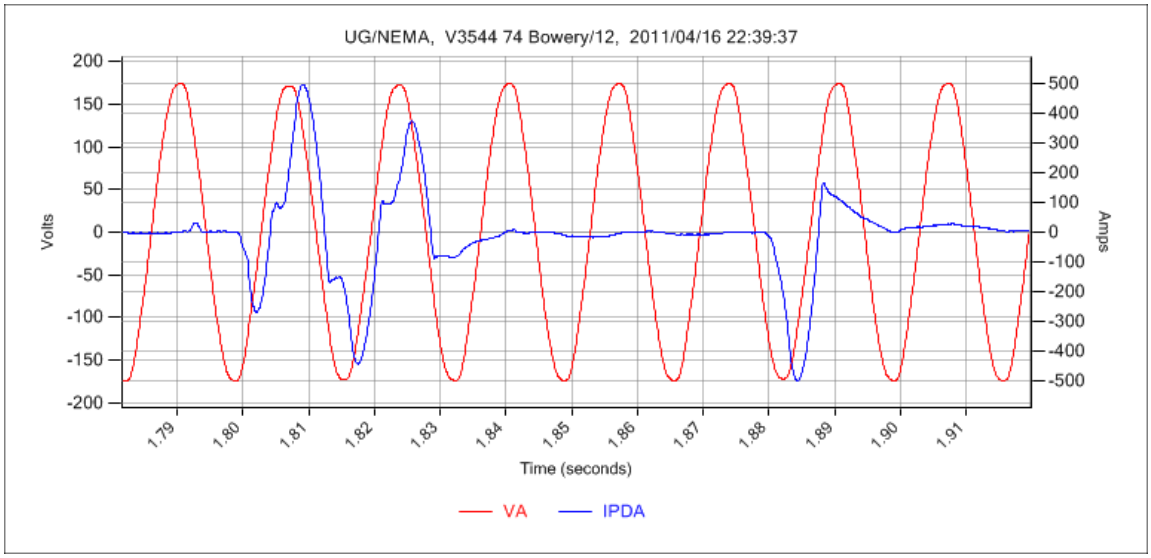

Figure 46: Phase-to-phase arcing fault, voltage and differenced current, Phase A

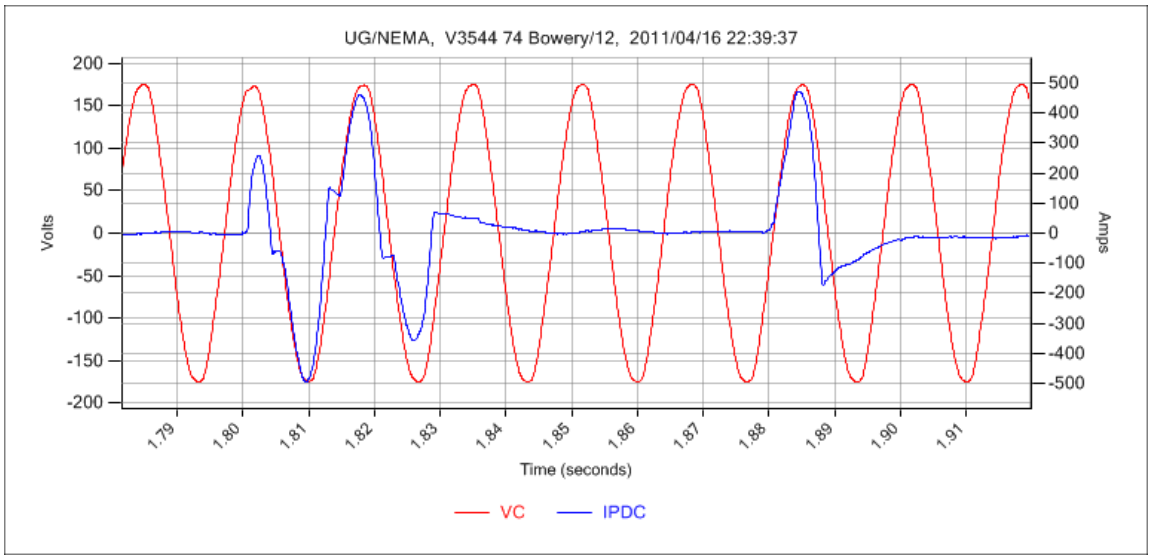

Figure 47: Phase-to-phase arcing fault, voltage and differenced current, Phase C

Figure 48 shows a case which contains phase-to-phase arcing involvement, but also involves system neutral. In practice, any given fault can, and often does, evolve between multiple electrical configurations in a span of cycles to seconds, transitioning between single-phase, phase-to-phase with no neutral involvement, phase-to-phase with neutral involvement, individual phases involved independently with system neutral, and a variety of complicated three-phase interactions.

This fact owes to the highly unstable mechanical conditions generally present at the fault point. Electrical behavior of arcing faults is dominated by the contact impedance at the fault point. Changing mechanical conditions are easily imagined in a conduit with multiple exposed phase cables, each being subjected to strong mechanical forces produced by rapidly changing electric and magnetic fields. Ionized gasses, arc plasma, expelled gaseous metal, the mechanical action of the arc itself, progressive

physical damage, as well as whatever water, mud, sludge, and other conductive media that may exist in the conduit at the fault point, all contribute to this mechanical instability. As a result, developing any kind of model to predict the behavior of an underground arcing fault once it begins is not straightforward.

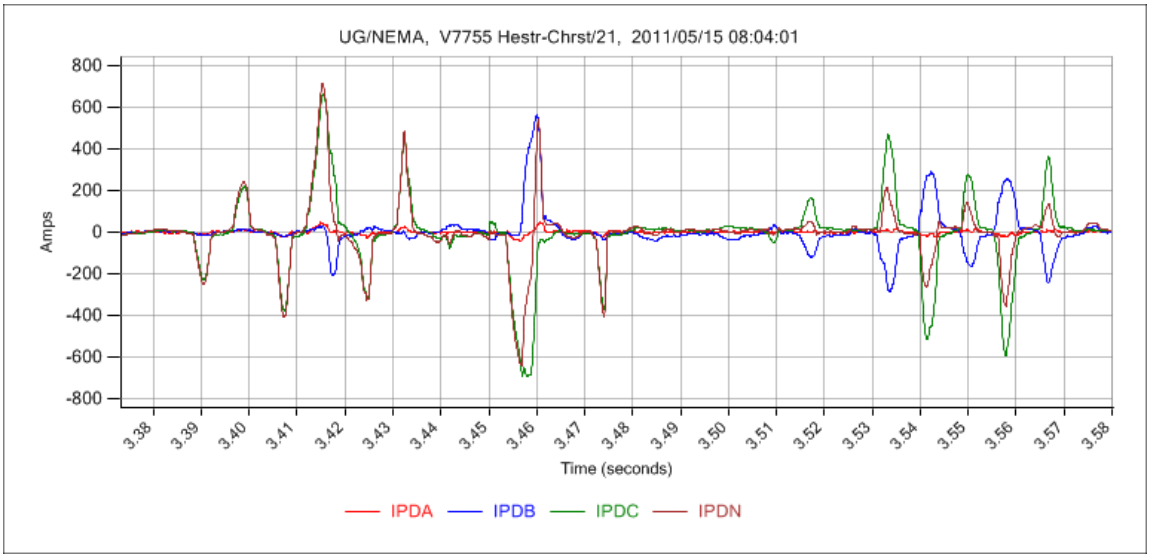

Figure 48: Phase-to-phase fault with ground involvement, differenced currents

6.2.3 Three-phase Arcing Events

As discussed in the previous section, attempting to predict the behavior of arcing faults by modeling is perilous once multiple phases are involved. Arcing where all three-phases are involved within a relatively short temporal window is not uncommon, particularly in the final stages of an event. What is considerably more difficult, however,

is describing exactly which phases are involved with which other phases. This is again caused by the complicated, uncertain, and possibly continually changing conditions at the fault point, and further complicated by induced, sympathetic currents on non-faulted phases. Figure 49 shows a sample of relatively straightforward three-phase interactions. Even in this relatively simple case, phase currents display erratic and unusual behavior as arcing transitions between phases. Figure 50 shows the same data, but with only Phase C plotted. In particular, the "notch" observable between 1.18 and 1.19 seconds is an unusual phenomenon not observed in single-phase or phase-to-phase arcing.

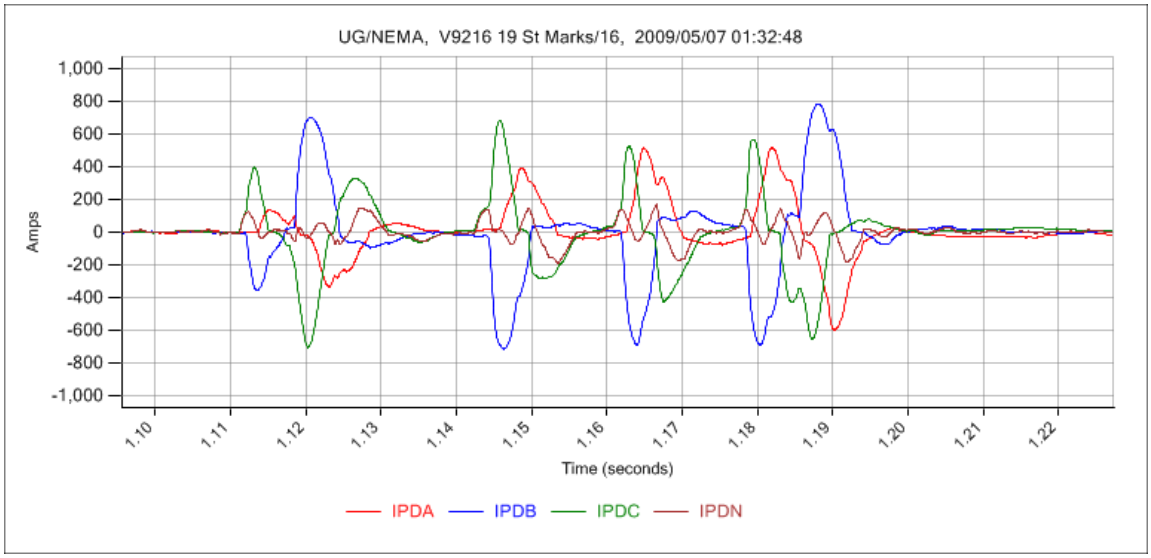

Figure 49: Three-phase arcing fault

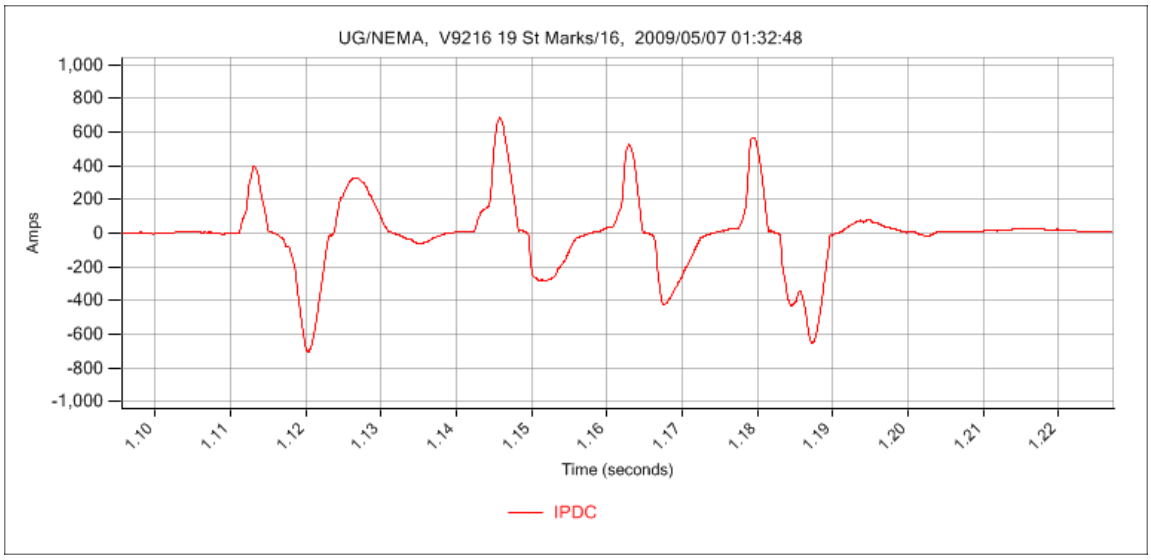

Figure 50: Three-phase arcing event, Phase C shown

In Section 4.4.2.1 it was mentioned that large three-phase events could have a noticeable effect on system voltage, but that significant current levels were required for this to be observed. Figure 51 shows the RMS currents from a waveform file containing an arcing fault. While this fault produced RMS currents of over 2,500A, it reduced the phase voltage only by approximately 4V RMS, as observed in Figure 52. This represents a change of less than three percent out of the 126V RMS initial signal. It is debatable whether this three percent change in voltage would even be visible in the form of flickering lights. Arcing associated with this event eventually caused a report of a manhole event less than one block from the structure which observed these currents.

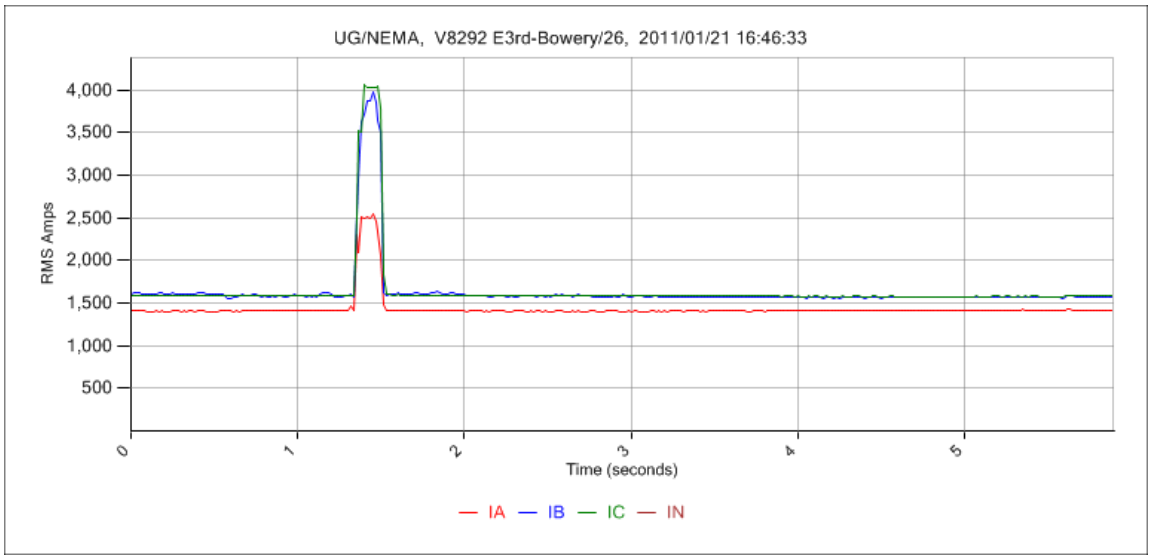

Figure 51: Arcing fault burst, RMS currents

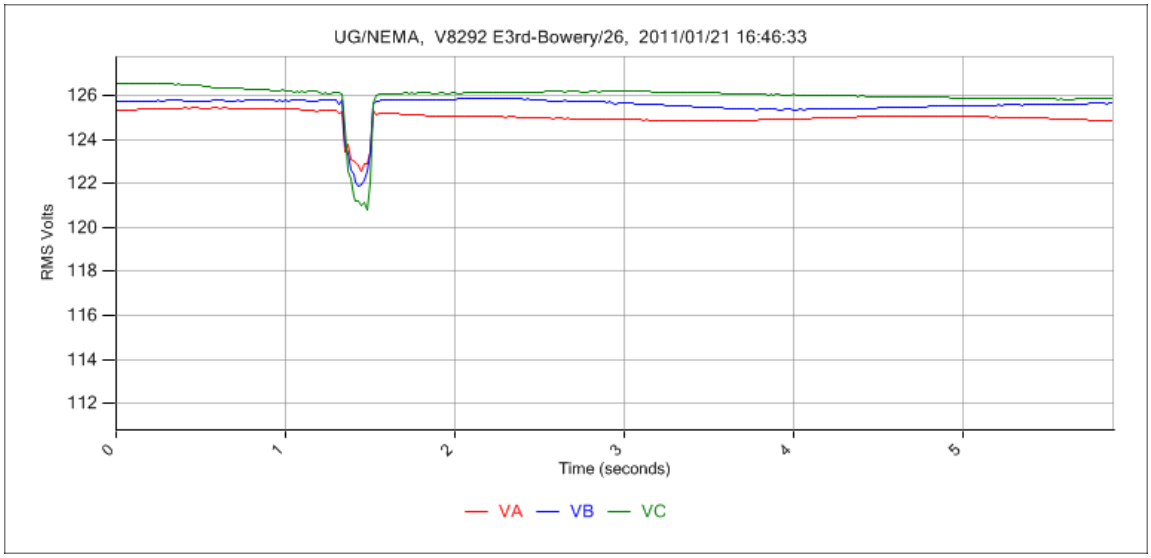

Figure 52: Arcing fault burst, RMS voltages

6.3 Variations Between Simultaneous Captures Observed at Multiple Locations

On the afternoon of January 21, 2011, four underground DCD's recorded a simultaneous arcing fault. This arcing activity, as well as additional bursts captured in the surrounding time period, resulted in a manhole event. Figure 53 shows the location of underground monitors which observed the event in green and the location of the faulted structure in red. The maximum point of estimated peak current is shown below the vault number in red text. Figure 54-Figure 57 show waveform recordings of the arcing fault as observed in multiple locations.

Figure 53: Location of structures observing manhole event, faulted structure in red

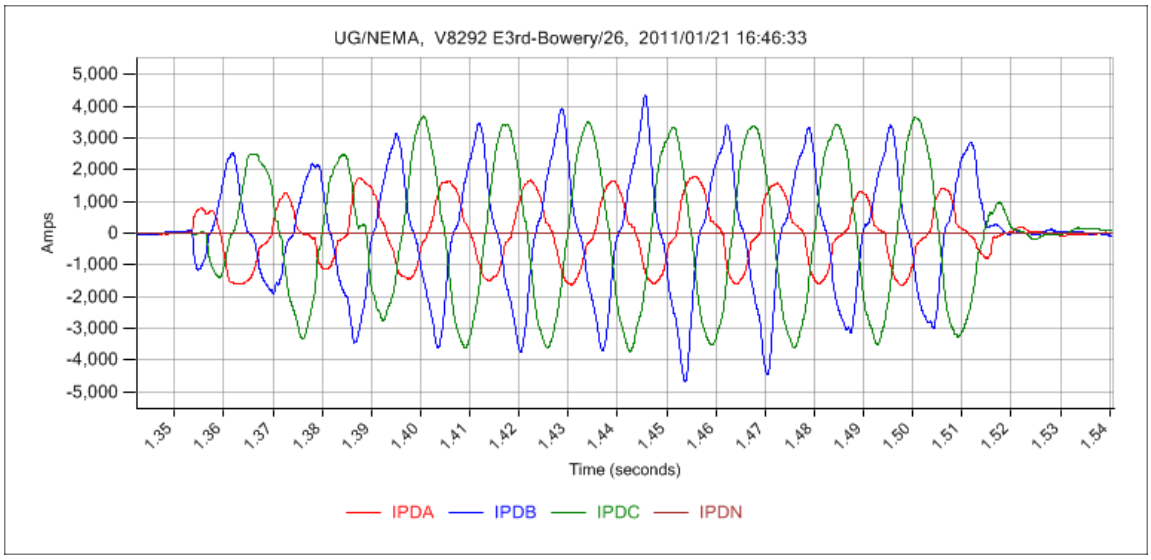

Figure 54: Three-phase arcing fault, V8292

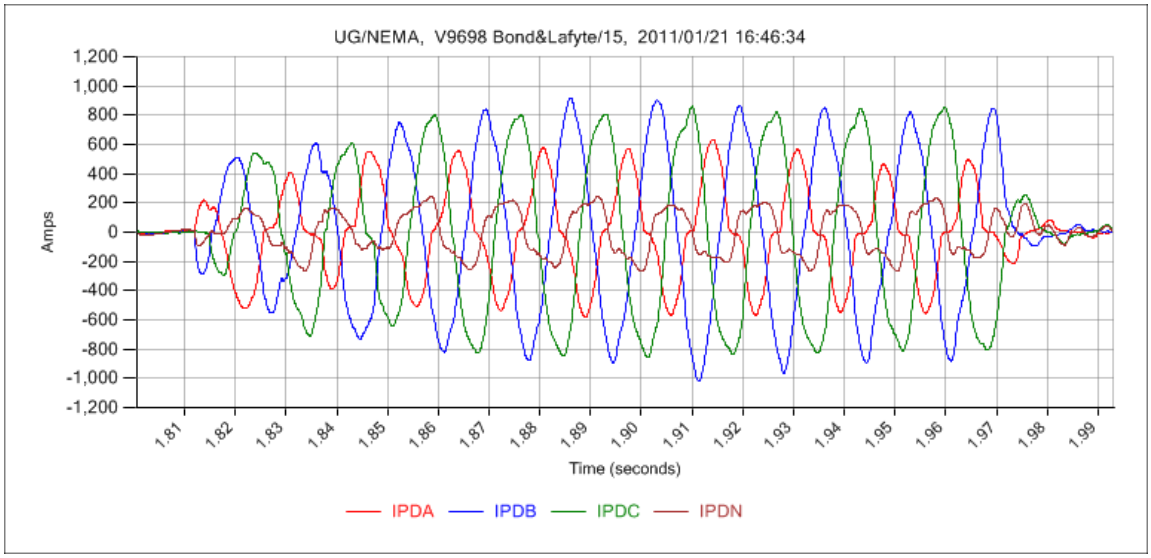

Figure 55: Three-phase arcing fault, V9698

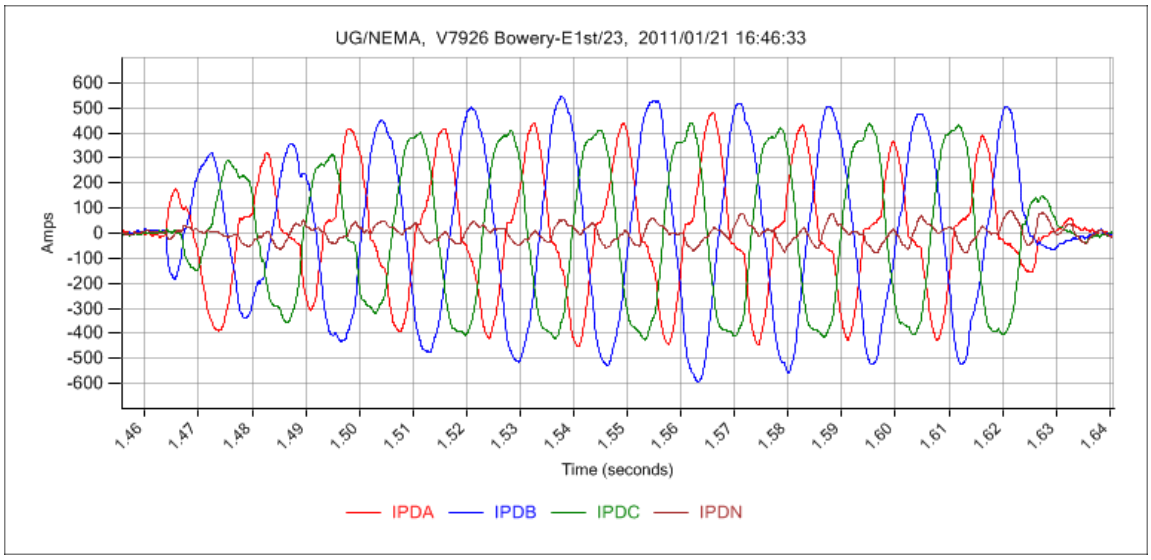

Figure 56: Three-phase arcing fault, V7926

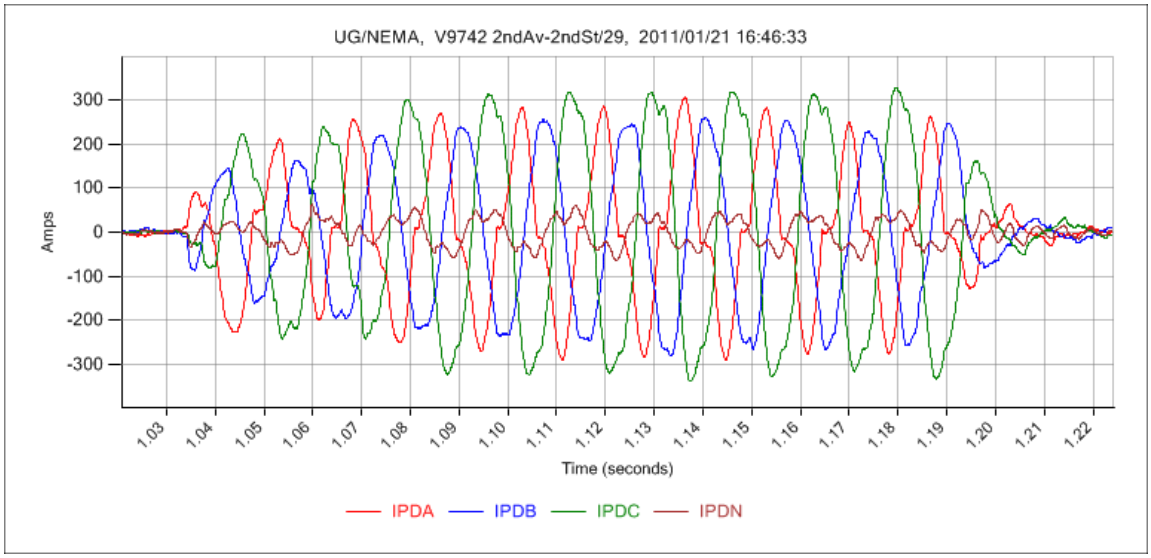

Figure 57: Three-phase arcing fault, V9742

Multiple conclusions are clear from close inspection of the graphs. First, the general structure of the arcing fault is more or less unchanged from structure to structure for this particular fault. However, certain subcycle waveshape differences are clearly apparent. For example, the positive peak behavior of Phase C differs significantly between observations at V7926 and V9742, seen in Figure 56 and Figure 57 respectively. Additionally, the relative magnitudes of fault current between phases is not consistent between faulted locations. Note that at all locations except V9742, Phase B current exceeds Phase C current, while at V9742 the opposite is true. More study remains to be done, but this is believed to be caused by out of service cables in the vicinity of one or more devices, either through intentional utility operation or unintentional damage caused by previous, yet undiscovered faulted conditions.

Figure 58-Figure 65 serve to further illustrate this point. Figure 58 and Figure 59 show all three fault current waveforms for an event observed at two locations, V7755 and V3544, on August 14, 2010. The next six figures show individual phase currents for each phase measured at V7755 and V3544 respectively. For this event, investigation of the individual phases shows that, with very few exceptions, the signals agree quite closely in waveshape. The relative magnitudes, however, vary considerably. Phase A maintains a fairly consistent ratio of approximately 1:1 between locations throughout the capture file. For Phase B, measurements at V3544 are larger than measurements at V7755, on the order of 30%. In contrast, Phase C measurements at V3544 are almost 100% greater than Phase C measurements at V7755. These measurements suggest that network topology can significantly affect localized fault current flows.

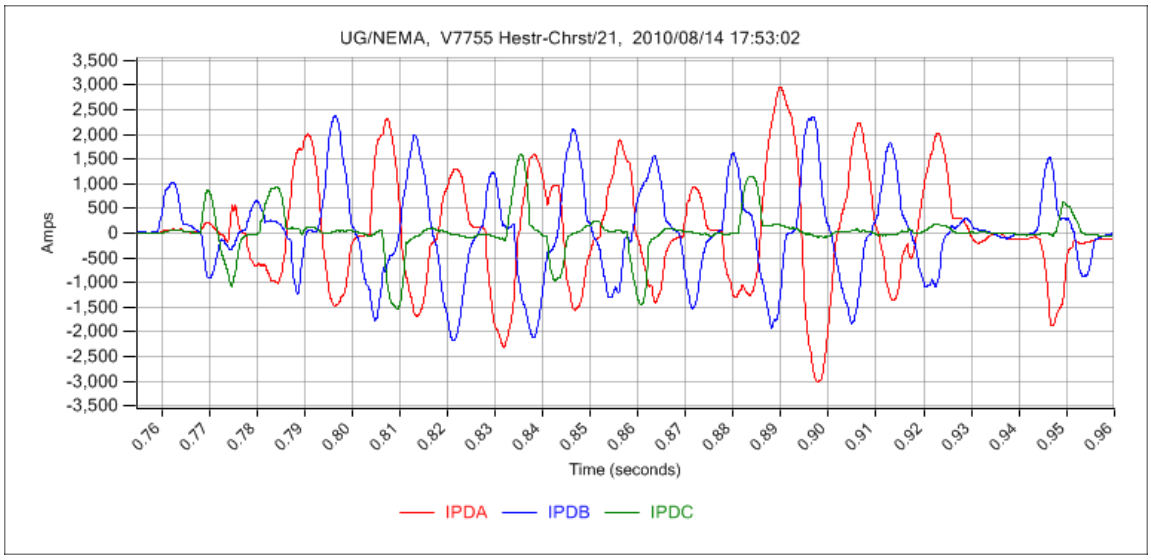

Figure 58: Three-phase arcing fault observed at V7755

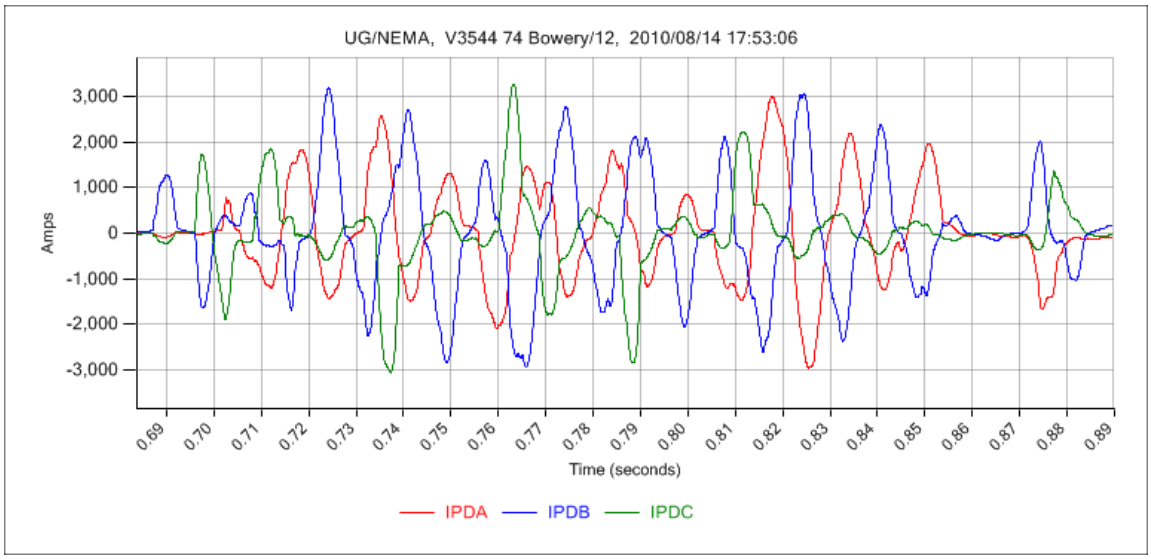

Figure 59: Three-phase arcing fault observed at V3544

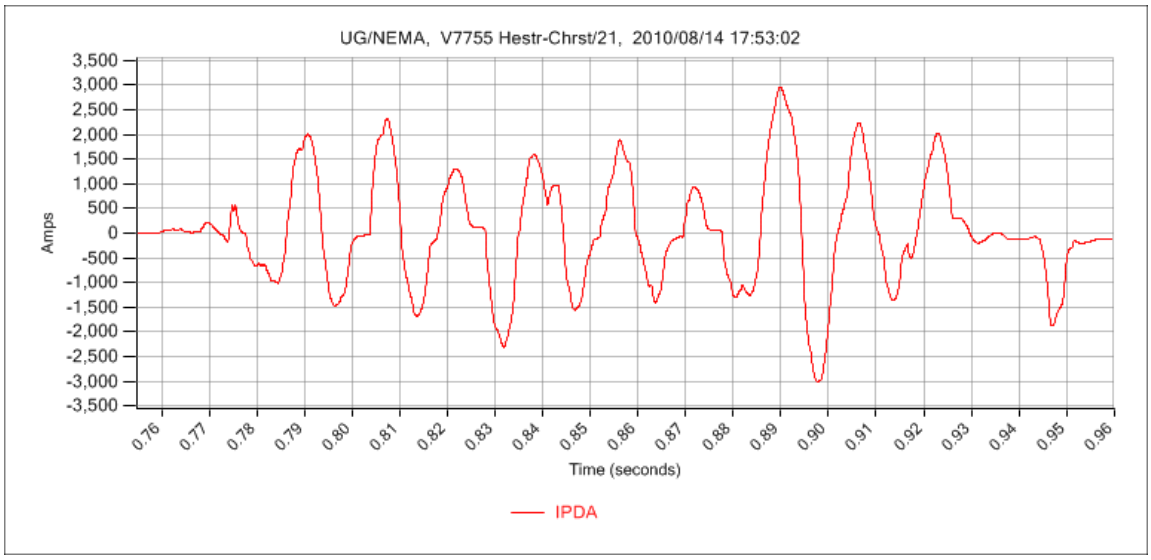

Figure 60: Three-phase arcing fault observed at V7755, Phase A

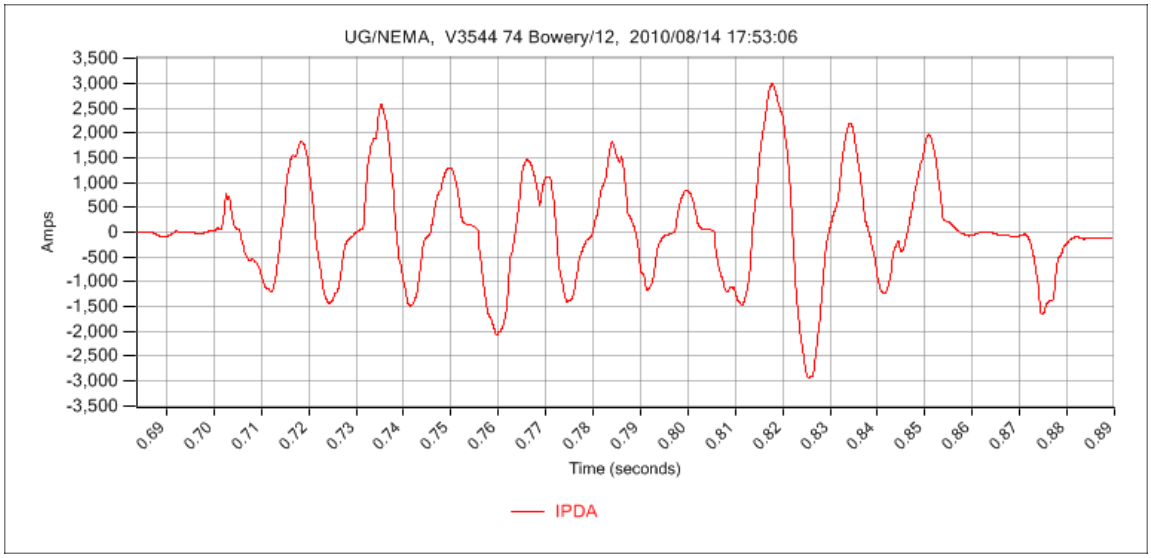

Figure 61: Three-phase arcing fault observed at V3544, Phase A

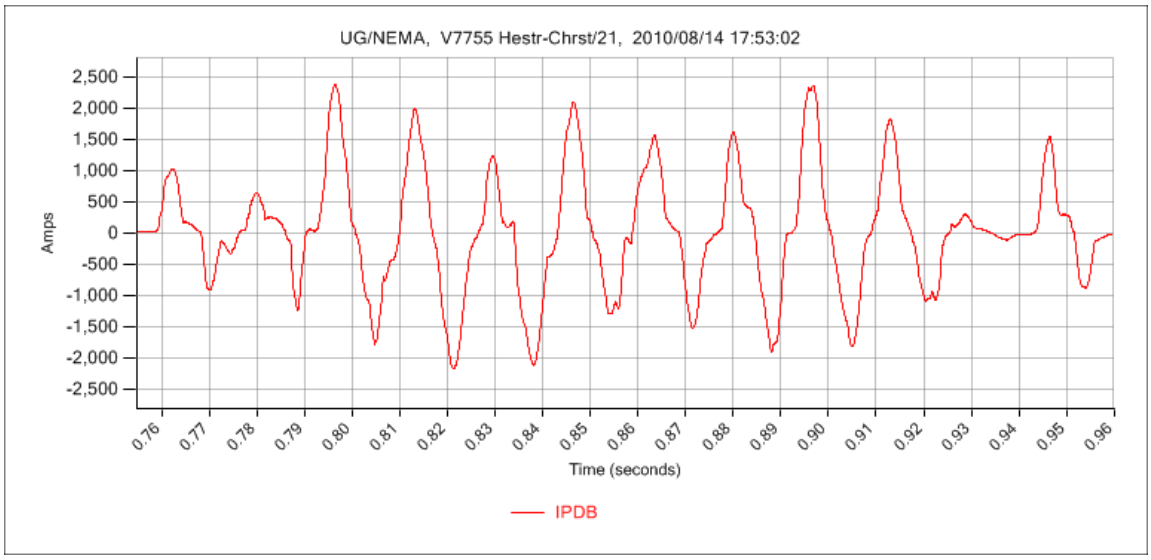

Figure 62: Three-phase arcing fault observed at V7755, Phase B

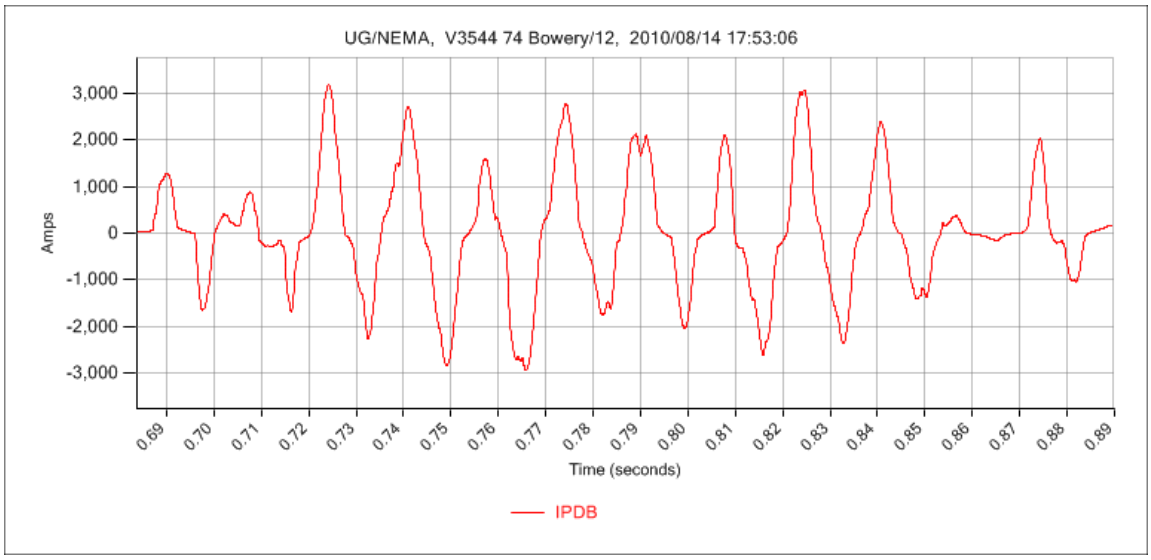

Figure 63: Three-phase arcing fault observed at V3544, Phase B

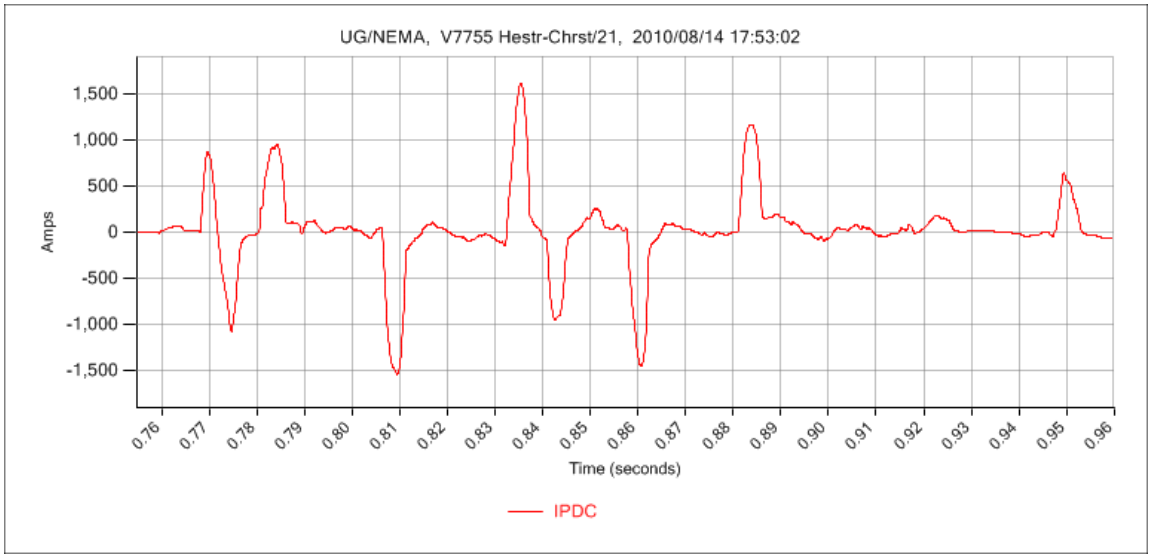

Figure 64: Three-phase arcing fault observed at V7755, Phase C

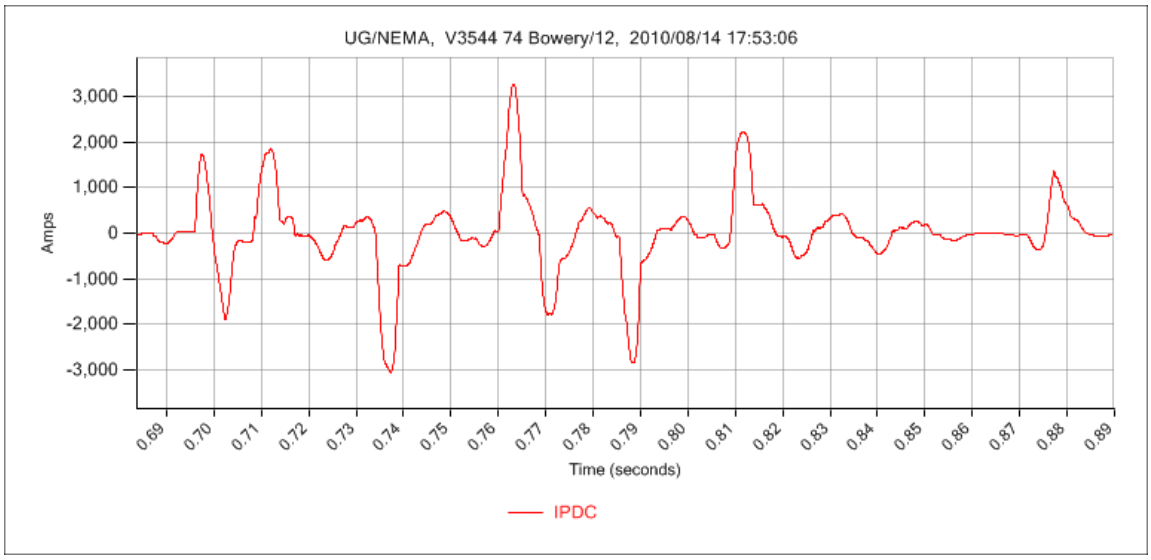

Figure 65: Three-phase arcing fault observed at V3544, Phase C

While the event detailed in Figure 58-Figure 65 maintained a generally constant ratio of currents between the monitored points as the event progressed, this is not always the case. Figure 66 and Figure 67 show an arcing fault simultaneously recorded at two locations, V8442 and V9742. During the course of the event, current waveforms at V8442 drop off significantly, with current peaks near the end of the event approaching 25% of those near the event's inception. By contrast, the measurements taken at V9742 show arc current increasing near the end of the event, in the case of Phase C to levels significantly higher than observed at the beginning of the event. It is incidental, but interesting to note that the maximum current observed at V9742, even near the end of the event remains smaller than the smallest currents observed at V8442. As discussed in Section 6.2, the most likely cause of these changes is variable mechanical conditions near the fault point fundamentally altering the observed impedance between source and fault. As cables are damaged by the fault, it is conceivable that the mechanical condition could be altered differently on either "side" of the fault. As damage continues to progress, the fault impedance might rise or fall depending on mechanical conditions at the faulted point. Without knowing the precise mechanical conditions at the point of the fault, all detailed hypotheses about relative fault current ratios remain little more than speculation.

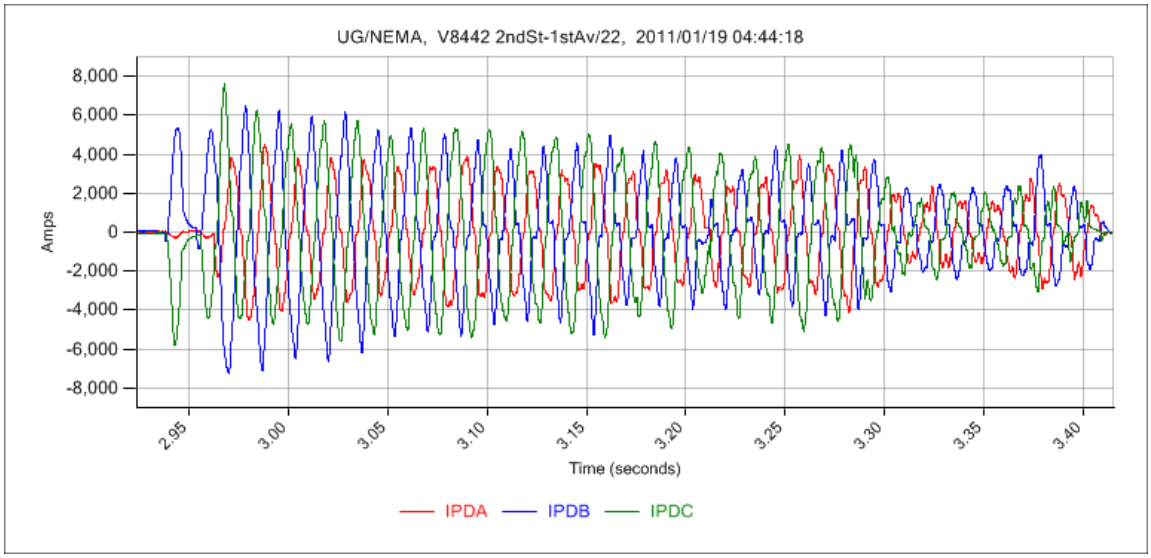

Figure 66: Three-phase arcing fault, V8442

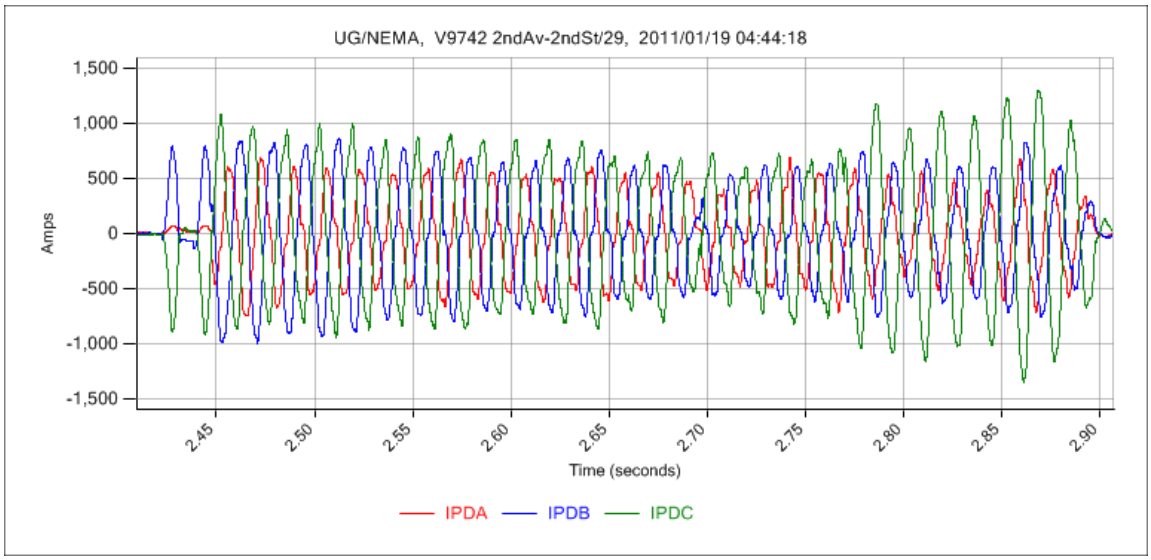

Figure 67: Three-phase arcing fault, V9742

6.4 Persistence and Duration

One major finding observed multiple times in the course of this project involves the length of time arcing bursts can persist near-continuously without self-extinguishing or causing enough damage to be reported through conventional means. In contrast to conventional wisdom claims that arcing faults on 120/208V networks do not sustain themselves for any significant amount of time, researchers documented multiple instances where arcing persisted at monitored locations for hours. Figure 68 shows a sixty-second portion of one such arc burst, which continued unabated for four-hours before utility crews located and repaired the underlying problem. In some instances, these faults produced high fault currents, with the combined total of fault current at all monitored locations measuring thousands of amperes. While many of these events are eventually reported as manhole events, some eventually self-extinguish, though potentially remain incipient conditions.

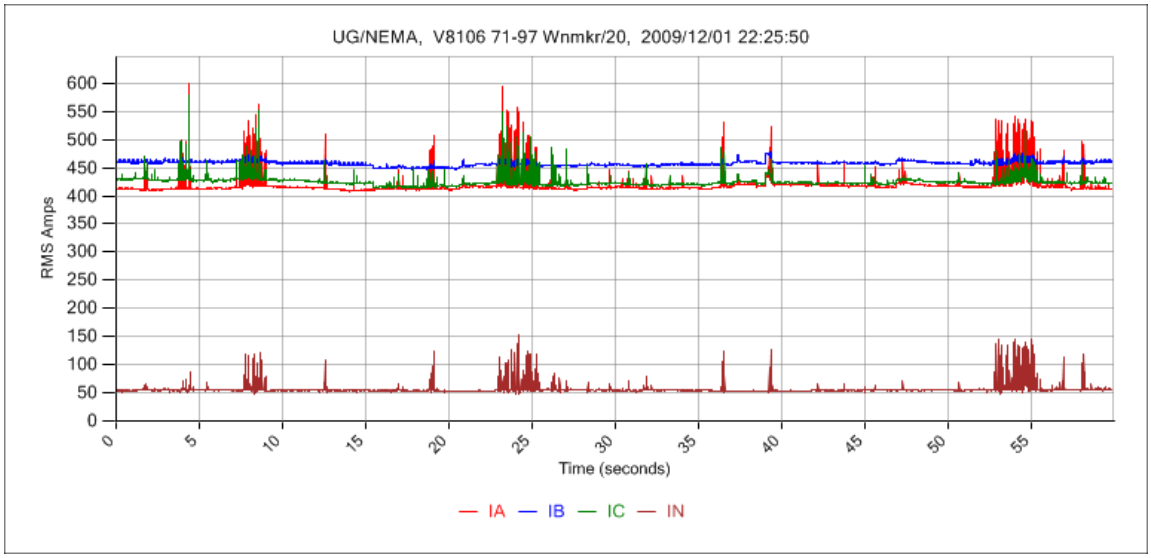

Figure 68: Sixty seconds of arcing activity

7.1 CONCLUSIONS

7.1 Overview

The research presented in this dissertation fundamentally alters the landscape of knowledge about arcing faults on 120/208V networks. Before this investigation, the behavior of arcing faults on 120/208V networks was a poorly understood phenomenon, and virtually no high-fidelity data existed of naturally occurring arcing faults on an operational system. Beliefs about arcing at 120/208V were largely dominated by conventional wisdom claims, with few statements based on scientific measurements. In contrast, this research has produced an expansive database of arcing fault waveforms, believed to be the most extensive such database currently in existence.

7.2 Proof of Hypothesis

With regard to the hypotheses and research goals set forth in this study, the results of this project have exceeded expectations. Selected case studies are presented in Section 8, which serve as representative of the results documented during this course of research. These selected cases, as well as others, provide sufficient evidence of the following:

1) Arcing faults can persist for minutes, hours, days, or weeks before producing enough physical or electrical evidence to be detected by a utility company or the public. This finding is substantiated by multiple cases, including those presented in Appendix A, Appendix B, and Appendix D.

2) Arcing faults at 120V can persist near-continuously for hours without self-extinguishing or operating any protective device. Cases studies presented in Appendix A and Appendix B show clear examples of this behavior.
3) Arcing faults on low-voltage secondary networks can be detected by monitoring primary feeders serving network transformers geographically proximate to the faulted location. One such case is detailed in Appendix Appendix C.
4) Arcing faults can be readily detected by electrically monitoring secondary cables; both low and high current faults can be detected. All cases studes presented in Appendix A-Appendix E show a diversity of arcing behavior, including both high and low current faults.
5) Arcing fault current is served predominantly by network transformers closest to the fault location. Appendix E shows a current distribution observed by multiple units, substantiating this finding.
6) Monitors not electrically near the fault location do not observe the fault. All studied cases where the actual fault location is known confirm that monitors which are not electrically proximate to the fault do not observe the event.
7) Faults can be located using multiple, simultaneous measurements of fault current on secondary cables. Case studies presented in Appendix D and Appendix E show that, in some cases, arcing faults can be located based on multiple, simultaneous measurements of fault current on secondary cables.

7.3 Additional Research

Considerable work remains before arcing on low-voltage networks will be fundamentally understood as well as arcing faults at higher voltages. In particular, additional studies are needed with a greater density of monitored points on multiple utility's networks to ensure the conclusions set forth in this research, primarily drawn from the ConEdison system, can be generalized to all low-voltage networks. Investigation is needed in detecting secondary network arcing from primary feeder measurement points, with the potential to achieve maximum network coverage while substantially reducing the number of data collection devices required. On the secondary network, additional study is needed to understand how many network monitors would be required to enable reliable fault location, and where to place those monitors for maximum effectiveness. A study applying similar methods to 480V networks would explore the now-existing gap in understanding between 120V and 480V arcing.

In summary, this research provides a foundational, scientific basis for future research to detect, locate, and possibly prevent arcing faults on low-voltage secondary networks. It is hoped that this and future work will have a serious impact on mitigating arcing faults on 120/208V networks, reducing the safety hazards they produce and thereby improving network reliability.

REFERENCES

[1] H. Cheng, X. Chen, F. Liu, and C. Wang, "Series arc fault detection and implementation based on the short-time fourier transform," in *Power and Energy Engineering Conference (APPEEC), 2010 Asia-Pacific*, 2010, pp. 1-4.

[2] O. Karacasu, M. H. Hocaoglu, "Simulational analysis of a novel arcing fault detection method," in *Electrical, Electronics and Computer Engineering (ELECO), 2010 National Conference on*, 2010, pp. 118-122.

[3] A. Siadatan, H. K. Karegar, and V. Najmi, "New high impedance fault detection," in *Power and Energy (PECon), 2010 IEEE International Conference on*, 2010, pp. 573-576.

[4] J. Vico, M. Adamiak, C. Wester, and A. Kulshrestha, "High impedance fault detection on rural electric distribution systems," in *Rural Electric Power Conference (REPC), 2010 IEEE*, 2010, pp. B3-B3-8.

[5] G. Idarraga Ospina, D. Cubillos, and L. Ibanez, "Analysis of arcing fault models," in *Transmission and Distribution Conference and Exposition: Latin America, 2008 IEEE/PES*, 2008, pp. 1-5.

[6] B. M. Aucoin and B. D. Russell, "Distribution high impedance fault detection utilizing high frequency current components," *Power Engineering Review, IEEE*, vol. PER-2, pp. 46-47, 1982.

[7] M. Aucoin, "Status of high impedance fault detection," *Power Apparatus and Systems, IEEE Transactions on*, vol. PAS-104, pp. 637-644, 1985.

[8] M. Aucoin, J. Zeigler, and B. D. Russell, "Feeder protection and monitoring system, Part II: staged fault test demonstration," *Power Apparatus and Systems, IEEE Transactions on,* vol. PAS-104, pp. 1455-1462, 1985.

[9] M. Aucoin, J. Zeigler, and B. D. Russell, "Feeder protection and monitoring system, Part I: design, implementation and testing," *Power Apparatus and Systems, IEEE Transactions on,* vol. PAS-104, pp. 873-880, 1985.

[10] M. Aucoin and B. D. Russell, "Detection of distribution high impedance faults using burst noise signals near 60 HZ," *Power Delivery, IEEE Transactions on,* vol. 2, pp. 342-348, 1987.

[11] B. D. Russell, R. P. Chinchali, and C. J. Kim, "Behaviour of low frequency spectra during arcing fault and switching events," *Power Delivery, IEEE Transactions on,* vol. 3, pp. 1485-1492, 1988.

[12] B. D. Russell, K. Mehta, and R. P. Chinchali, "An arcing fault detection technique using low frequency current components-performance evaluation using recorded field data," *Power Delivery, IEEE Transactions on,* vol. 3, pp. 1493-1500, 1988.

[13] M. Aucoin, B. D. Russell, and C. L. Benner, "High impedance fault detection for industrial power systems," in *Industry Applications Society Annual Meeting, 1989., Conference Record of the 1989 IEEE,* 1989, pp. 1788-1792 vol.2.

[14] B. D. Russell and R. P. Chinchali, "A digital signal processing algorithm for detecting arcing faults on power distribution feeders," *Power Delivery, IEEE Transactions on,* vol. 4, pp. 132-140, 1989.

[15] C. J. Kim, B. D. Russell, and K. Watson, "A parameter-based process for selecting high impedance fault detection techniques using decision making under incomplete knowledge," *Power Delivery, IEEE Transactions on,* vol. 5, pp. 1314-1320, 1990.

[16] B. D. Russell and C. L. Benner, "Arcing fault detection for distribution feeders: security assessment in long term field trials," *Power Delivery, IEEE Transactions on,* vol. 10, pp. 676-683, 1995.

[17] B. M. Aucoin and R. H. Jones, "High impedance fault detection implementation issues," *Power Delivery, IEEE Transactions on,* vol. 11, pp. 139-148, 1996.

[18] C. L. Benner and B. D. Russell, "Practical high impedance fault detection for distribution feeders," in *Rural Electric Power Conference, 1996. Papers Presented at the 39th Annual Conference*, 1996, pp. B2-1.

[19] C. L. Benner and B. D. Russell, "Practical high-impedance fault detection on distribution feeders," *Industry Applications, IEEE Transactions on,* vol. 33, pp. 635-640, 1997.

[20] H. Ching-Lien, C. Hui-Yung, and C. Ming-Tong, "Algorithm comparison for high impedance fault detection based on staged fault test," *Power Delivery, IEEE Transactions on,* vol. 3, pp. 1427-1435, 1988.

[21] S. Ebron, D. L. Lubkeman, and M. White, "A neural network approach to the detection of incipient faults on power distribution feeders," *Power Delivery, IEEE Transactions on,* vol. 5, pp. 905-914, 1990.

[22] A. E. Emanuel, D. Cyganski, J. A. Orr, S. Shiller, and E. M. Gulachenski, "High impedance fault arcing on sandy soil in 15 kV distribution feeders: contributions to the evaluation of the low frequency spectrum," *Power Delivery, IEEE Transactions on,* vol. 5, pp. 676-686, 1990.

[23] A. A. Girgis, W. Chang, and E. B. Makram, "Analysis of high-impedance fault generated signals using a Kalman filtering approach," *Power Delivery, IEEE Transactions on,* vol. 5, pp. 1714-1724, 1990.

[24] D. I. Jeerings and J. R. Linders, "Unique aspects of distribution system harmonics due to high impedance ground faults," *Power Delivery, IEEE Transactions on,* vol. 5, pp. 1086-1094, 1990.

[25] D. I. Jeerings and J. R. Linders, "A practical protective relay for down-conductor faults," *Power Delivery, IEEE Transactions on,* vol. 6, pp. 565-574, 1991.

[26] A. F. Sultan and G. W. Swift, "Security testing of high impedance fault detectors," in *WESCANEX '91 'IEEE Western Canada Conference on Computer, Power and Communications Systems in a Rural Environment',* 1991, pp. 191-197.

[27] K. Wook Hyun, L. Gi Wen, P. Young Moon, Y. Man Chul, and Y. Myeong Ho, "High impedance fault detection utilizing incremental variance of normalized even order harmonic power," *Power Delivery, IEEE Transactions on,* vol. 6, pp. 557-564, 1991.

[28] J. A. Momoh, A. U. Chuku, L. G. Dias, and Z. Z. Zhang, "Integrated detection and protection schemes for high-impedance faults on distribution systems," in

Systems, Man and Cybernetics, 1992., IEEE International Conference on, 1992, pp. 1102-1109 vol.2.

[29] L. L. Lai and D. J. Daruvala, "A new approach to arcing fault detection on overhead distribution feeders," in *Electricity Distribution, 1993. CIRED. 12th International Conference on*, 1993, pp. 2.7/1-2.7/5 vol.2.

[30] A. M. Sharaf, L. A. Snider, and K. Debnath, "A neural network based relaying scheme for distribution system high impedance fault detection," in *Artificial Neural Networks and Expert Systems, 1993. Proceedings., First New Zealand International Two-Stream Conference on*, 1993, pp. 321-324.

[31] A. W. Sharaf, L. A. Snider, and K. Debnath, "A third harmonic sequence ANN based detection scheme for high impedance faults," in *Electrical and Computer Engineering, 1993. Canadian Conference on*, 1993, pp. 802-806 vol.2.

[32] A. M. Sharat, L. A. Snider, and K. Debnath, "A neural network based back error propagation relay algorithm for distribution system high impedance fault detection," in *Advances in Power System Control, Operation and Management, 1993. APSCOM-93., 2nd International Conference on*, 1993, pp. 613-620 vol.2.

[33] P. R. Silva, A. Santos, Jr., W. C. Boaventura, G. C. Miranda, and J. A. Scott, "Impulse response analysis of a real feeder for high impedance fault detection," in *Transmission and Distribution Conference, 1994., Proceedings of the 1994 IEEE Power Engineering Society*, 1994, pp. 276-283.

[34] A. F. Sultan, G. W. Swift, and D. J. Fedirchuk, "Detecting arcing downed-wires using fault current flicker and half-cycle asymmetry," *Power Delivery, IEEE Transactions on*, vol. 9, pp. 461-470, 1994.

[35] D. C. Yu and S. H. Khan, "An adaptive high and low impedance fault detection method," *Power Delivery, IEEE Transactions on*, vol. 9, pp. 1812-1821, 1994.

[36] M. B. Djuric and V. V. Terzija, "A new approach to the arcing faults detection for fast autoreclosure in transmission systems," *Power Delivery, IEEE Transactions on*, vol. 10, pp. 1793-1798, 1995.

[37] A. V. Mamishev, B. D. Russell, and C. L. Benner, "Analysis of high impedance faults using fractal techniques," in *Power Industry Computer Application Conference, 1995. Conference Proceedings., 1995 IEEE*, 1995, pp. 401-406.

[38] R. Patterson, "Signatures and software find high impedance faults," *Computer Applications in Power, IEEE*, vol. 8, pp. 12-15, 1995.

[39] P. R. Silva, A. Santos, Jr., and F. G. Jota, "An intelligent system for automatic detection of high impedance faults in electrical distribution systems," in *Circuits and Systems, 1995., Proceedings., Proceedings of the 38th Midwest Symposium on*, 1995, pp. 453-456 vol.1.

[40] A. V. Mamishev, B. D. Russell, and C. L. Benner, "Analysis of high impedance faults using fractal techniques," *Power Systems, IEEE Transactions on*, vol. 11, pp. 435-440, 1996.

[41] A. M. Sharaf, R. M. El-Sharkawy, R. Al-Fatih, and M. Al-Ketbi, "High impedance fault detection on radial distribution and utilization systems," in

Electrical and Computer Engineering, 1996. Canadian Conference on, 1996, pp. 1012-1015 vol.2.

[42] J. T. Tengdin, E. E. Baker, J. J. Burke, B. D. Russell, R. H. Jones, T. E. Wiedman, and N. J. Johnson, "Application of high impedance fault detectors: a summary of the panel session held at the 1995 IEEE PES summer meeting," in *Transmission and Distribution Conference, 1996. Proceedings., 1996 IEEE*, 1996, pp. 116-122.

[43] V. V. Terzija, Z. M. Radojevic, and M. B. Djuric, "A new approach for arcing faults detection and fault distance calculation in spectral domain," in *Transmission and Distribution Conference, 1996. Proceedings., 1996 IEEE*, 1996, pp. 573-578.

[44] K. L. Butler, J. A. Momoh, and D. J. Sobajic, "Field studies using a neural-net-based approach for fault diagnosis in distribution networks," *Generation, Transmission and Distribution, IEE Proceedings-*, vol. 144, pp. 429-436, 1997.

[45] M. B. Duric, Z. M. Radojevic, and V. V. Terzija, "Time domain solution of arcing faults detection and fault distance calculation on distribution lines," in *Electricity Distribution. Part 1: Contributions. CIRED. 14th International Conference and Exhibition on (IEE Conf. Publ. No. 438)*, 1997, pp. 1/1-1/5 vol.1.

[46] J. Lorenc, K. Marszalkiewicz, and J. Andruszkiewicz, "Admittance criteria for earth fault detection in substation automation systems in Polish distribution power networks," in *Electricity Distribution. Part 1: Contributions. CIRED. 14th*

International Conference and Exhibition on (IEE Conf. Publ. No. 438), 1997, pp. 19/1-19/5 vol.4.

[47] J. A. Momoh, L. G. Dias, and D. N. Laird, "An implementation of a hybrid intelligent tool for distribution system fault diagnosis," *Power Delivery, IEEE Transactions on*, vol. 12, pp. 1035-1040, 1997.

[48] L. A. Snider and S. Yuen Yee, "The artificial neural networks based relay algorithm for distribution system high impedance fault detection," in *Advances in Power System Control, Operation and Management, 1997. APSCOM-97. Fourth International Conference on (Conf. Publ. No. 450)*, 1997, pp. 100-106 vol.1.

[49] K. Jae-Ho, S. Jae-Chul, R. Chang-Wan, P. Chan-Gook, and Y. Wha-Yeong, "Detection of high impedance faults using neural nets and chaotic degree," in *Energy Management and Power Delivery, 1998. Proceedings of EMPD '98. 1998 International Conference on*, 1998, pp. 399-404 vol.2.

[50] K. J. Jensen, S. M. Munk, and J. A. Sorensen, "Feature extraction method for high impedance ground fault localization in radial power distribution networks," in *Acoustics, Speech and Signal Processing, 1998. Proceedings of the 1998 IEEE International Conference on*, 1998, pp. 1177-1180 vol.2.

[51] F. G. Jota and P. R. S. Jota, "High-impedance fault identification using a fuzzy reasoning system," *Generation, Transmission and Distribution, IEE Proceedings-*, vol. 145, pp. 656-661, 1998.

[52] T. S. Sidhu, G. Singh, and M. S. Sachdev, "A new technique for detection and location of arcing faults in power system apparatus," in *Electrical and Computer Engineering, 1998. IEEE Canadian Conference on*, 1998, pp. 185-188 vol.1.

[53] C. G. Wester, "High impedance fault detection on distribution systems," in *Rural Electric Power Conference, 1998. Papers Presented at the 42nd Annual Conference*, 1998, pp. c5-1-5.

[54] I. K. Yu and Y. H. Song, "Wavelet analysis of arcing fault phenomena with particular reference to development of new protection and control techniques," in *Control '98. UKACC International Conference on (Conf. Publ. No. 455)*, 1998, pp. 1011-1016 vol.2.

[55] M. Al-Dabbagh and L. Al-Dabbagh, "Neural networks based algorithm for detecting high impedance faults on power distribution lines," in *Neural Networks, 1999. IJCNN '99. International Joint Conference on*, 1999, pp. 3386-3390 vol.5.

[56] M. B. Djuric, Z. M. Radojevic, and V. V. Terzija, "Time domain solution of fault distance estimation and arcing faults detection on overhead lines," *Power Delivery, IEEE Transactions on*, vol. 14, pp. 60-67, 1999.

[57] L. Keng-Yu, C. Shi-Lin, L. Ching-Jung, G. Tzong-Yih, L. Tsair-Ming, and S. Jer-Sheng, "Energy variance criterion and threshold tuning scheme for high impedance fault detection," *Power Delivery, IEEE Transactions on*, vol. 14, pp. 810-817, 1999.

[58] K. L. Butler and J. A. Momoh, "A neural net based approach for fault diagnosis in distribution networks," in *Power Engineering Society Winter Meeting, 2000. IEEE*, 2000, pp. 1275-1278 vol.2.

[59] A. Lazkano, J. Ruiz, E. Aramendi, and L. A. Leturiondo, "A new approach to high impedance fault detection using wavelet packet analysis," in *Harmonics and Quality of Power, 2000. Proceedings. Ninth International Conference on*, 2000, pp. 1005-1010 vol.3.

[60] A. Lazkano, J. Ruiz, E. Aramendi, L. A. Leturiondo, and J. A. Gonzalez, "Study of high impedance fault detection in Levante area in Spain," in *Harmonics and Quality of Power, 2000. Proceedings. Ninth International Conference on*, 2000, pp. 1011-1016 vol.3.

[61] A. Lazkano, J. Ruiz, L. A. Leturiondo, and E. Aramendi, "High impedance arcing fault detector for three-wire power distribution networks," in *Electrotechnical Conference, 2000. MELECON 2000. 10th Mediterranean*, 2000, pp. 899-902 vol.3.

[62] Z. M. Radojevic, V. V. Terzija, and N. B. Djuric, "Numerical algorithm for overhead lines arcing faults detection and distance and directional protection," *Power Delivery, IEEE Transactions on*, vol. 15, pp. 31-37, 2000.

[63] R. Keyhani, M. Deriche, and E. Palmer, "A high impedance fault detector using a neural network and subband decomposition," in *Signal Processing and its Applications, Sixth International, Symposium on. 2001*, 2001, pp. 458-461 vol.2.

[64] A. Lazkano, J. Ruiz, E. Aramendi, and L. A. Leturiondo, "Evaluation of a new proposal for arcing fault detection method based on wavelet packet analysis," in *Power Engineering Society Summer Meeting, 2001. IEEE*, 2001, pp. 1328-1333 vol.3.

[65] L. Li and M. A. Redfern, "A review of techniques to detect downed conductors in overhead distribution systems," in *Developments in Power System Protection, 2001, Seventh International Conference on (IEE)*, 2001, pp. 169-172.

[66] T. M. Lai, L. A. Snider, E. Lo, C. H. Cheung, and K. W. Chan, "High impedance faults detection using artificial neural network," in *Advances in Power System Control, Operation and Management, 2003. ASDCOM 2003. Sixth International Conference on (Conf. Publ. No. 497)*, 2003, pp. 821-826.

[67] H. Belka and M. Michalik, "Application of the continuous wavelet transform to intermittent high impedance ground fault detection in MV networks," in *Developments in Power System Protection, 2004. Eighth IEE International Conference on*, 2004, pp. 473-476 Vol.2.

[68] R. Das and S. A. Kunsman, "A novel approach for ground fault detection," in *Protective Relay Engineers, 2004 57th Annual Conference for*, 2004, pp. 97-109.

[69] H. Khorashadi-Zadeh, "A novel approach to detection high impedance faults using artificial neural network," in *Universities Power Engineering Conference, 2004. UPEC 2004. 39th International*, 2004, pp. 373-376 Vol. 1.

[70] Y. Ming-Ta, G. Jhy-Cheng, J. Chau-Yuan, and K. Wen-Shiow, "Detection of high impedance fault in distribution feeder using wavelet transform and artificial

neural networks," in *Power System Technology, 2004. PowerCon 2004. 2004 International Conference on*, 2004, pp. 652-657 Vol.1.

[71] Y. Ming-Ta, G. Jhy-Cherng, H. Wen-Shing, C. Yuan-Chi, and C. Chiang, "A novel intelligent protection scheme for high impedance fault detection in distribution feeder," in *TENCON 2004. 2004 IEEE Region 10 Conference*, 2004, pp. 401-404 Vol. 3.

[72] A. M. Sharaf and W. Guosheng, "High impedence fault detection using low - order pattern harmonic detection," in *Electrical, Electronic and Computer Engineering, 2004. ICEEC '04. 2004 International Conference on*, 2004, pp. 883-886.

[73] S. Yong and S. M. Rovnyak, "Decision tree-based methodology for high impedance fault detection," *Power Delivery, IEEE Transactions on*, vol. 19, pp. 533-536, 2004.

[74] I. Baqui, A. J. Mazon, I. Zamora, and R. Vicente, "High impedance faults detection in power distribution system by combination of artificial neural network and wavelet transform," in *Electricity Distribution, 2005. CIRED 2005. 18th International Conference and Exhibition on*, 2005, pp. 1-4.

[75] M. Carpenter, R. R. Hoad, T. D. Bruton, R. Das, S. A. Kunsman, and J. M. Peterson, "Staged-fault testing for high impedance fault data collection," in *Protective Relay Engineers, 2005 58th Annual Conference for*, 2005, pp. 9-17.

[76] A. Gaudreau and B. Koch, "Evaluation of LV and MV Arc Parameters," *Power Delivery, IEEE Transactions on*, vol. 23, pp. 487-492, 2008.

[77] Z. Lily, S. A. Boggs, and S. Livanos, "Manhole Events Caused by Secondary Cable Insulation Breakdown," in *Electrical Insulation and Dielectric Phenomena, 2008. CEIDP 2008. Annual Report Conference on*, 2008, pp. 107-110.

[78] A. K. Mishra, A. Routray, and A. K. Pradhan, "Detection of arcing in low voltage distribution systems," in *Industrial and Information Systems, 2008. ICIIS 2008. IEEE Region 10 and the Third international Conference on*, 2008, pp. 1-3.

[79] T. A. Kawady, A. Taalab, and M. Z. Elgeziry, "Experimental investigation of high impedance faults in low voltage distribution networks," in *Power & Energy Society General Meeting, 2009. PES '09. IEEE*, 2009, pp. 1-6.

[80] W. Charytoniuk, L. Wei-Jen, C. Mo-Shing, J. Cultrera, and M. Theodore, "Arcing fault detection in underground distribution networks-feasibility study," *Industry Applications, IEEE Transactions on,* vol. 36, pp. 1756-1761, 2000.

[81] A. Hamel, A. Gaudreau, and M. Cote, "Intermittent arcing fault on underground low-voltage cables," *Power Delivery, IEEE Transactions on,* vol. 19, pp. 1862-1868, 2004.

[82] W. Huaren, L. Xiaohui, D. Stade, and H. Schau, "Arc fault model for low-voltage AC systems," *Power Delivery, IEEE Transactions on,* vol. 20, pp. 1204-1205, 2005.

[83] T. L. Gammon, "Improved arcing-fault current models for low-voltage power systems (<1 kV)," Ph.D. 9966950, Georgia Institute of Technology, United States -- Georgia, 1999.

[84] D. G. Ece and F. M. Wells, "Analysis and detection of arcing faults in low-voltage electrical power systems," in *Electrotechnical Conference, 1994. Proceedings., 7th Mediterranean*, 1994, pp. 929-935 vol.3.

[85] D. G. Ece, "Behavior of system voltage during arcing faults and switching events," in *Electrotechnical Conference, 1996. MELECON '96., 8th Mediterranean*, 1996, pp. 757-760 vol.2.

[86] J. Slepian and A. P. Strom, "Arcs in low-voltage AC networks," *American Institute of Electrical Engineers, Transactions of the,* vol. 50, pp. 847-852, 1931.

[87] G. Sutherland and D. S. Maccorkle, "Burn-off characteristics of AC low-voltage network cables," *American Institute of Electrical Engineers, Transactions of the,* vol. 50, pp. 831-844, 1931.

[88] Central Station Engineers of the Westinghouse Electric Corporation., *Electrical Transmission and Distribution Reference Book*, 4th ed. East Pittsburgh, Pennsylvania, Westinghouse Electric Corporation, 1950.

[89] Edison Electric Institute. Transmission and Distribution Committee. and National Electric Light Association. Underground Systems Committee., *Underground Systems Reference Book*. New York, Edison Electric Institute, 1957.

[90] R. D. Christie, H. Zadehgol, and M. M. Habib, "High impedance fault detection in low voltage networks," *Power Delivery, IEEE Transactions on,* vol. 8, pp. 1829-1836, 1993.

[91] A. H. Kehoe, "Underground Alternating Current Network Distribution for Central Station Systems," *American Institute of Electrical Engineers, Transactions of the*, vol. XLIII, pp. 844-853, 1924.

[92] D. W. Roop and N. G. Vidonic, "Arcing fault protection on Vepco's 480Y/277 volt secondary spot Networks," *Power Apparatus and Systems, IEEE Transactions on*, vol. PAS-102, pp. 364-372, 1983.

[93] B. Koch and Y. Carpentier, "Manhole explosions due to arcing faults on underground secondary distribution cables in ducts," *Power Delivery, IEEE Transactions on*, vol. 7, pp. 1425-1433, 1992.

[94] L. Zhang, S. A. Boggs, S. Livanos, G. Varela, and A. Prazan, "The electro-chemical basis of manhole events," *Electrical Insulation Magazine, IEEE*, vol. 25, pp. 25-30, 2009.

[95] B. P. Walsh and W. Z. Black, "Thermodynamic and mechanical analysis of short circuit events in an underground vault," *Power Delivery, IEEE Transactions on*, vol. 20, pp. 2235-2240, 2005.

[96] Underwriters Laboratories, "Evaluation of Gases Generated by Heating and Burning of Cables," EPRI Final Report TR-106394, Palo Alto, CA. 1996.

[97] "Assessment of the Underground Distribution System of the Potomac Electric Power Company," Stone & Webster Consultants, Washington D.C. 2001.

[98] W. Charytoniuk, W. J. Lee, M. S. Chen, J. Cultrera, and T. Maffetone, "Arcing fault detection in underground distribution networks feasibility study," in *Industrial and Commercial Power Systems Technical Conference, 2000.*

Conference Record. Papers Presented at the 2000 Annual Meeting. 2000 IEEE, 2000, pp. 15-20.

[99] R. J. Landman, "Underground secondary AC networks, a brief history," in *Electric Power, 2007 IEEE Conference on the History of*, 2007, pp. 140-151.

[100] C. P. Xenis, "The limiter - its basic functions in network distribution systems," *Power Apparatus and Systems, Part III. Transactions of the American Institute of Electrical Engineers*, vol. 74, pp. 913-950, 1955.

[101] C. P. Xenis, "Short-circuit protection of distribution networks by the use of limiters," *American Institute of Electrical Engineers, Transactions of the*, vol. 56, pp. 1191-1196, 1937.

[102] F. Heller and I. Matthysse, "Limiters, their design characteristics and application," *Power Apparatus and Systems, Part III. Transactions of the American Institute of Electrical Engineers*, vol. 74, pp. 924-950, 1955.

[103] I. Matthysse, "Classification and standardization of cables and limiters for secondary network systems," *Power Apparatus and Systems, Part III. Transactions of the American Institute of Electrical Engineers*, vol. 78, pp. 315-323, 1959.

[104] L. L. Grigsby, Ed., *The Electric Power Engineering Handbook* (Electrical engineering handbook series. Boca Raton, Fl.: CRC Press, 2001,

[105] "IEEE Guide for Performing Arc-Flash Hazard Calculations," *IEEE Std 1584-2002*, pp. i-113, 2002.

[106] C. A. Larkin, J. Ferrera, R. Kohl, C. Lamb, P. Margetts, and R. F. Ammerman, "Arc flash evaluation and hazard mitigation for the Colorado School of Mines electrical power distribution system," in *North American Power Symposium (NAPS), 2009*, 2009, pp. 1-6.

[107] C. Inshaw and R. A. Wilson, "Arc flash hazard analysis and mitigation," in *Protective Relay Engineers, 2005 58th Annual Conference for*, 2005, pp. 145-157.

[108] J. Sperl, C. Whitney, and A. Milner, "Arc flash hazard regulation and mitigation," in *Protective Relay Engineers, 2009 62nd Annual Conference for*, 2009, pp. 417-425.

[109] H. L. Floyd, D. R. Doan, C. T. Wu, and S. L. Lovasic, "Arc flash hazards and electrical safety program implementation," in *Industry Applications Conference, 2005. Fourtieth IAS Annual Meeting. Conference Record of the 2005*, 2005, pp. 1919-1923 Vol. 3.

[110] I. H. Landis Floyd, "Arc-Flash Hazard Mitigation," *Industry Applications Magazine, IEEE*, vol. PP, pp. 1-1, 2011.

[111] H. Landis Floyd, "Closing the gaps in arc flash hazard mitigation a review of US, Canada, and EU Standards," in *Industry Applications Society Annual Meeting, 2009. IAS 2009. IEEE*, 2009, pp. 1-5.

[112] D. C. Mohla, T. Driscoll, P. S. Hamer, and S. A. R. Panetta, "Mitigating electric shock and arc flash energy; A total system approach for personnel and equipment protection," in *Petroleum and Chemical Industry Conference (PCIC), 2010*

Record of Conference Papers Industry Applications Society 57th Annual, 2010, pp. 1-10.

[113] J. Simms and G. Johnson, "Protective relaying methods for reducing arc flash energy," in *Protective Relay Engineers, 2010 63rd Annual Conference for*, 2010, pp. 1-15.

[114] H. W. Tinsley, M. Hodder, and A. M. Graham, "Arc flash hazard calculations: myths, facts and solutions," in *Pulp and Paper Industry Technical Conference, 2006. Conference Record of Annual*, 2006, pp. 1-7.

[115] R. F. Ammerman, P. K. Sen, and J. P. Nelson, "Arc flash hazard incident energy calculations a historical perspective and comparative study of the standards: IEEE 1584 and NFPA 70E," in *Petroleum and Chemical Industry Technical Conference, 2007. PCIC '07. IEEE*, 2007, pp. 1-13.

[116] "Arc-flash hazard in wind power plants," in *Transmission and Distribution Conference and Exposition, 2010 IEEE PES*, 2010, pp. 1-8.

[117] J. C. Das, "Design aspects of industrial distribution systems to limit arc flash hazard," in *Pulp and Paper Industry Technical Conference, 2005. Conference Record of 2005 Annual*, 2005, pp. 179-190.

[118] H. W. Tinsley, III and M. Hodder, "A practical approach to arc flash hazard analysis and reduction," in *Pulp and Paper Industry Technical Conference, 2004. Conference Record of the 2004 Annual*, 2004, pp. 111-119.

[119] M. Hodder, W. Vilcheck, F. Croyle, and D. McCue, "Practical methods in reducing the dangerous arc flash hazard areas in large industrial facilities," in

Pulp and Paper Industry Technical Conference, 2005. Conference Record of 2005 Annual, 2005, pp. 191-198.

[120] G. T. Homce and J. C. Cawley, "Understanding and quantifying arc flash hazards in the mining industry," in *Industry Applications Conference, 2007. 42nd IAS Annual Meeting. Conference Record of the 2007 IEEE*, 2007, pp. 1364-1372.

[121] K. J. Lippert, D. M. Colaberardino, and C. W. Kimblin, "Understanding arc flash hazards," in *Pulp and Paper Industry Technical Conference, 2004*, pp. 120-129.

APPENDIX A: CASE STUDY 1 - NETWORK ARCING FAULT OBSERVED AT TWO UNDERGROUND LOCATIONS LEADS TO MANHOLE EVENT

A.1 Summary

On the evening of August 14, 2010, two proximate underground DCDs recorded simultaneous arcing signatures with high magnitude. High magnitude arcing signatures generally result when an event is particularly severe, or when the monitoring device is sufficiently close to the faulted point. Arcing continued violently at the monitored location over an eight minute period. This arcing activity resulted in the report of a manhole event to ConEdison, located approximately half a block from each DCD.

A.2 Detailed narrative

This event was selected for presentation as a case study for multiple reasons. First, high-speed waveforms from this arcing event were used multiple times in the main body of this dissertation, as they provide excellent examples of high magnitude, three-phase arcing. The inclusion of these high-speed waveforms at other points in the presentation allows this narrative to focus on the behavior of the event as a whole, as opposed to focusing on specific details of waveforms. Discussion of high-speed waveforms related to this event can be found in Sections 6.2.3 and 6.3. Second, the entire event lasted only eight minutes, and resulted in fewer than one hundred total waveform files, compared to other major arcing episodes, which may generate several hundred waveform files over many hours. The shorter time duration and lower number of files allows a higher percentage of important data to be presented in this case study,

allowing easier diagnosis of high level trends. Finally, it represents a clear case where multiple transformers observed significant currents, with waveform peaks of well over 3,000A, and RMS fault currents of several hundred amperes.

Figure 69 shows a street map of the neighborhood local to this event. V7755 and V3544 are located approximately one electrical block from each other, but on two separate streets. The arcing fault occurred at the intersection of Hester and Bowery, located approximately at the midpoint of the two locations.

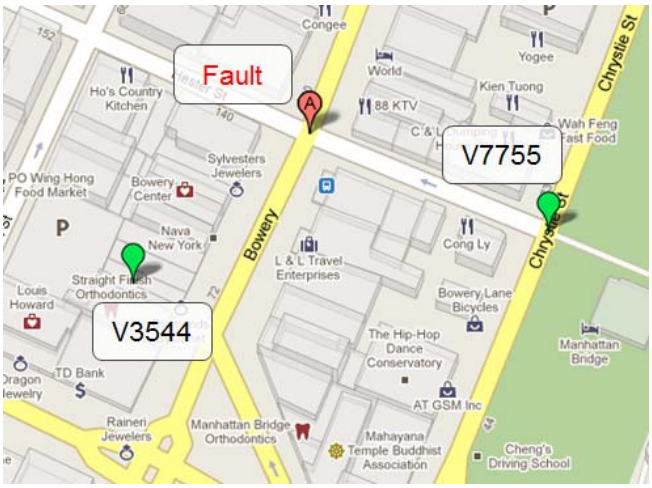

Figure 69: Street map showing locations of V7755, V3544, and resultant manhole event

Because several high-speed waveforms from this event are used in the main body of this dissertation, graphs presented in this case study will focus on RMS signals calculated from the calculated phasor differenced quantities. These graphs represent the

best estimate of the RMS of the fault current at each location. It is important to note that this is not the RMS cycle-to-cycle difference parameter used for triggering, which is calculated by the unit from a simple point-by-point subtraction and is used only for the purposes of triggering waveform files. Instead, the graphs presented in Section 0 account for both phase shifts and harmonic content in the load and event signals. As one final note, because arcing faults are not steady-state sinusoidal signals, the RMS values calculated do not have a simple "square root 2" relationship with peak current values. For each of the waveforms presented below, peak values substantially exceed those expected by a square root 2 approximation.

Figure 70 and Figure 71 show the initial major burst recorded in this event. The event begins entirely on Phase A, but quickly progresses to involve Phase C and system neutral as well. Following the burst in Figure 70 and Figure 71, sporadic half cycle arcing continued on Phase B for the next minute and a half, which eventually resulted in a brief, eight cycle burst which involved all three-phases at 17:51.

Sporadic Phase B arcing continued for the next minute with greater persistence before resulting in the bursts seen in Figure 72 and Figure 73. In these graphs, low level Phase B arcing activity can be seen in the initial second, followed by a brief, half-cycle phase-to-phase arc burst on Phases A and B, which immediately transitions into a significant, three-phase burst. Contrasting Figure 70 and Figure 71 with Figure 72 and Figure 73, we can already see a shift in the relative magnitudes of the phase. In Figure 70 and Figure 71, both V3544 and V7755 share roughly the same ratio of C to A current, with the magnitude of Phase C being approximately 33% larger than the magnitude of

Phase A. In Figure 72, by contrast, Phase C is 43% larger than Phase A, while in Figure 73, Phase C is only 20% larger than Phase A.

Low level arcing continued for the next twenty seconds before producing the graphs shown in Figure 74 and Figure 75. High-speed waveforms from this current burst were discussed extensively in Section 6.3, and extended discussion will not be repeated here.

For the next minute and a half, arcing continued primarily on Phase B, but with occasional involvement on Phase A and Phase C. Arcing peaks in these bursts consistently reached over 1,500 amperes, with some peaks reaching greater than 2,000 amperes.

At 17:54, three-phase arcing resumed, as seen in Figure 76 and Figure 77. This was followed quickly by phase-to-phase bursts shown in Figure 78 and Figure 79. Lower level single-phase arcing was observed on Phase B for the next two minutes. While this could be considered a sort of quiescent period, arc bursts continued to have peak magnitudes of over 800A. After the two minute quiescent period, arcing resumed with the bursts shown in Figure 80 and Figure 81. Three additional phase-to-phase and three-phase bursts occurred over the next minute and a half, but none differ significantly from graphs already presented. The final observed bursts are shown in Figure 82 and Figure 83.

Several important conclusions can be drawn from this series of waveforms. First, secondary network arcing faults can evolve in unpredictable ways, transitioning between single-phase, phase-to-phase, and three-phase involvement, sometimes in a span of a few

cycles. Second, mechanical changes at the fault point can result in significant changes to the ratios between phase magnitudes observed at various locations during the course of an event. Finally, there is not a certain correlation between the duration of a burst and a report of a manhole event. This event was over in eight minutes, yet generated a report of a manhole fire, while similar bursts have continued for hours with no such report.

A.3 Waveforms

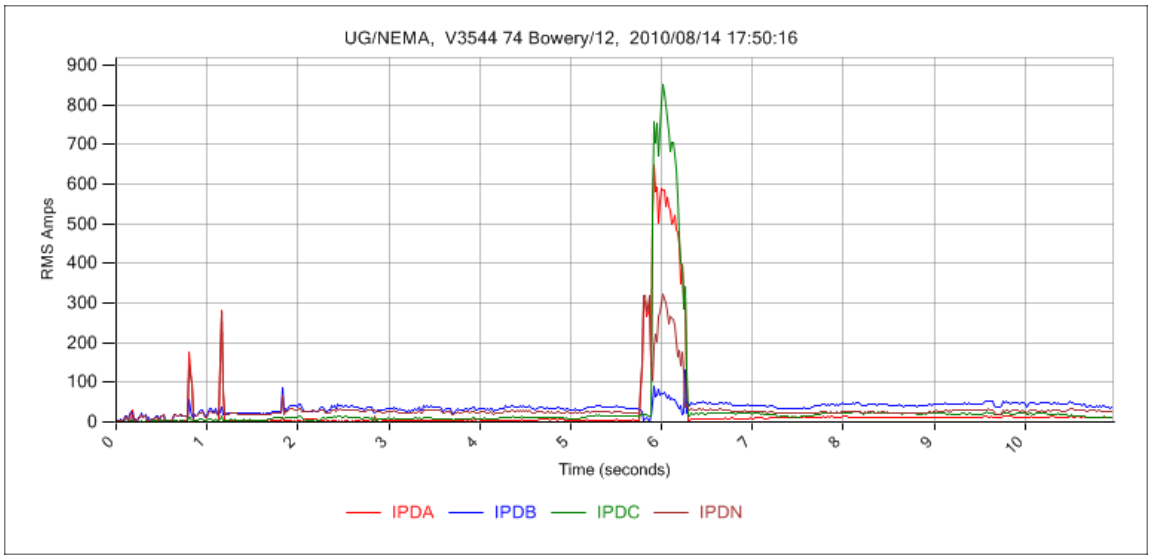

Figure 70: Initial burst, V3544, 17:50

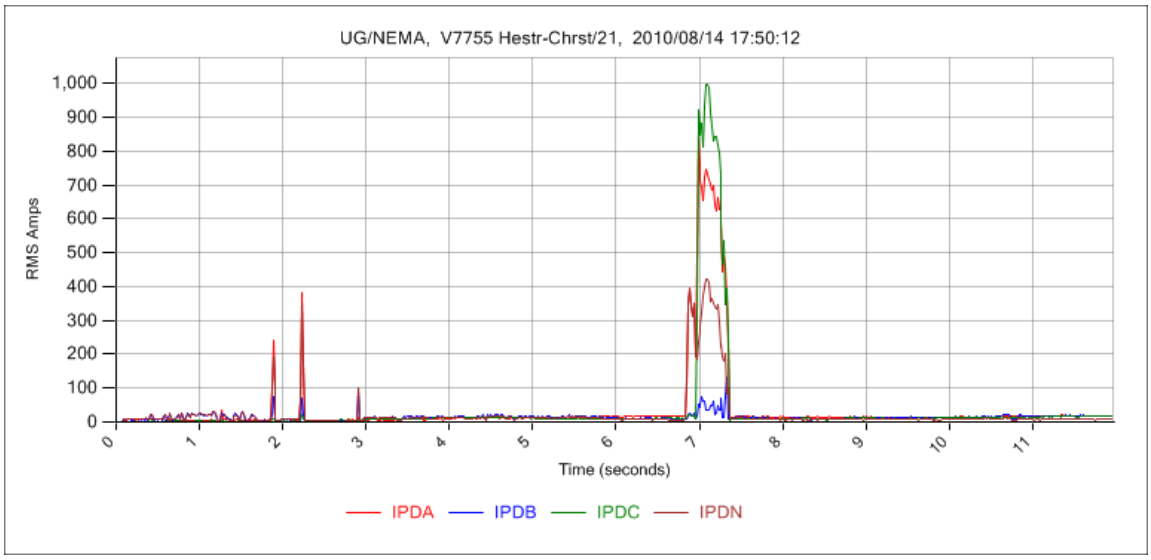

Figure 71: Initial burst, V7755, 17:50

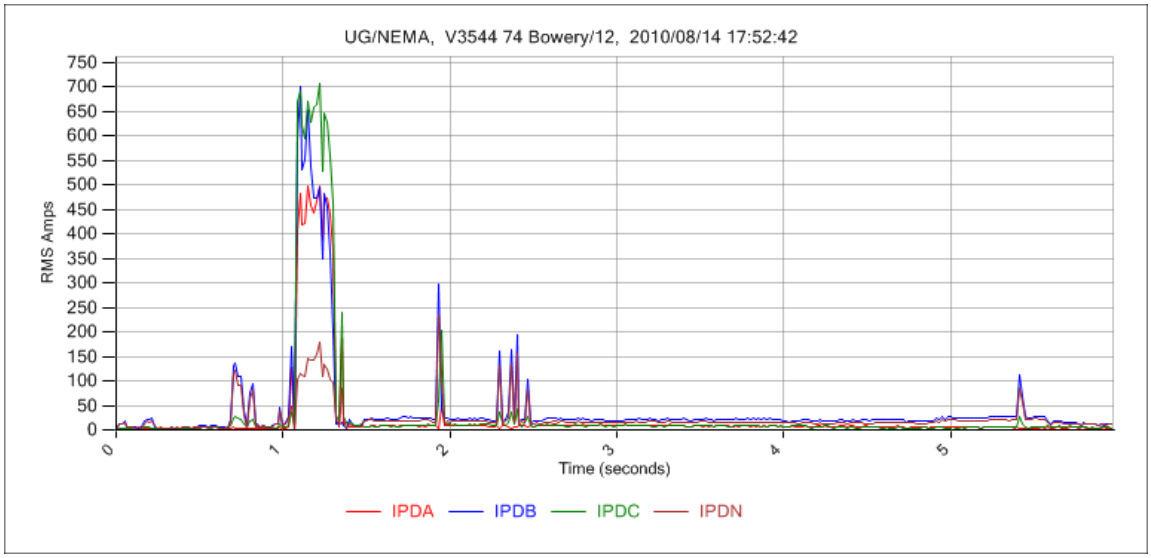

Figure 72: Three-phase burst, V3544, 17:52

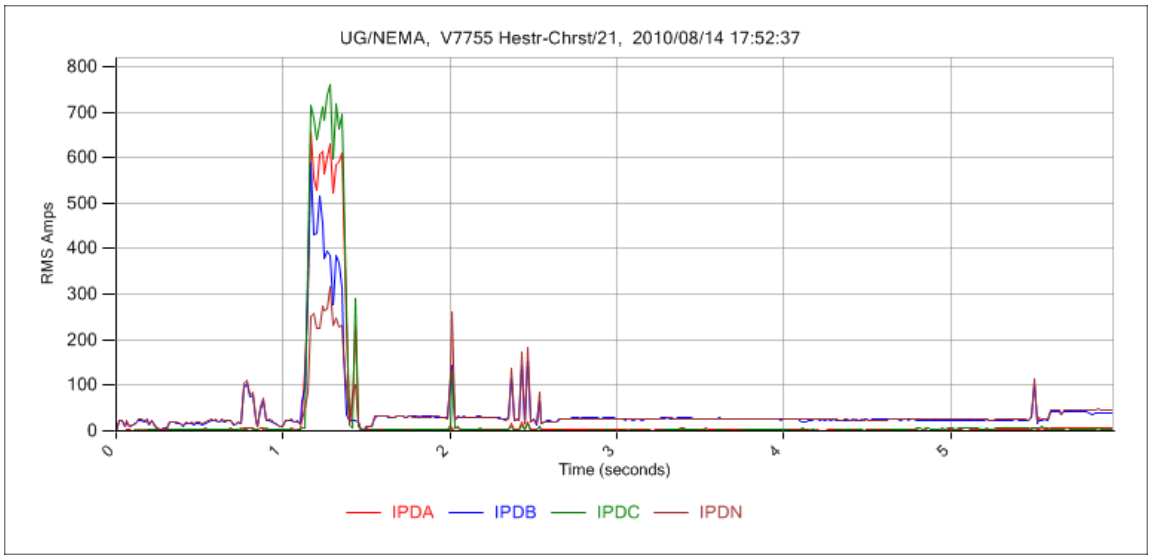

Figure 73: Three-phase burst, V7755, 17:52

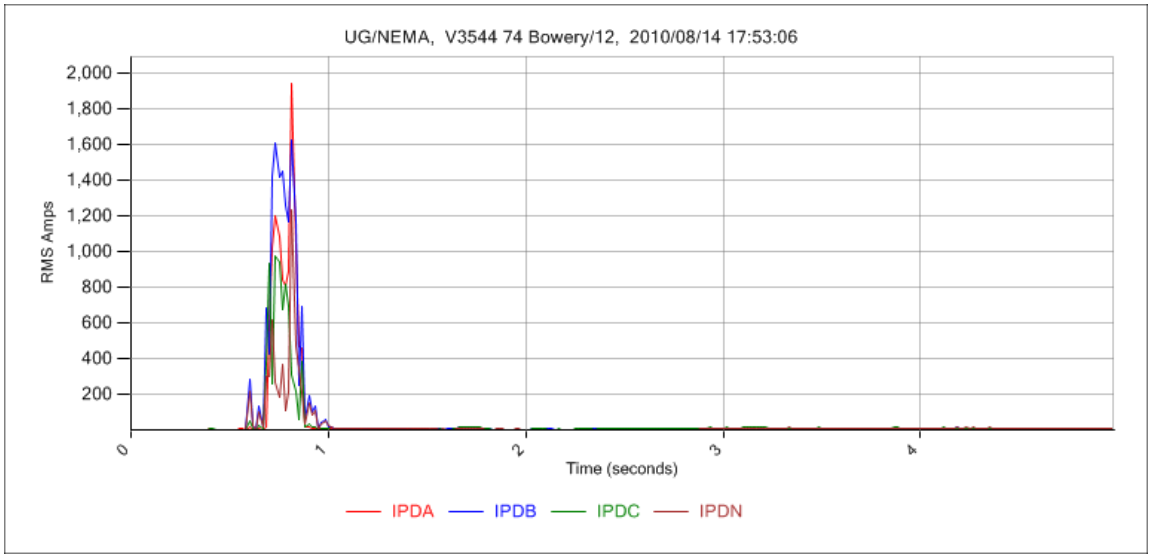

Figure 74: Major three-phase burst, V3544, 17:53

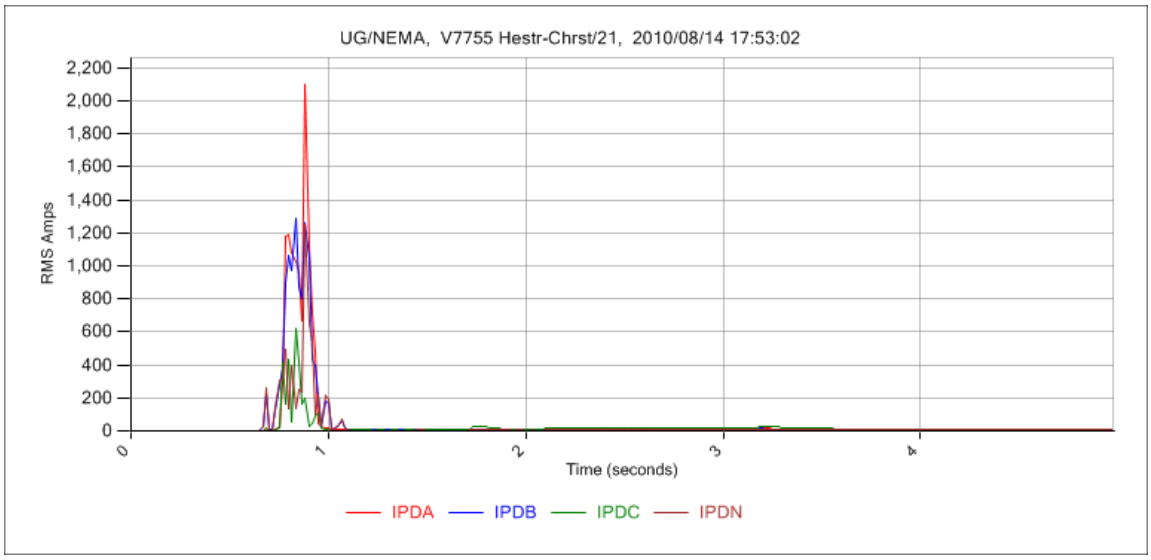

Figure 75: Major three-phase burst, V7755, 17:53

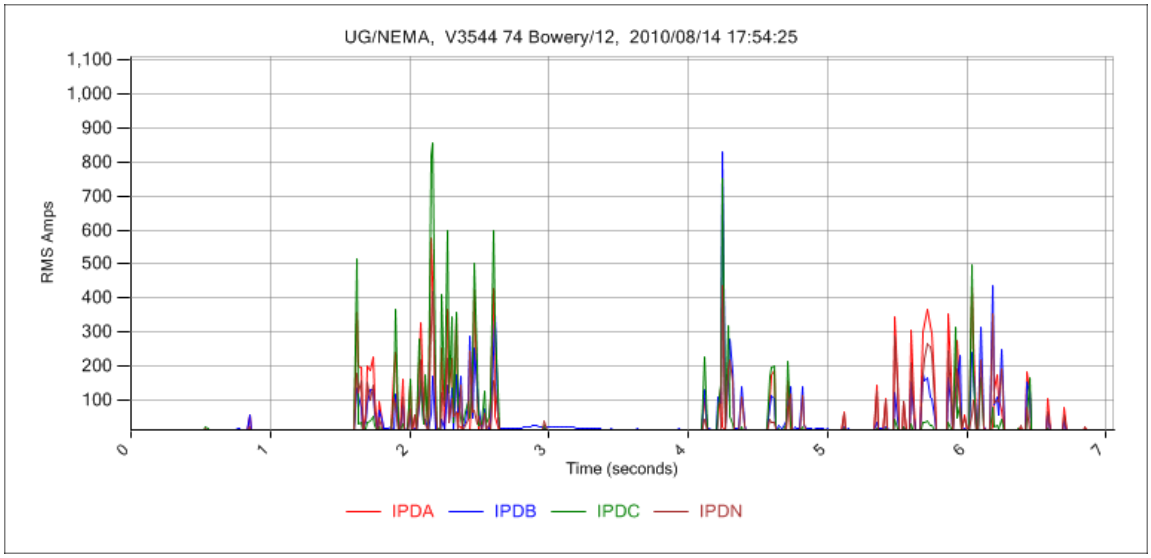

Figure 76: Three-phase burst, V3544, 17:54

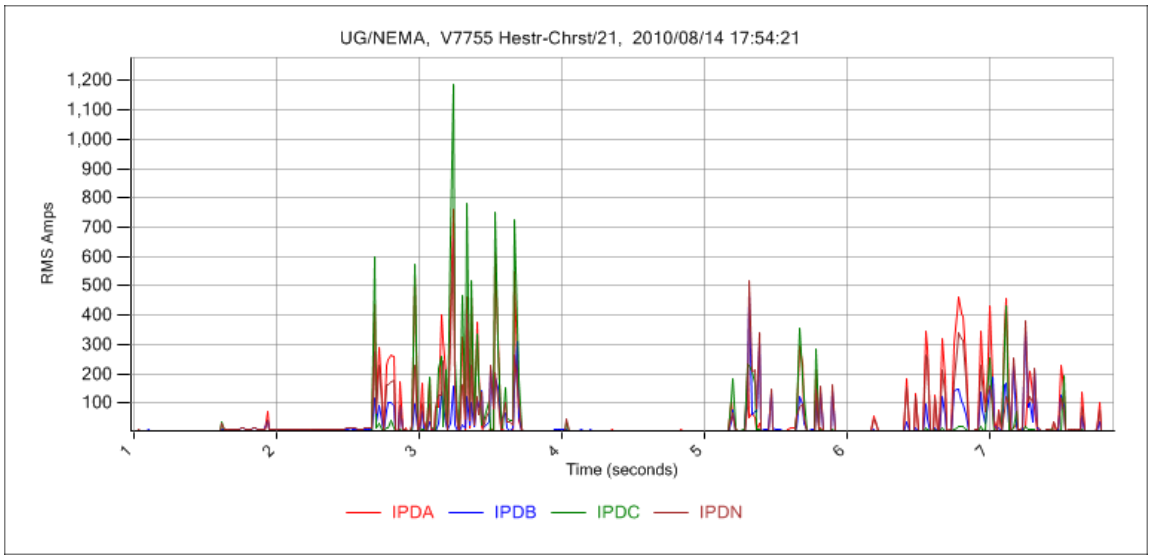

Figure 77: Three-phase burst, V7755, 17:54

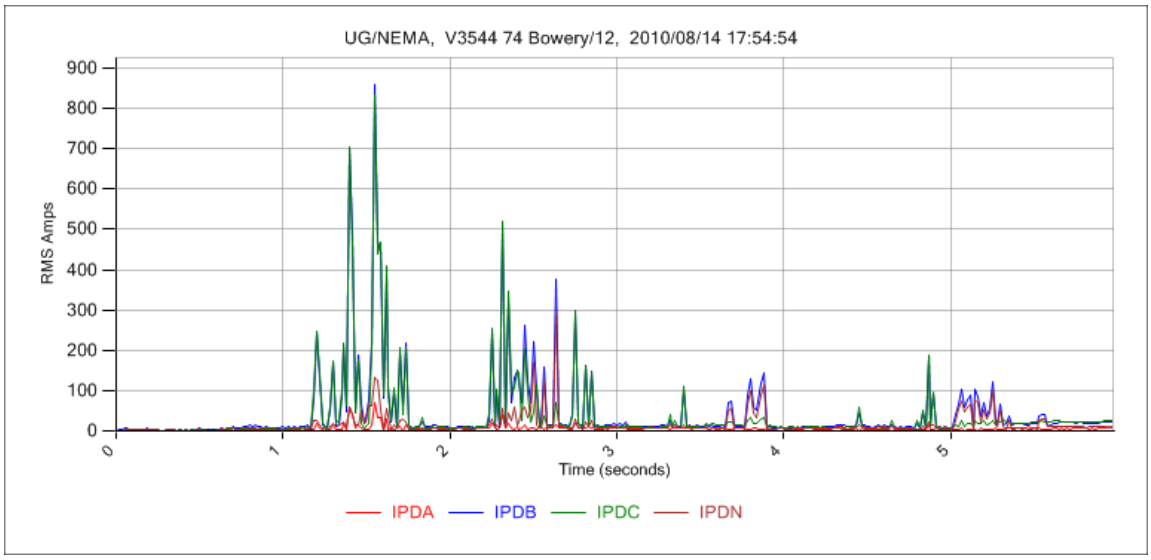

Figure 78: Phase-to-phase burst, V3544, 17:54

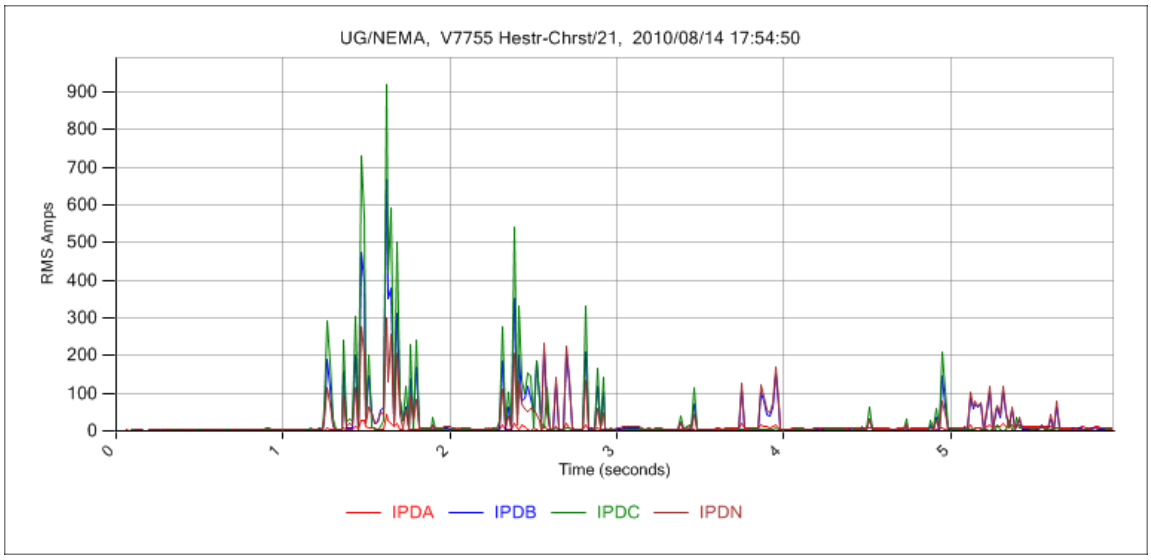

Figure 79: Phase-to-phase burst, V7755, 17:54

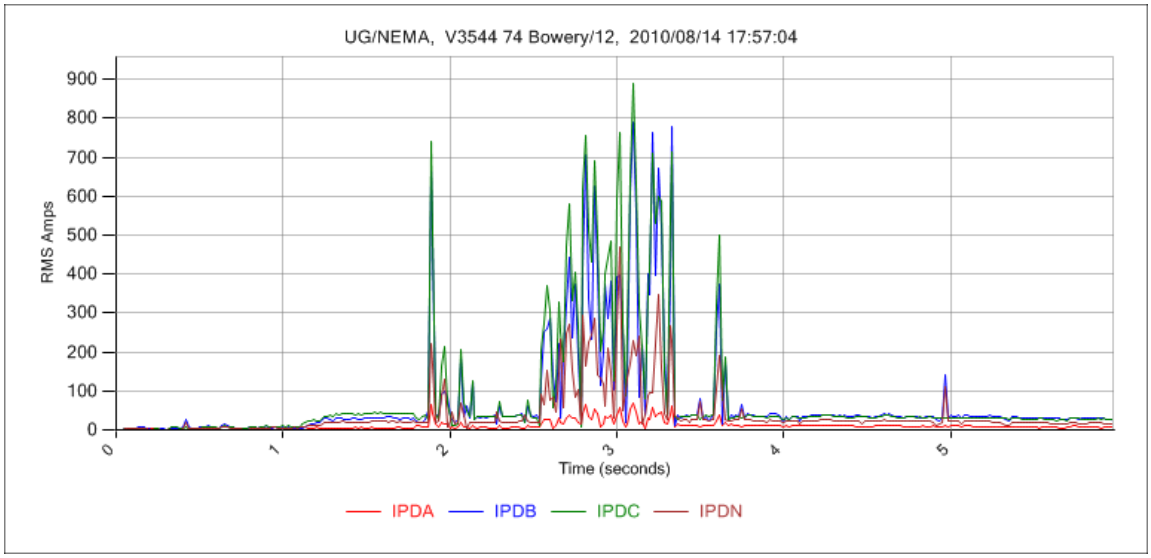

Figure 80: Phase-to-phase burst, V3544, 17:57

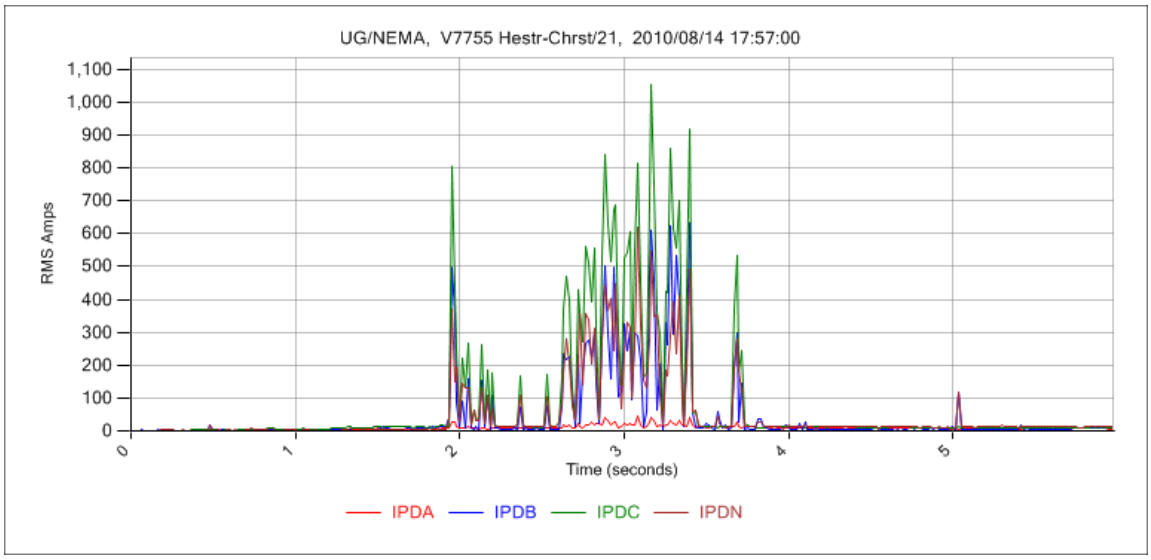

Figure 81: Phase-to-phase burst, V7755, 17:57

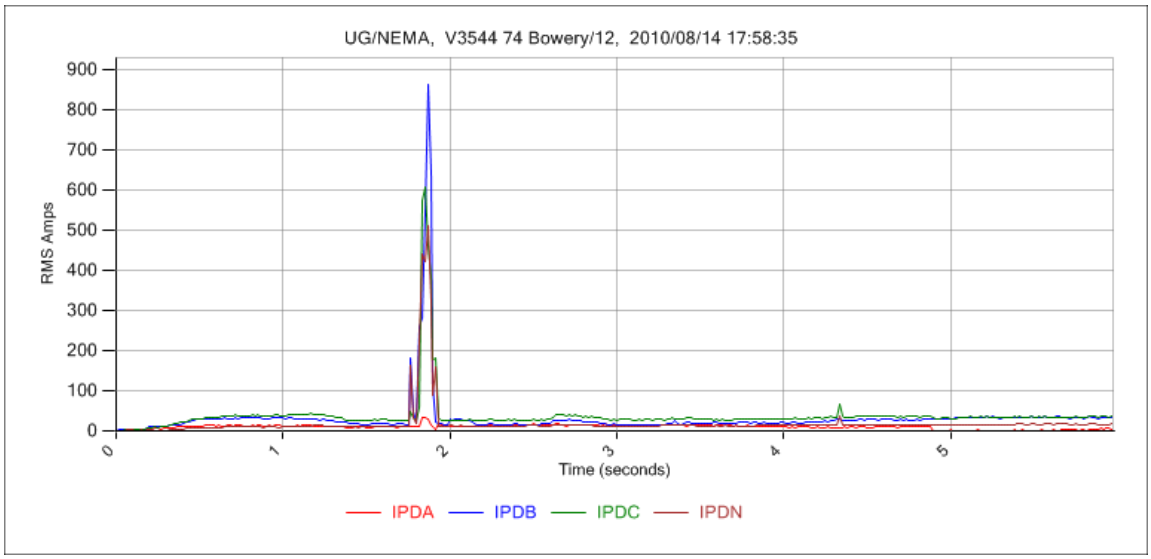

Figure 82: Final burst, V3544, 17:58

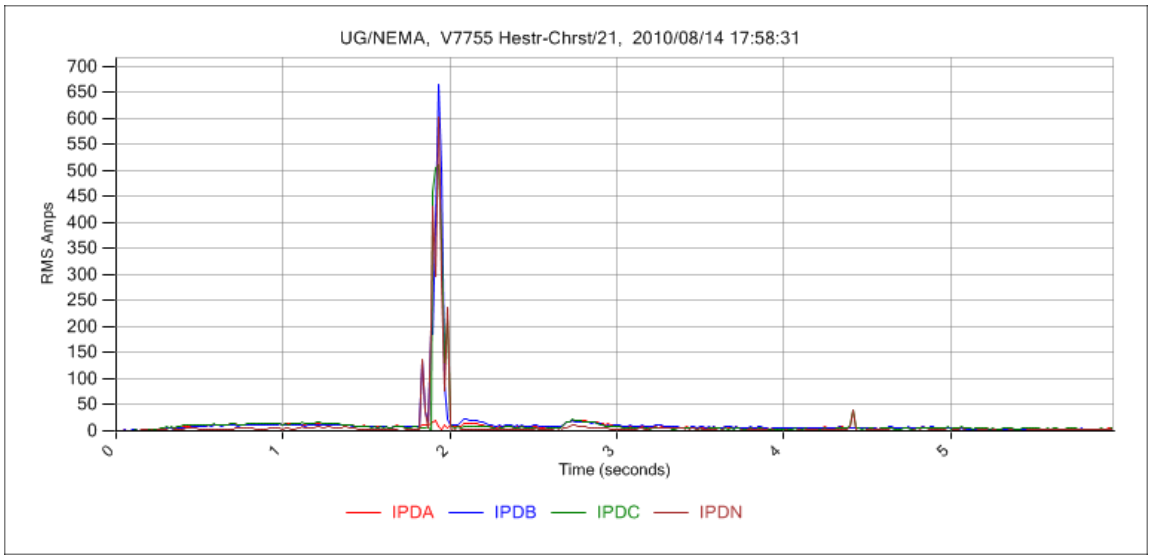

Figure 83: Final burst, V7755, 17:58

APPENDIX B: CASE STUDY 2 - NETWORK ARCING FAULT PERSISTS NEAR-CONTINUOUSLY FOR 72 HOURS

B.1 Summary

Over a 72 hour period from December 30, 2010 to the early morning hours of January 2, 2011, a single DCD located at V4413 recorded over 2,000 separate waveform captures containing arcing-related signatures. While arcing did not persist on a continuous basis, at least one arcing burst with RMS current greater than 500A was recorded for the majority of intervals recorded during this period. No manhole event was reported as a result of this activity. This case represents the longest period of time over which arcing was observed on a consistent basis at the same location without self-extinguishing, or generating enough evidence to be reported to ConEdison.

B.2 Detailed narrative

On December 26 and 27, 2010, New York City received a cumulative 20 inches of snowfall. Temperatures remained below freezing until December 30, when the high reached 40 F. Temperatures remained above freezing for all of December 31, when the recorded low was 36 F. Higher temperatures combined with record snowfalls resulted in abnormally high snow runoff, a condition believed to be closely tied with arcing activity underground.

On the morning of December 30, the DCD installed at V4413 began to observe significant numbers of arcing transients. Initially, the transients were primarily half-cycle and single-phase or phase-to-phase, though occurring once every few minutes,

with some minutes having multiple bursts. Figure 84 shows a representative example of these early waveforms. By midday on the 30th, the frequency and intensity of the bursts had increased. Due to the rate at which captures were generated, waveform files from 10:41 on December 30 to December 31 at 7:26 were not retrieved. A total of 2063 waveform captures were triggered over the three day period. All capture files retrieved contained arcing signatures.

Interval data from this period suggests arcing continued on a persistent basis for virtually the entire three day period. Figure 85 shows a plot of interval data collected over an 8 day period beginning at midnight on December 28. Data on this plot represents the maximum value of differenced current recorded over fifteen minute intervals. Of 289 interval data points observed between midnight on December 30 and 01:00 on January 2, 240 contained at least one major arcing signature, a rate of 83%.

Figure 86-Figure 91show typical waveforms captured during this period. While the majority of bursts lasted only a few cycles, they did show significant fault current magnitudes, with peaks reaching over 1,000A. The final burst, shown in Figure 91, represents much more sustained arcing activity. In spite of the significant arcing activity over an extended period of time, no manhole events were reported in the area.

This case represents one of multiple instances where arcing was recorded on a consistent basis over a period of many hours without the fault self-extinguishing or generating enough evidence to be detected by conventional means. This finding is contrary to conventional wisdom claims that arcing faults quickly burn clear in 120/208V networks.

B.3 Waveforms

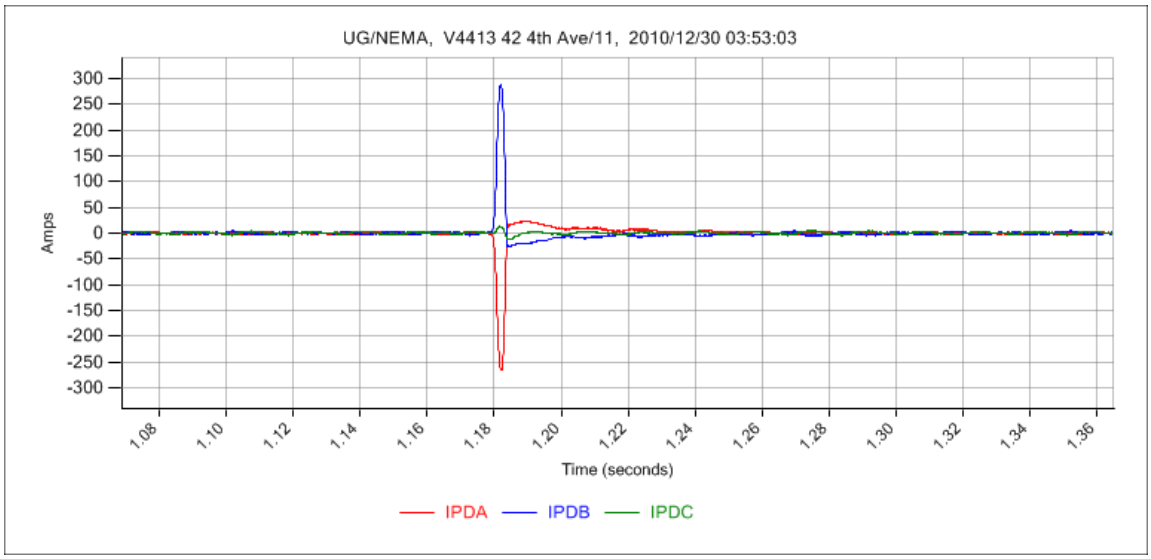

Figure 84: Early arc burst, 12/30 03:53

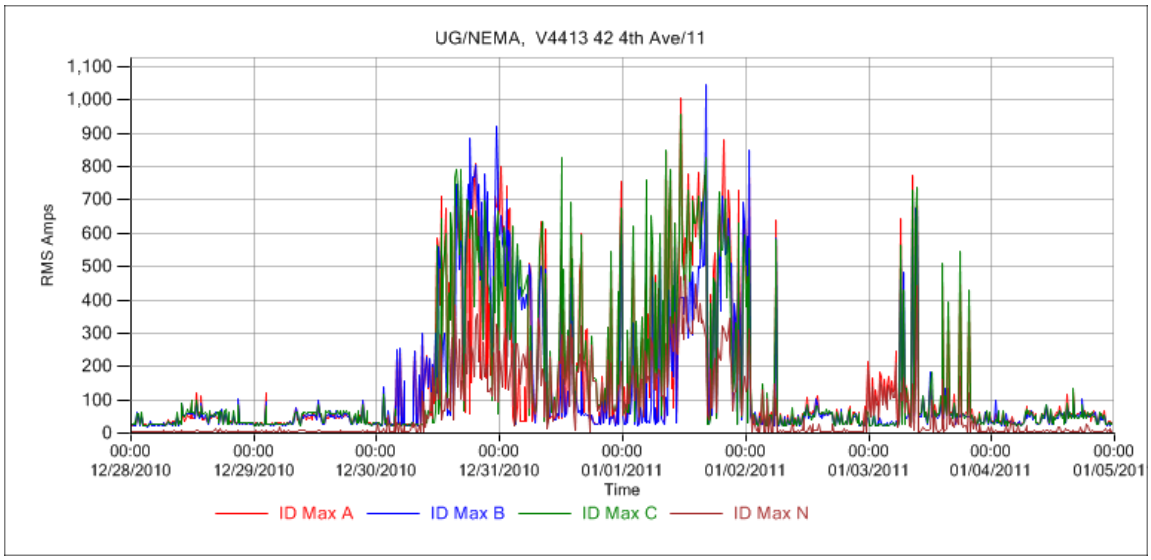

Figure 85: Interval data of maximum recorded differenced current, 12/28/2010-1/04/2011

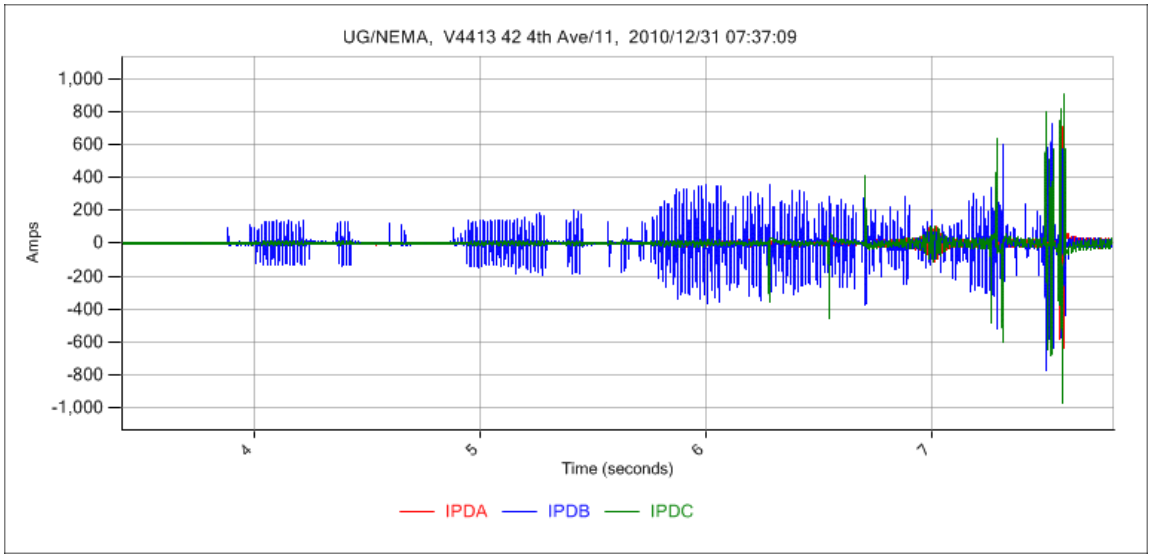

Figure 86: Multi-phase burst, 12/31 07:37

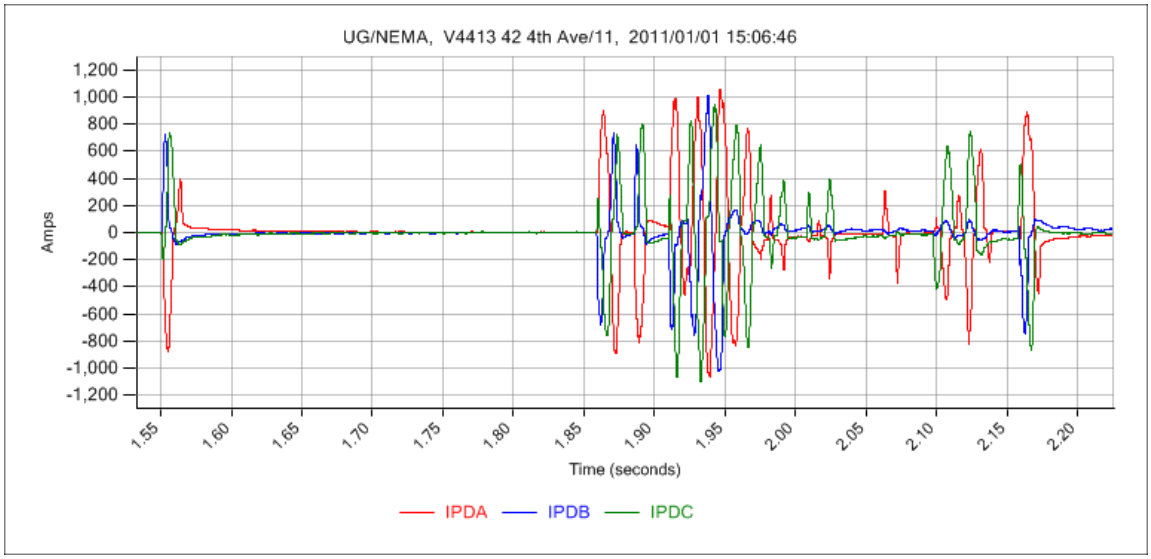

Figure 87: Three-phase burst, 1/1/2011 15:06

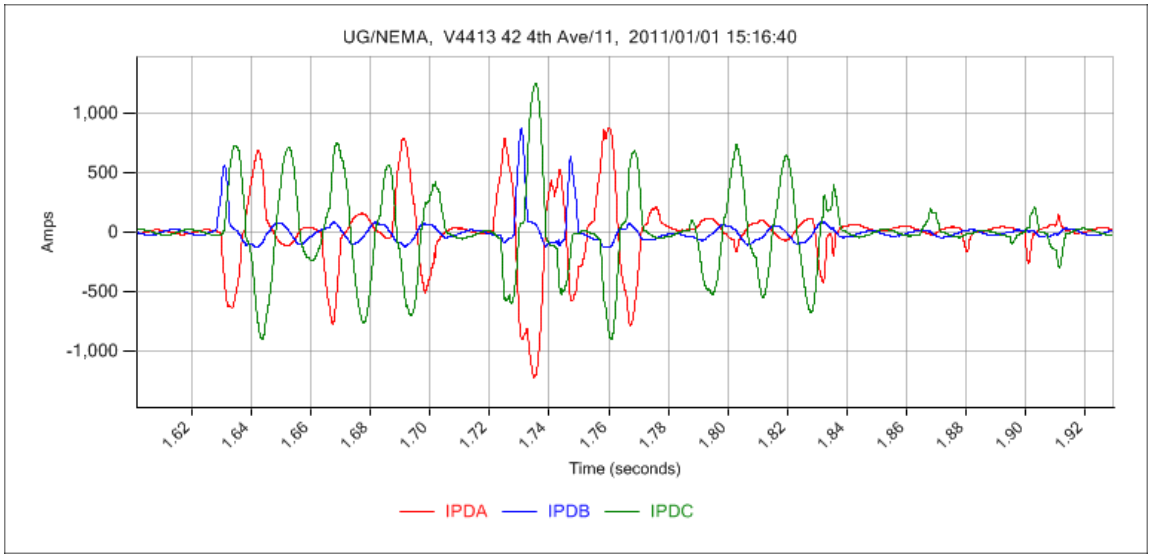

Figure 88: Three-phase burst, 1/1/2011 15:16

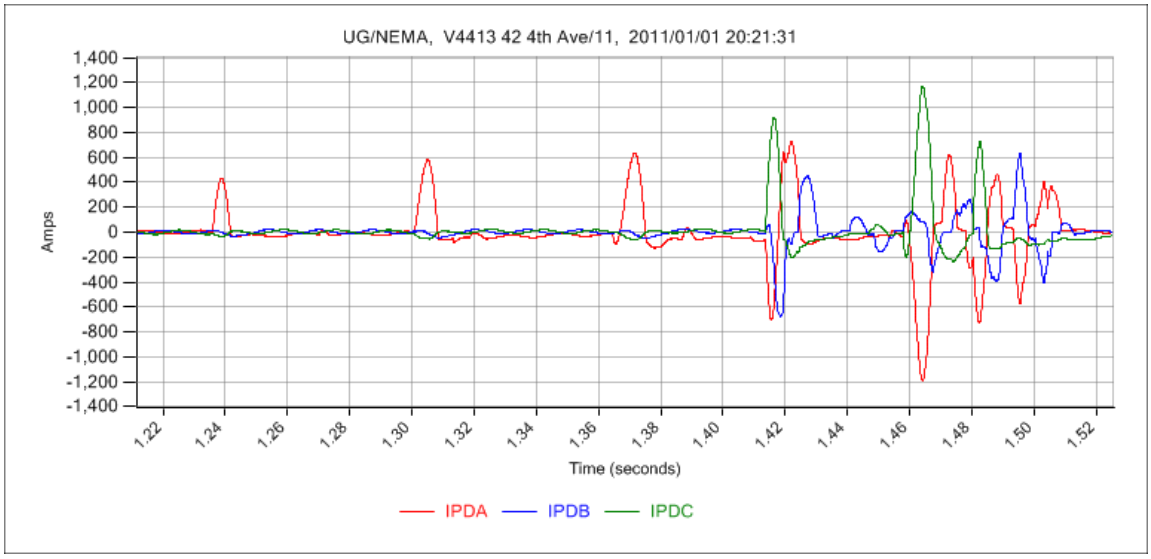

Figure 89: Three-phase burst, 1/1/2011 20:21

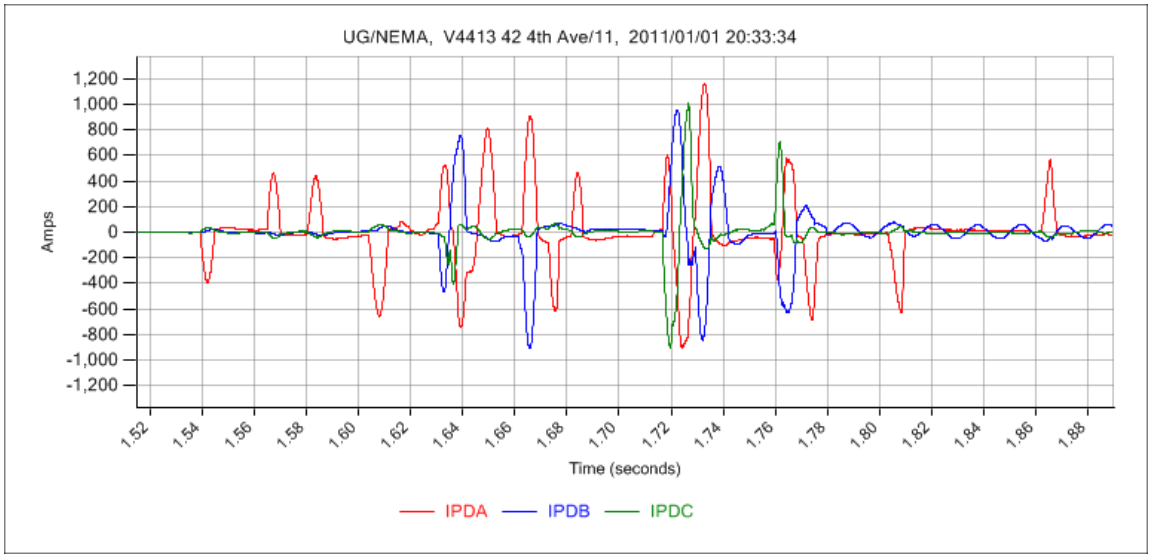

Figure 90: Three-phase burst, 1/1/2011 20:33

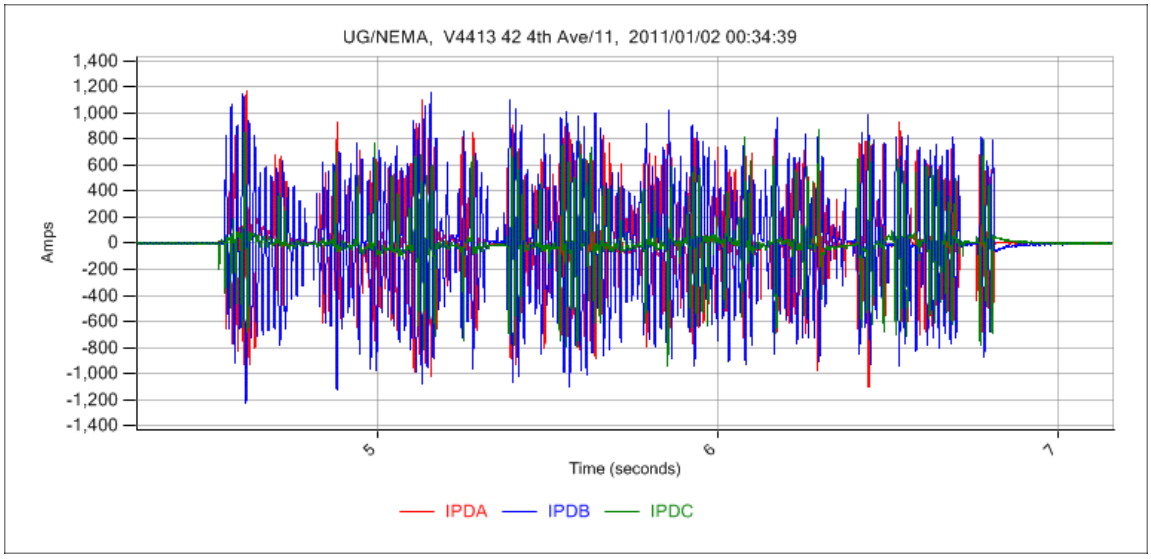

Figure 91: Three-phase extended burst, 1/2/2011 00:34

APPENDIX C: CASE STUDY 3 - SECONDARY NETWORK ARCING FAULT OBSERVED ON PRIMARY FEEDER

C.1 Summary

On the evening of November 30, 2009, two underground DCDs and a DCD monitoring a primary feeder serving the Cooper Square network simultaneously recorded a secondary network arcing fault. Fault activity continued over a period of seven hours. Following a fifteen-hour quiescent period, arcing resumed the following evening. During a four-hour period on the evening of December 1, 2009, three underground DCDs and the substation monitor recorded simultaneous arcing measurements. A timeline of events is contained in Figure 92. This is believed to be the first time secondary network arcing has been simultaneously measured on the secondary network and a primary feeder serving the network.

C.2 Detailed narrative

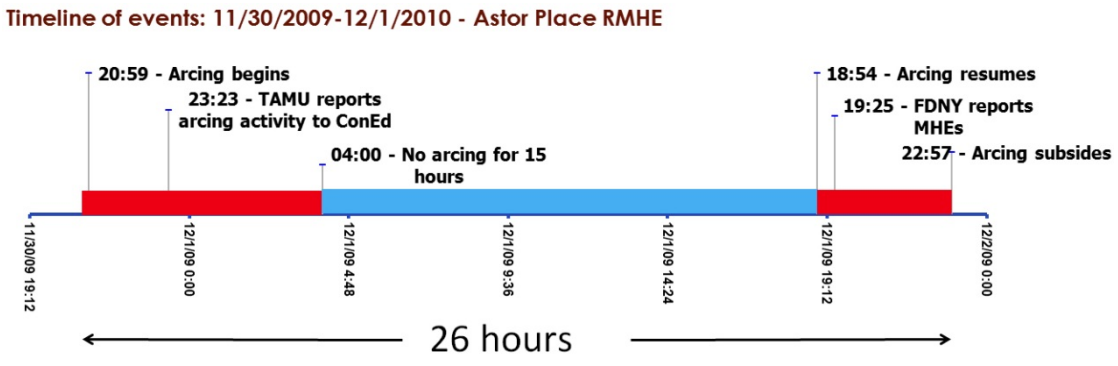

Figure 92: Timeline for Case Study 8.3

At approximately 21:00 on the evening of November 30, 2009, two underground DCDs and a DCD at the Ave. A. Area substation recorded substantial arcing signatures. Arcing continued intermittently at all three locations for the next seven hours. By chance, researchers noticed the activity on the evening of November 30, and reported it to ConEdison less than three hours after it began. The following morning, a search of outage tickets showed no report of a manhole event associated with arcing on the evening of November 30, or the morning of December 1.

At 18:54 on the evening of December 1, arcing resumed at all three installations which had observed arcing the previous evening, and was also detected at a third underground monitor. At 19:25, the Fire Department of New York (FDNY) reported two adjacent smoking manholes in the vicinity of the three underground monitors. All four monitors continued to observe significant arcing over the next four-hours, before crews were able to isolate the problem and cut the affected mains.

Figure 93-Figure 96 show waveforms recorded during the four-hour portion of near-continuous arcing observed on the night of December 1. Figure 93-Figure 95 show measurements recorded at underground locations, while Figure 96 shows the same recording as viewed from the primary. Figure 97-Figure 100 show a zoomed portion of the same waveforms.

There are several points of interest regarding these waveforms. First, secondary network arcing activity is clearly seen on the primary feeder. Once the transformer's turns ratio has been accounted for, the primary feeder is sourcing over 1,000A to the

fault on the secondary, in addition to the current coming from the three underground monitors, none of which are served by this feeder. Second, there is not a 1:1 correspondence in waveforms between primary and secondary measurements, which is expected since the primary monitor is viewing the fault from the delta side of a delta-wye transformer, and the fault is on the wye side. In more simple fault cases, predicting primary side fault behavior is relatively straightforward. For instance, a single-phase fault occurring on the secondary produces a phase-to-phase fault when seen on the other side of a delta-wye transformer. Once the fault becomes more complicated and involves several phases, however, such predictions become much more difficult.

The conclusion that secondary network arcing can be observed from primary feeders serving the network was a surprising finding for many engineers. Before these recordings, it was generally believed that arcing fault currents would be too small to be seen at the area substation. This finding does lay the possible foundation for a system which could be installed on primary feeders and used to detect arcing in underground structures.

Such a system would have numerous practical benefits over a system installed on the secondary. One obvious advantage would be a substantially reduced number of monitoring points. Most primary feeders on a network serve on the order of 10 transformers, implying a primary feeder-based system would only need 10% of the points for the same amount of coverage. Additionally, substation installations do not need to be field hardened to the same extent as devices intended to operate underground.

Most substations also have communication of some sort, while communication to underground devices is extremely challenging.

Significantly more research is needed before a substation-based system capable of detecting and locating arcing faults is a practical reality, but these recordings, as well as hundreds of others obtained from primary feeder measurements during this project, suggest the viability of such a system.

C.3 Waveforms

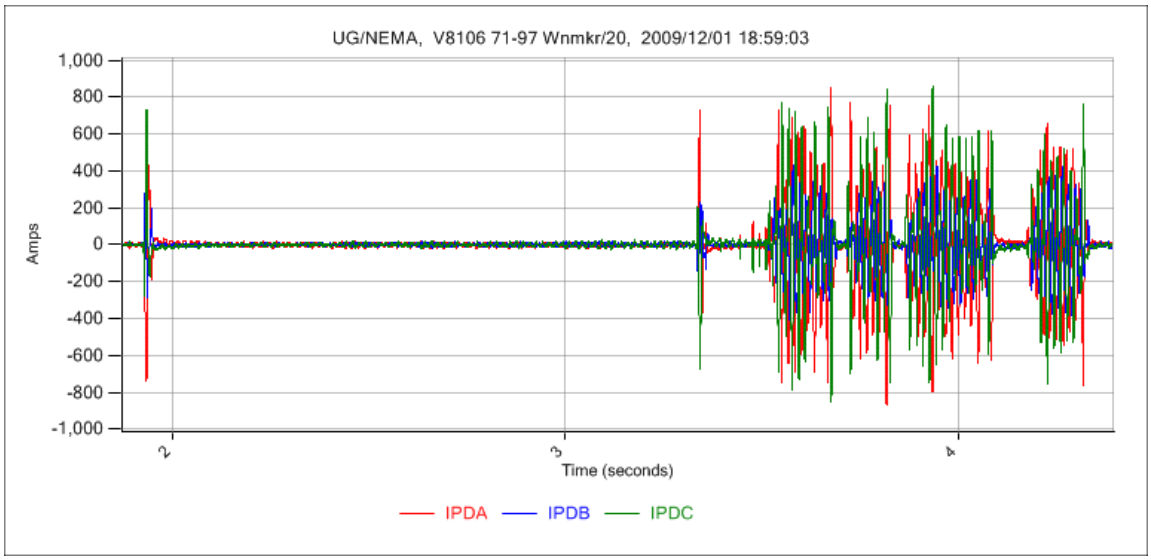

Figure 93: Simultaneous arcing fault, V8106 (secondary)

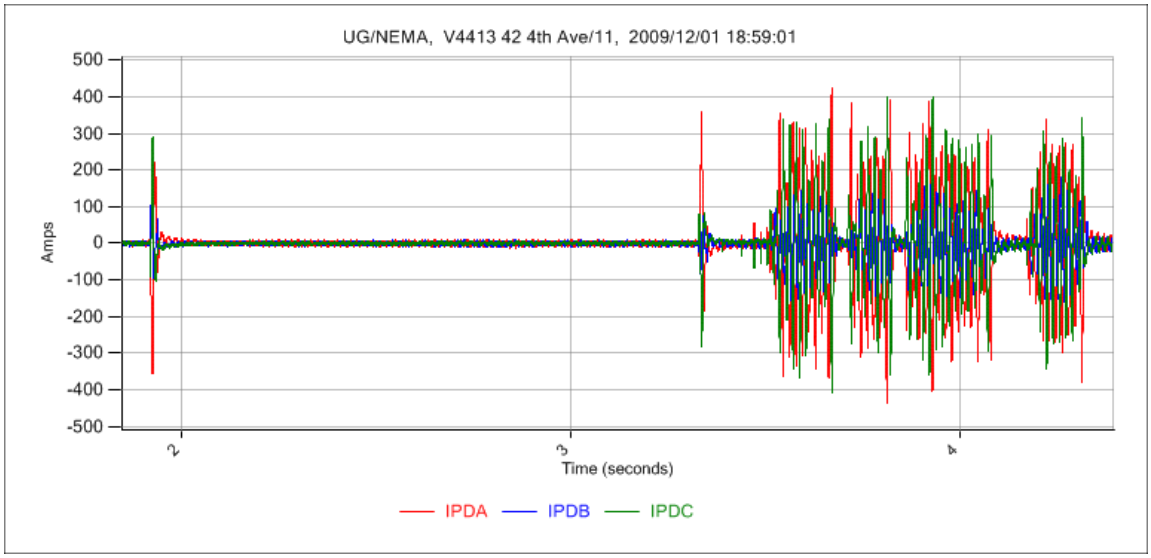

Figure 94: Simultaneous arcing fault, V4413 (secondary)

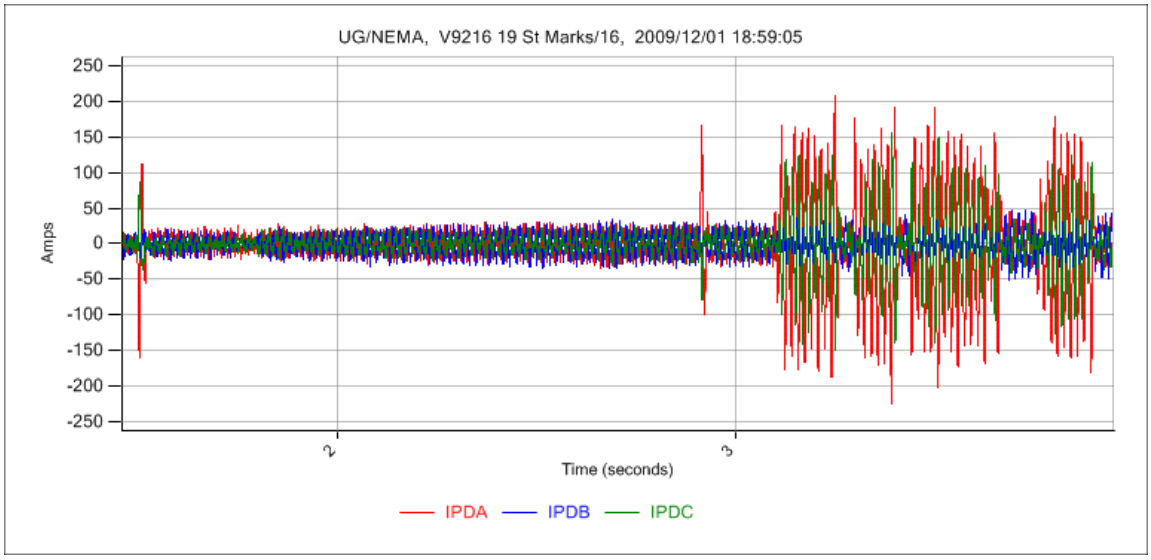

Figure 95: Simultaneous arcing fault, V9216 (secondary)

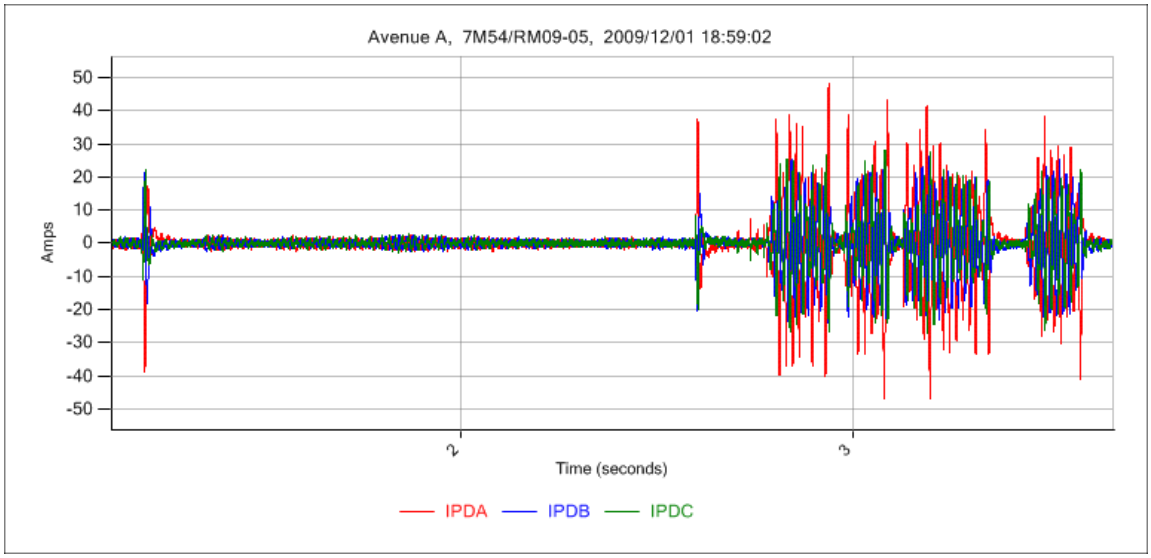

Figure 96: Simultaneous arcing fault, Ave. A. 7M54 (primary)

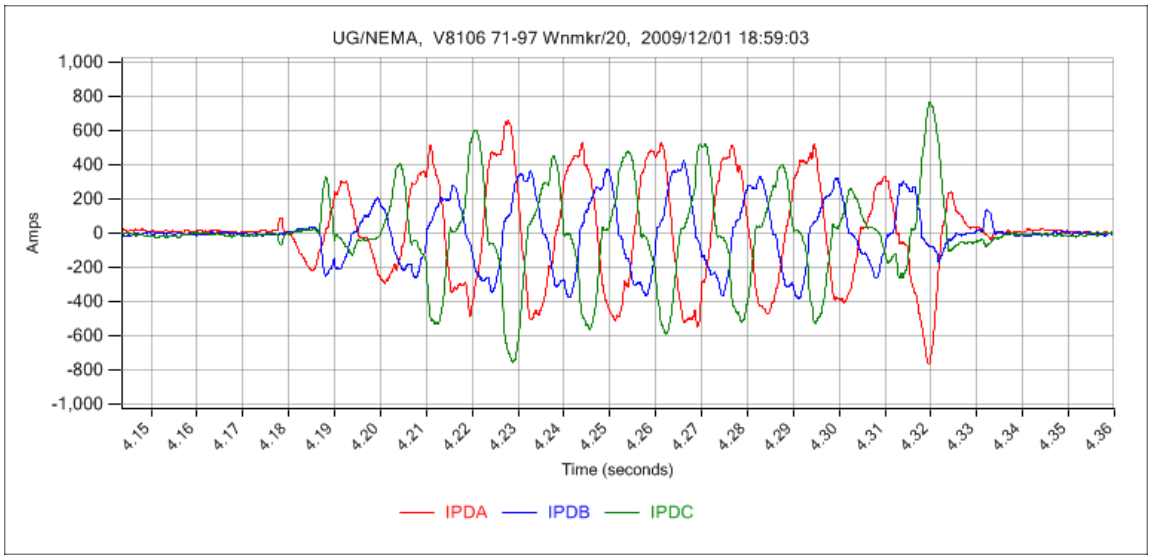

Figure 97: Simultaneous arcing fault, zoomed, V8106 (secondary)

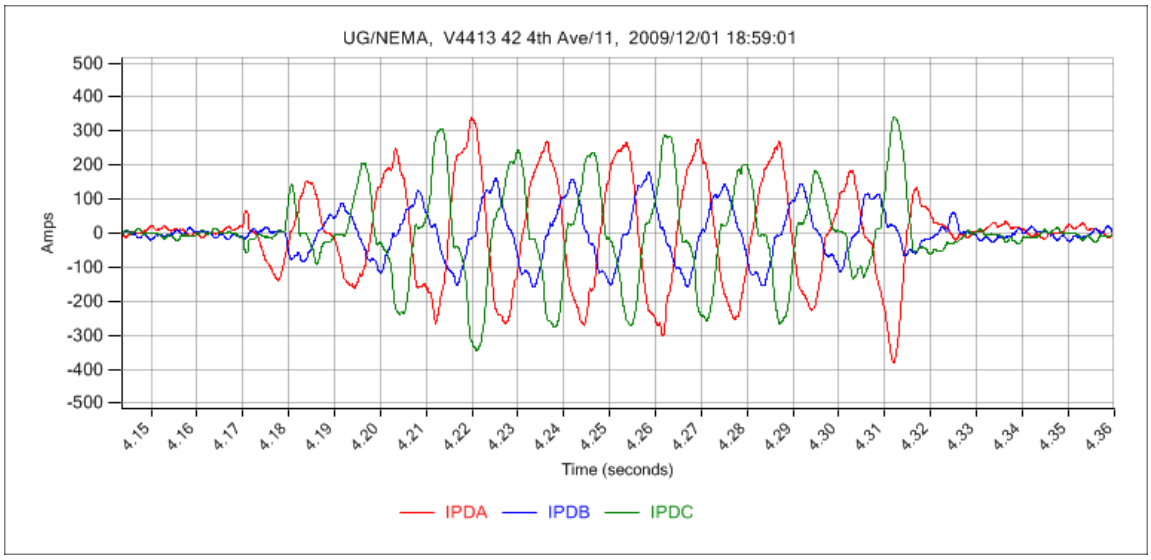

Figure 98: Simultaneous arcing fault, zoomed, V4413 (secondary)

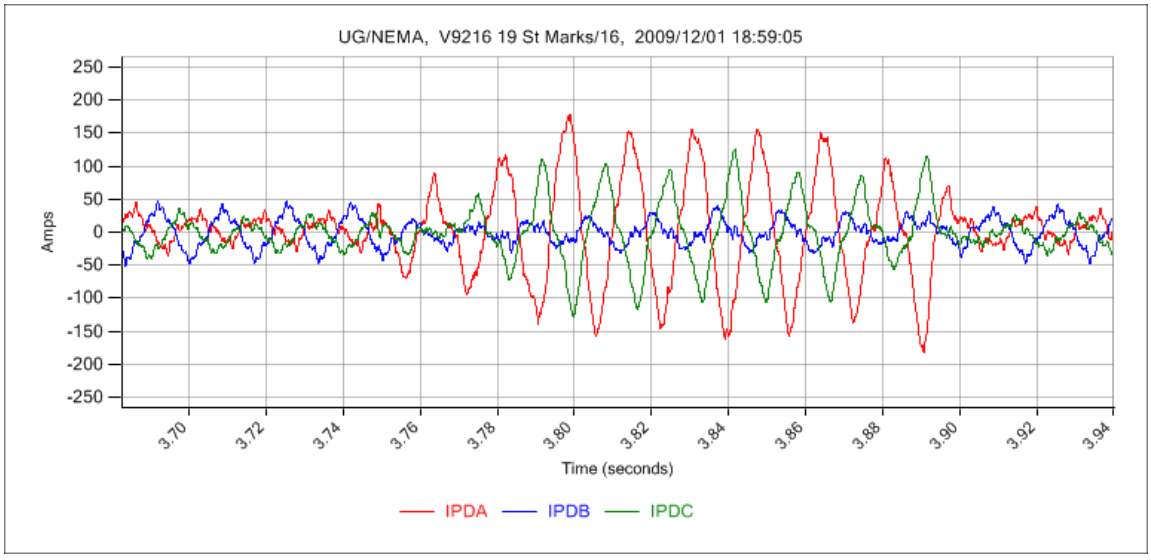

Figure 99: Simultaneous arcing fault, zoomed, V9216 (secondary)

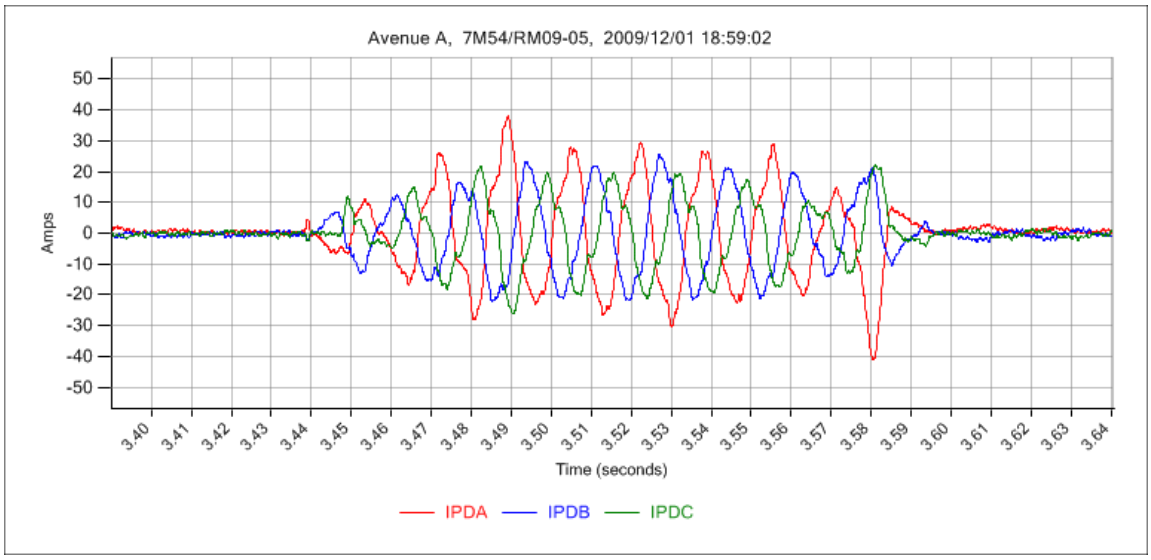

Figure 100: Simultaneous arcing fault, zoomed, Ave. A 7M54 (primary)

APPENDIX D: CASE STUDY 4 - ARCING FAULT PERSISTS FOR THREE WEEKS BEFORE BEING LOCATED

D.1 Summary

On March 13, 2010, two DCDs recorded significant arcing bursts. These bursts continued sporadically over the next 18 days. ConEdison was informed of the arcing activity on March 23. Acting on measurements obtained from the DCDs, ConEdison was able to use internal tools to locate the fault and make repairs. No further arcing episodes were observed, suggesting the problem was fixed.

D.2 Detailed narrative

On the morning of March 13, 2010, two underground DCDs recorded multiple three-phase arcing bursts. This arcing continued over a period of almost seven hours, with a two hour quiescent period in the middle. Over the next 21 hours, both data collection devices continued to record arcing-related signatures, with alternating periods of arcing and quiescence measured in hours.

Figure 101 shows the initial burst, as observed at one of the units. Figure 102 shows an additional burst captured 16 hours after the original observation. Figure 103 shows a burst captured 28 hours after the initial observation. Following the activity shown in Figure 103, no activity was observed at either unit for a period of five days. Additional episodes were observed on March 19, March 23, March 29, and March 30. Figure 104 shows a plot of arcing observed 16 days after the initial burst. On March 23, ConEdison was informed of the arcing activity. On March 25, based on information

obtained from DCD measurements, ConEdison dispatched trucks designed to detect elevated voltages on structures to the area proximate to the two DCSs. On March 31, after several nights of searching, one truck found multiple energized structures half a block from the two data collection devices. A crew was dispatched the next morning and found significant damage to mains in proximate structures. Following repairs, no additional arcing was detected, and the problem was considered to be resolved.

The plot in Figure 105 shows interval data collected from this DCD between March 13 and April 1, 2010. The plot represents the maximum value of cycle-to-cycle differenced current that was recorded in each 15 minute interval over this time period. In the graph, clear periods of activity are spaced with long periods of quiescence.

This case represents clearly that in some cases, arcing faults can continue over a period of weeks in an incipient condition without self-extinguishing. While there is no way to know how long the incipient fault would have persisted without utility action, it can be certain that, at least for a period of 18 days, the fault persisted in an incipient condition that had neither fully self-extinguished, nor generated any evidence to indicate there was a problem. This represents a clear contradiction to what most utility engineers perceive to be conventional wisdom. In short, arcing faults can, and many times do persist over days or weeks before causing a final failure.

D.3 Waveforms

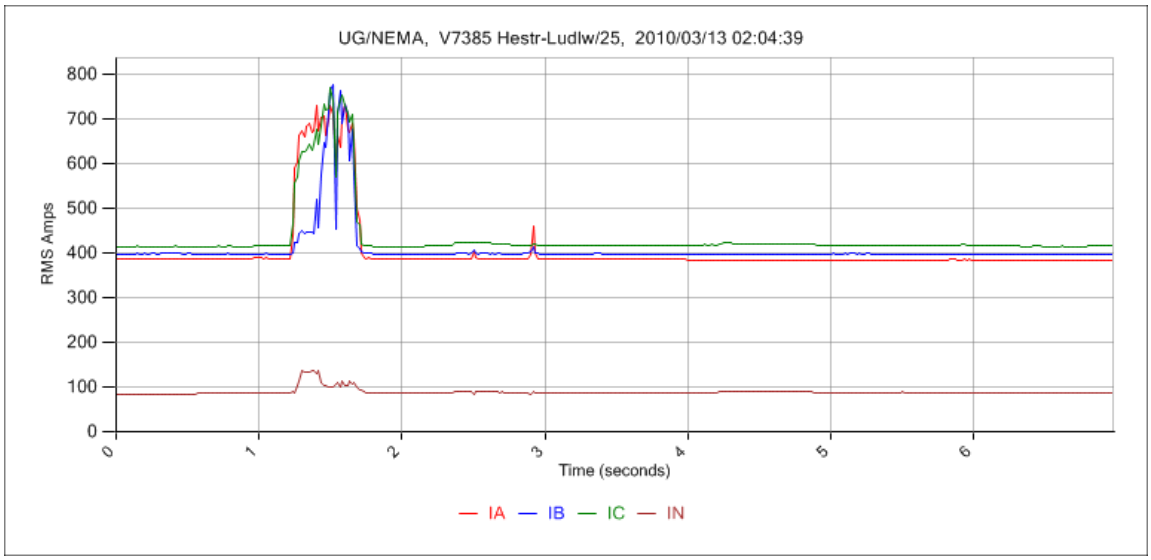

Figure 101: Initial observed arc burst

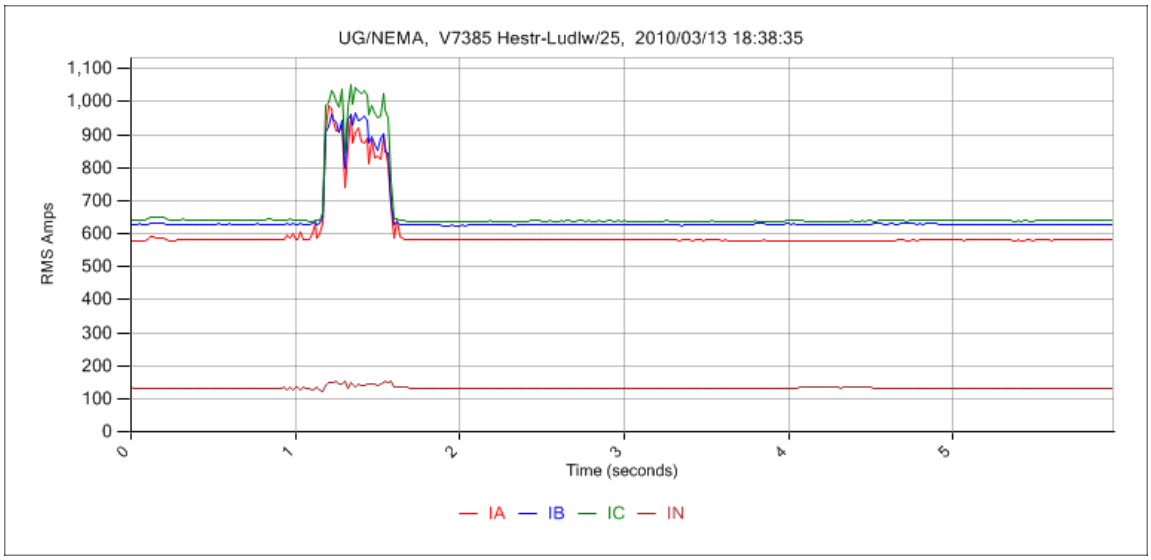

Figure 102: Additional arcing, observed 16 hours after original burst

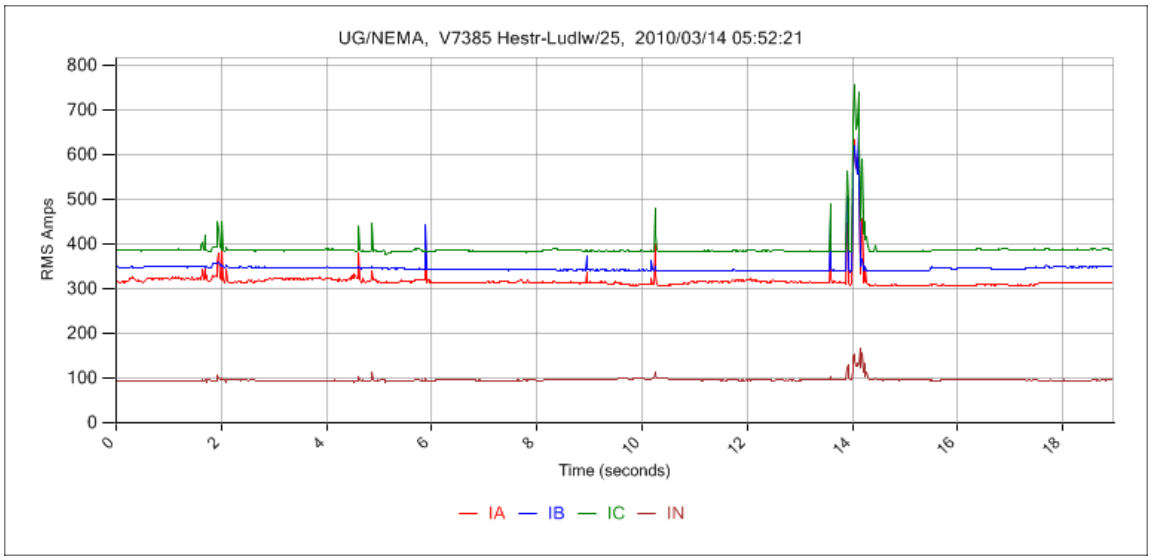

Figure 103: Additional arcing, observed 28 hours after initial burst

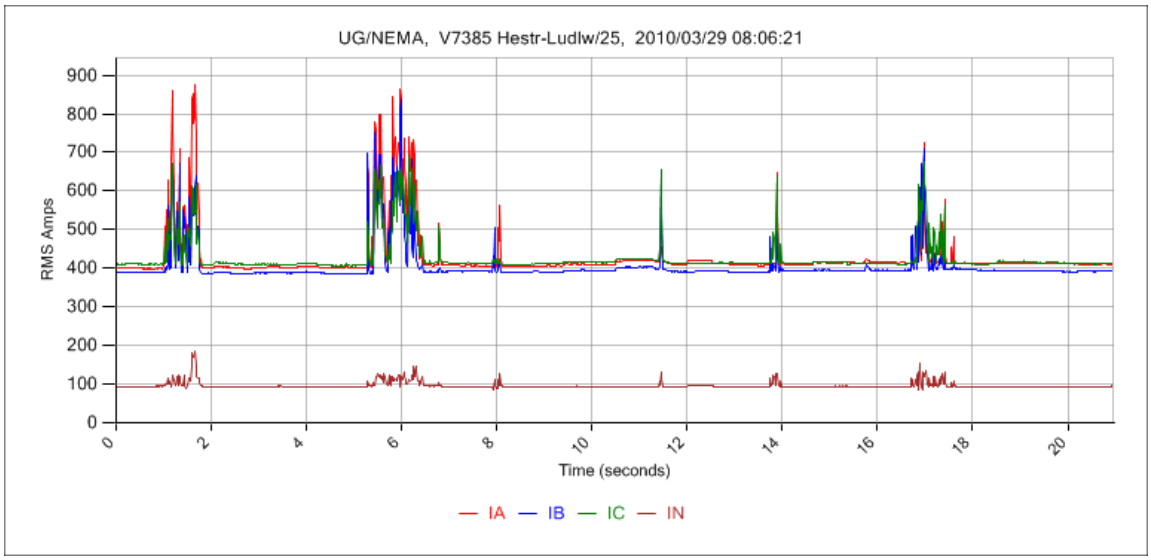

Figure 104: Additional arcing, observed 16 days after initial burst.

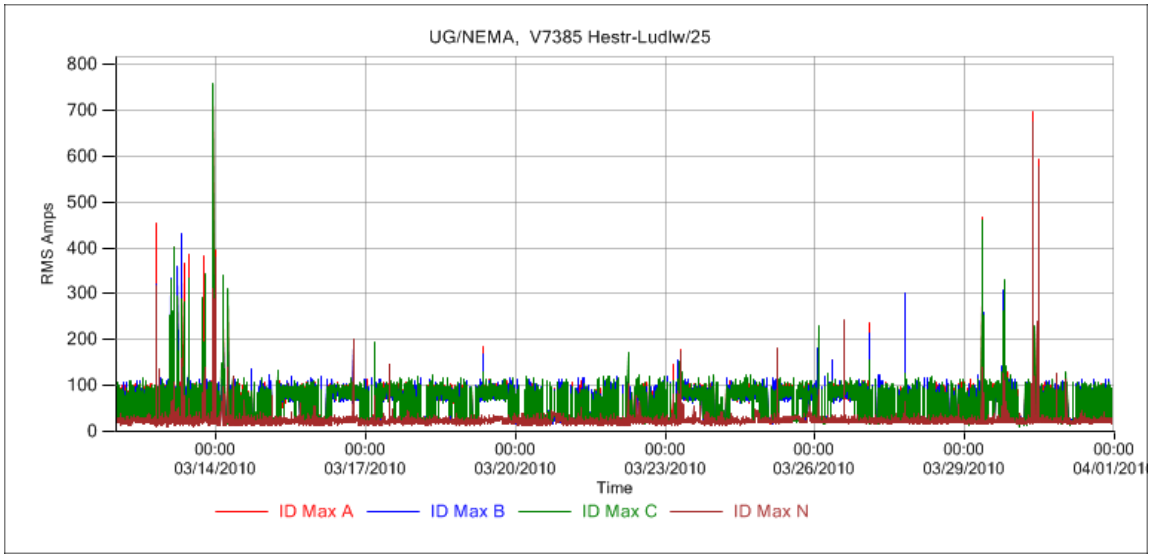

Figure 105: Plot of maximum transient currents observed during 15 minute intervals, March 13-April1, 2010

APPENDIX E: CASE STUDY 5 - ARCING FAULT OBSERVED AT FIVE UNDERGROUND LOCATIONS

E.1 Summary

On the evening of January 12, 2011, five proximate DCDs simultaneously recorded current from an arcing fault. Damaged cables from this fault then lay dormant for the next four months, resulting in an incipient condition and creating the potential for a future manhole event. Based on measurements obtained during this arcing fault, researchers used ConEdison's Poly-Voltage Loadflow (PVL) software to predict the structure most likely to contain the incipient event. A crew inspected the structure and found multiple burned out cables. Repairs were completed, avoiding future consequences.

E.2 Detailed narrative

On the evening of January 12, 2011, five proximate DCDs recorded a phase-to-phase arcing fault on the Cooper Square network. This represented the first time an event was observed simultaneously by five underground monitors. Because so many monitors observed the event, it provided an excellent test-case to explore how arcing fault currents distribute themselves around the network, and in particular how well real data matched modeling software used by ConEdison.

Figure 106 shows the locations of the five DCDs which observed the event, as well as the maximum peak fault current magnitudes observed at each location. Figure 107-Figure 111 show the actual recorded arcing waveforms for each of the five

locations. When the project began, there was a large degree of uncertainty about how far fault currents might travel across the network. Over the course of the project, researchers began to feel that a unit needed to be relatively “close” to an event to see any substantial fault current. Readings from this event would allow researchers to quantify that, if the location of the faulted structure could be found.

Figure 106: Locations of DCDs and fault currents observed

ConEdison provided researchers with access and training for their Poly-Voltage Loadflow program (PVL). PVL is an internal tool developed by ConEdison which performs a variety of functions, including allowing the user to simulate a bolted, three-phase fault at any structure on the network and calculate an expected fault current at every structure due to that fault. Arcing faults have a finite impedance and, by definition,

are not bolted faults. Many arcing faults, including this one, are also not three-phase events. As a result, it was expected that PVL estimates for fault current would be substantially greater than readings produced by the DCDs. However, it was hoped the relative magnitudes predicted by PVL would match the values observed by the DCDs.

Because the current observed at V9742 was extremely high, researchers began by running PVL simulations for faults in structures proximate to V9742. The first structure run was M53933, a structure adjacent to V9742, and the resulting current distribution fit reasonably well with observed values. A ConEdison crew was dispatched to the structure to check for damage, but found none. Following this, researchers ran PVL simulations at ten underground structures near V9742 and developed multiple error functions to quantify the structure with the best fit. Of the ten structures tested SB53931, SB53930, and M53933 consistently had the lowest error values.

Table 5 shows error values for the five underground structures with the lowest overall absolute error. Cells shaded red represent the highest error values on a per row basis, where cells shaded blue represent the lowest error values. SB53931 consistently showed the lowest error values across all functions tested. Based on these results, ConEdison dispatched a crew to SB53931 to inspect the structure for damage. The crew found multiple burned out cables, and made the appropriate repairs.

Table 5: Error values for PVL simulation

Error Function	M53934	M53933	53926	53931	53930
Percentage Difference	0.805	0.891	0.905	0.475	0.742
Weighted % Difference	0.046	0.050	0.052	0.021	0.039
Ratio Difference	0.073	0.042	0.087	0.021	0.057
Ratio Percentage Difference	1.258	0.726	1.518	0.477	1.140
Weighted Ratio % Difference	0.005	0.003	0.006	0.001	0.003

E.3 Waveforms

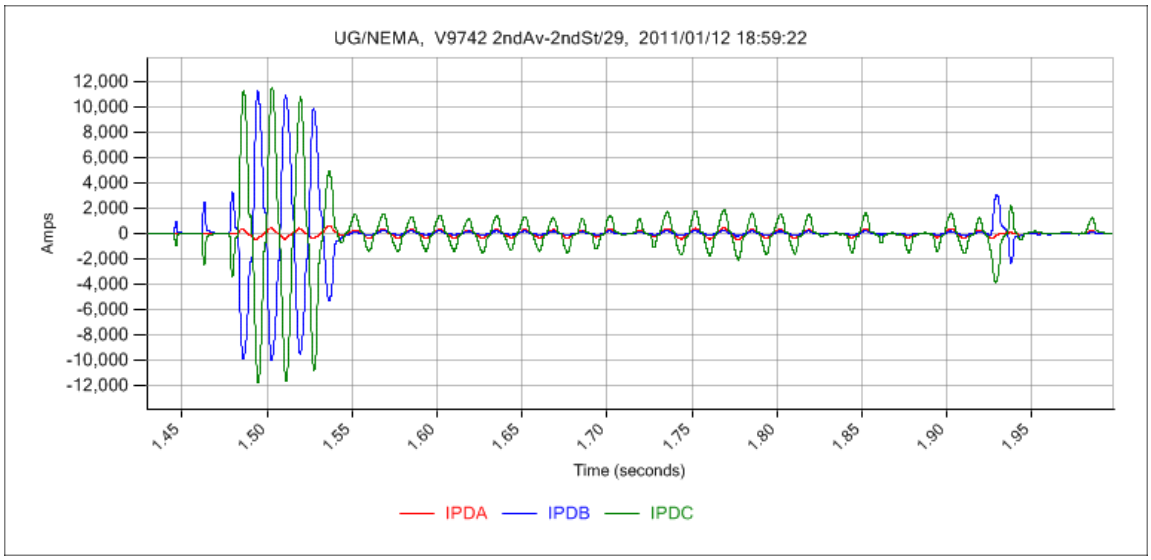

Figure 107: Arcing burst, V9742

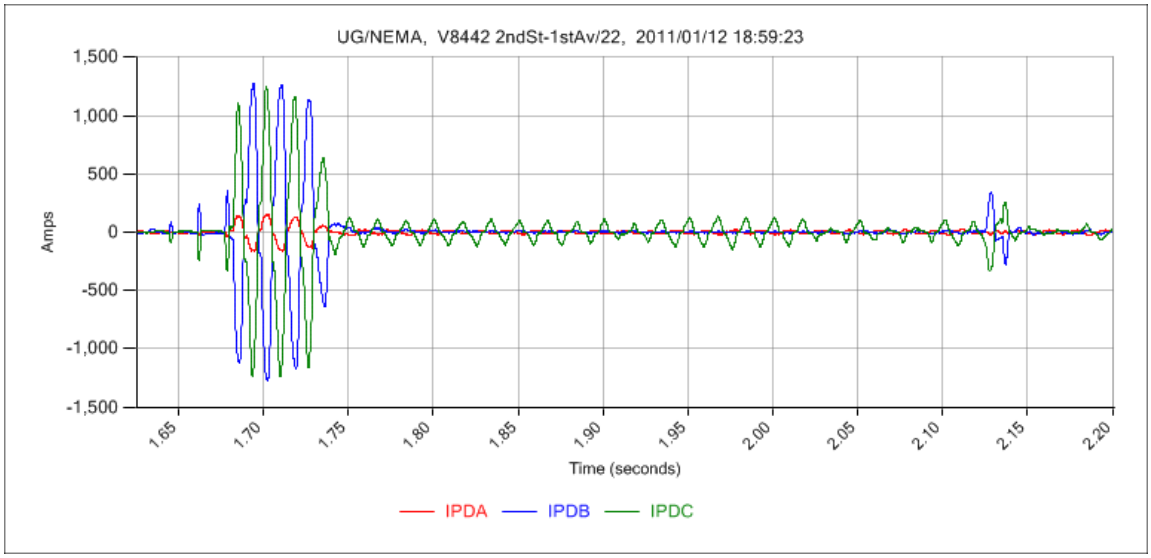

Figure 108: Arcing burst, V8442

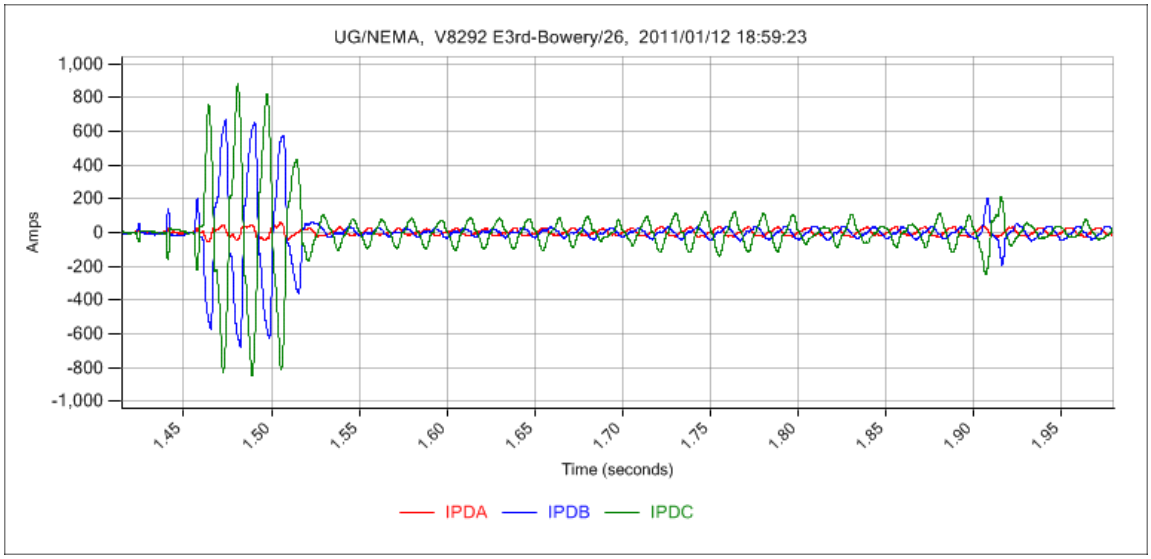

Figure 109: Arcing burst, V8292

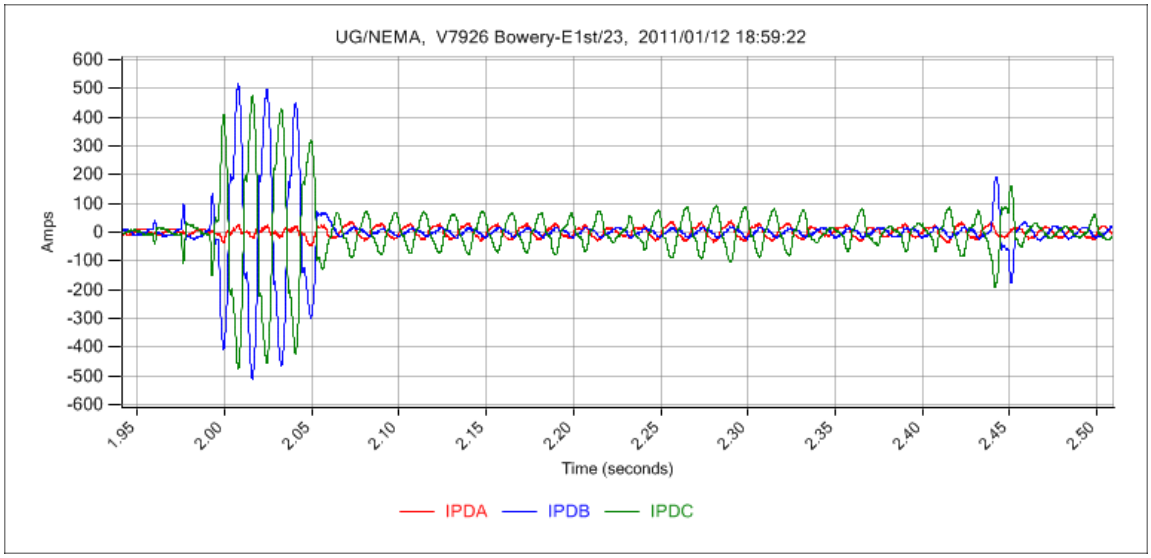

Figure 110: Arcing burst, V7926

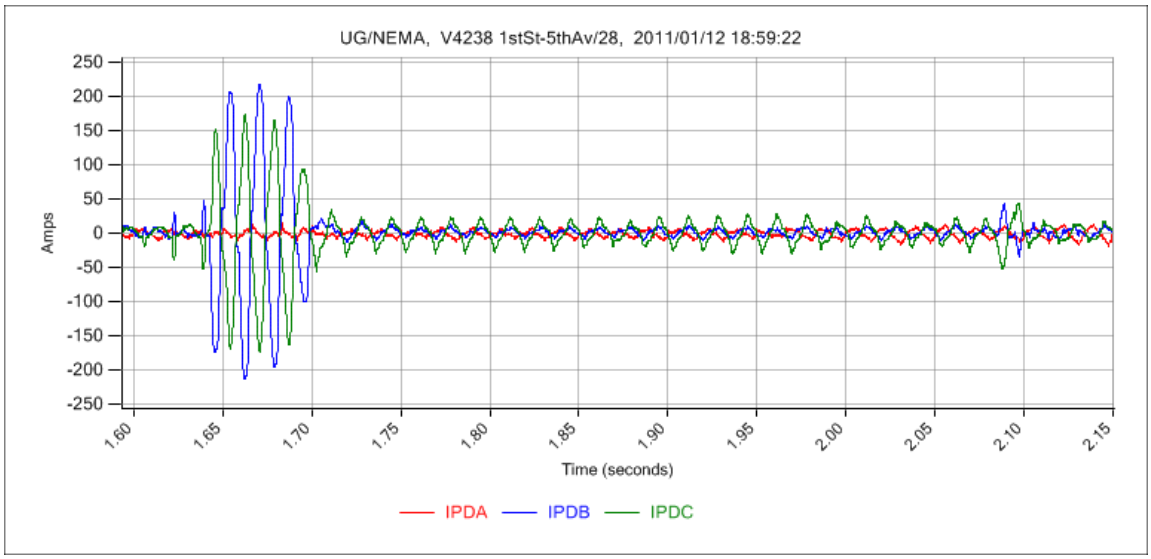

Figure 111: Arcing burst, V4238

VITA

Jeffrey Alan Wischkaemper received his Bachelor of Science degree in electrical engineering from Texas A&M University in 2003, and subsequently entered the graduate program pursuing his Doctorate of Philosophy, which he completed in 2011. His research interests include advanced monitoring and control of power distribution systems. Mr. Wischkaemper has previously worked on projects characterizing vegetation contacts with distribution feeders, and comparing characteristics of advanced distribution sensors.

Mr. Wischkaemper's email is jeffw@tamu.edu, and he may be reached at:

Department of Electrical Engineering

c/o Dr. B. Don Russell

Texas A&M University

College Station, TX 77843-3128